Evaluation of 2% CrMoWV HP/LP Rotor Forging for Single Cylinder Steam Turbine Use

TR-111219
Research Project WO4789-01

Final Report, August 1998

EPRI Project Manager
R. Viswanathan

EPRI • 3412 Hillview Avenue, Palo Alto, California 94304 • PO Box 10412, Palo Alto, California 94303 • USA
800.313.3774 • 650.855.2121 • askepri@epri.com • www.epri.com

DISCLAIMER OF WARRANTIES AND LIMITATION OF LIABILITIES

ORGANIZATION(S) THAT PREPARED THIS REPORT

Rolls-Royce International Research and Development Limited

ORDERING INFORMATION

Requests for copies of this report should be directed to the EPRI Distribution Center, 207 Coggins Drive, P.O. Box 23205, Pleasant Hill, CA 94523, (510) 934-4212.

CITATION

This report was prepared by

Rolls Royce Industrial Power Group
Shields Road
New Castle Upon Tyne NE 62YD, England

Principal Investigator
M. Beech

This report describes research sponsored by EPRI

The report is a corporate document that should be cited in the literature in the following manner:

Evaluation of 2% CrMoWV HP/LP Rotor Forging for Single Cylinder Steam Turbine Use, EPRI, Palo Alto, CA, 1998 Report TR-111219.

REPORT SUMMARY

There has been considerable industry interest in developing a single shaft rotor configuration that uses the same rotor in the high-pressure (HP) as well as the Low Pressure (LP) sections of a steam turbine. This report evaluates an HP/LP rotor forging for single cylinder steam turbines.

Background

Use of a single shaft HP/LP combination leads to a more compact turbine with a single casing, resulting in substantial savings. This is only possible if the combined rotor can meet the performance factors both of existing HP rotors, in particular with regard to creep strength requirements, and also to LP rotors, which require a combination of good toughness and tensile strength. To meet these prerequisites, various steelmakers have developed alloys, usually with higher chromium contents, with claims that all the key parameters of creep strength and toughness can be maintained. One such alloy, developed in the 80's and early 90's by Saarschmiede, has now been in extensive service for more than 10 years in HP/LP combination duty. EPRI undertook the present study because it was felt that this existing alloy could benefit from further optimization, particularly with respect to steel cleanliness and detailed attention to rotor composition.

Objectives

- To optimize the 2%CrMoNiWV Saarschmiede steel so that the HP properties are better than the existing 1CrMo1/4Vrotor steel and the LP properties are better than 31/2 %NiCrMoV steel
- To compare the results from the optimized HP/LP 1250mm/1750mm diameter trial rotor with the existing extensively evaluated 2%CrMoNiWV steel

Approach

Trial melts of the 2%CrMoNiWV steel were manufactured with reduced amounts of trace elements and silicon contents to approach a “clean steel” composition, together with variations to the molybdenum, tungsten, and niobium contents. The most promising candidate was then selected for the production of a trial HP/LP 1250/1750mm diameter rotor. This rotor was then evaluated against key properties for existing conventional HP and LP rotor steels.

Results

Melt trials of 2%CrMoNiWV alloys consisted of improved cleanliness, additions of Mo and W, or additions of Nb. Increasing the Mo and W contents promised a better FATT, but only in the rim region of the rotors, and even this advantage was offset by poorer creep properties. Addition of 0.04%Nb led to better toughness due to grain refinement, but was detrimental to the creep-rupture properties and resulted in an unacceptable formation of ferrite and carbide. The clean steel composition resulted in the best combination of toughness and creep properties and was chosen for trial rotor studies. A trial rotor manufactured from the optimized 2%CrMoNiWV steel with a LP diameter of 1750mm exhibited better toughness compared to previous 2%CrMoNiWV rotors of much smaller diameters. The creep strength of the HP portion lies in the upper scatterband of 1%CrMoV rotor steel with a comparable yield strength.

EPRI Perspective

The properties reported here for the optimized 2%CrMoNiWV steel make this material very attractive for use as a HP/LP combi-rotor. In addition, the material can be used as a retrofit for existing HP rotors, due to the ability of the material to use its greater toughness to allow faster startup and shut-down times.

TR-111219

Interest Categories

Applied science & technology
Combustion turbine/combined cycle plants
State-of-the-art power plants
Fossil steam plants O&M cost reduction

Keywords

Steam turbines
Alloys
Rotors
Motors
High Pressure
Low Pressure

ABSTRACT

In order to improve the properties of a 2%CrMoNiWV HP/LP combi-rotor steel, the composition was optimized with respect to Mo, W and Nb contents. The level of residual elements were at the same time reduced, and in this way, better FATT values were obtained, and long term embrittlement was reduced. A large trial HP/LP rotor forging was then produced having a maximum LP diameter of 1750mm, heat treated to yield strengths of up to 700 MPa. This trial rotor was extensively evaluated to determine whether the properties met the criteria both for existing LP and HP rotors.

The trial rotor exhibited excellent toughness levels compared to 1CrMo¼V HP rotors, and it was possible to attain the toughness level of previously investigated 2%CrMoNiWV rotors with an increased diameter and a yield strength of >690 MPa. Other mechanical, creep and fatigue properties were found to compare favorably with HP or LP rotor forgings, and consequently makes this material very attractive for use as a HP/LP combi-rotor, or even as a retrofit for existing HP rotors due to the ability to use its greater toughness to allow faster start-up and shut-down times.

ACKNOWLEDGMENTS

The author is grateful to Dr I. H. Craig for assistance with the graphics for this report, and to Dr R. Viswanathan for reviewing the manuscript and giving many helpful comments. The work contained in this report was sponsored by EPRI, and the data were gathered in a collaborative program by the following organizations:

ABB Power Generation, Switzerland

GEC-ALSTHOM, United Kingdom

GEC-ALSTHOM Energie, Germany

Parsons Power Generation Systems, United Kingdom

Siemens Power Generation KWU, Germany

Saarschmiede, Germany

CONTENTS

LIST OF FIGURES

LIST OF TABLES

1

INTRODUCTION

In conventional steam turbines, the high pressure and intermediate-pressure sections of rotors must be made from creep-resistant steel. For temperatures up to 545°C (±10°C) the 1%CrMoV type steels, for example ASTM A470 - Class 8 are well suited, and are often used for rotors and a similar material is also used for casings. They were developed 30 to 40 years ago to have a high creep resistance, but as a consequence, they have only a limited fracture toughness and creep-rupture ductility. These limitations are taken into account during turbine design, and are considered when establishing operating the parameters for the turbine. Within these limits however, turbine components made from 1%CrMo¼V steel have proved to be extremely successful worldwide.

The low pressure end of a steam turbine typically uses a rotor material manufactured from 3½%NiCrMoV which was developed in parallel to the higher temperature grades. The steel has a relatively high proof strength in order to withstand the blade loading from the long last row blades, together with a good fracture toughness that is required because of the large forging section sizes, and hence stresses that are generated at the rotor core. This grade of steel typically has poor creep rupture strength [1], but this can be improved by improved steelmaking techniques to a maximum operating temperature of approximately 520°C. Hence this grade, even in a superclean condition cannot be used at normal maximum operating temperatures.

Today, an increasing number of turbines feature a high-temperature - high-pressure section and a low-temperature - low-pressure section combined on one rotor and in one casing. The value of such a combination rotor is clear with respect to lower civil engineering costs, and lower manufacturing costs. Such turbines require a combination of tensile, creep strength and fracture toughness for which neither the high temperature 1%CrMo¼V steel nor the low temperature 3½%NiCrMoV steel is well suited, the former due to inadequate toughness in the LP section and the latter because of its poorer creep resistance in the HP section. It is clear then, that creep-resistant steels with higher toughnesses offer greater operational flexibility, particularly with respect to start-up and shut-down times, and as a result, would be particularly well suited for use as HP-LP combination rotors. To meet these requirements various steelmakers [2 - 17] around the world have developed alloys, usually with higher chromium, with claims that creep rupture strength can be maintained with a much greater fracture toughness. However most of these alloys have drawbacks to their use which would

potentially preclude their use. For example, the development of a superclean 2½%NiCrMoV steel was made [12] which showed considerable promise in developing a considerably higher toughness than conventional high temperature rotor material. The creep strength was also comparable to 1%CrMoV steel, however the notch bar creep rupture testing showed a tendency for notch weakening [12 - 14]. Other workers [15,16] preferred 2¼% Cr steel as the basis for a rotor steel. Other variants include the modified composition 2%Cr1.5%Ni1.7%Mo.

There has also been a development of a similar steel to the one used in the present investigation [13,15]. Its composition of 2.2%Cr1%MoNiVNbW had a higher nickel content than other variants (1.7%) and also had additions of niobium and tungsten. Also a superclean 0.2%Mn1.8%NiCrMoV steel with high toughness has been developed which apparently exhibits no degradation in creep rupture strength [14,17].

Trial HP-LP combination rotors have been manufactured from all of these newly developed steels. The chemical analyses and dimensions of these rotors are presented in the table below (Table 1-1):

Table 1-1
Chemical composition of HP-LP combination trial rotors reported in various studies

Steel Grade	C	Si	Mn	P	S	Cr	Mo	Ni	W	V	Nb	HP/LP diameter, mm	Reference
2%CrMoNiWV	0.22	0.06	0.70	0.005	0.001	2.13	0.86	0.76	0.65	0.32	-	1250/1750	RP 1403-21 EPRI-Europe rotor
2.5%NiCrMoV Superclean	0.23	0.03	0.03	0.003	0.001	1.60	1.20	2.50	-	0.24	-	1270/1750	EPRI-Japan rotor RP 1403-55 [13]
2.2%CrNiMoVNbW	0.24	0.02	0.45	0.004	0.0009	2.22	1.08	1.69	0.19	0.19	0.015	1000/1750	[16]
2%CrMoNiV	0.24	0.02	0.20	0.004	0.004	1.99	1.69	1.48	-	0.23	-	935/1380	[15]
1.8%NiCrMoV	0.23	0.01	0.20	0.004	0.002	2.03	1.17	1.74	-	0.26	-	1320/1720	[17]

Saarschmiede was the first to develop such an alloy (DIN: 23CrMoNiWV88) during the late 1970's (Table 1- 2). This new 2%CrMoNiWV steel shows real advantages for combi-rotor applications, and to date, Saarshmiede have now manufactured 108 rotors that have been manufactured (see Appendix A).

Table 1-2
Saarschmiede 2%CrMoNiWV Target Chemical Composition

C	Si	Mn	P	S	Cr	Mo	Ni	V	W	Al	Cu	Sn	Sb	As
0.22	< 0.10	0.70	<0.01	< 0.01	2.10	0.85	.75	0.32	0.65	< 0.010	< 0.10	< 0.01	< 0.002	< 0.015

This 2%CrMoNiWV steel was first reported to the public in 1980 [2], and was first commercially used in an HP/LP rotor placed in service during 1984 [7]. Developments and details have been described in other publications [3 - 11]. This advanced steel offers a creep-rupture behavior quite similar to the best oil quenched or air melted 1%CrMoV, together with a markedly higher fracture toughness, even after long-time high-temperature thermal exposure. Creep rupture ductility, which is considered to be important in European designs, remains high out to long durations. Consequently, this steel is superior to conventional 1%CrMo¼V for HP and IP rotors in machines operating under two shift conditions, and is also a good option for retrofit applications. It allows turbines to be operated with only minor startup limitations, due to the typically very much higher critical crack sizes [9]. The following figure shows an HP/LP combination rotor manufactured by Saarschmiede for Parsons TG Ltd at La Collette.

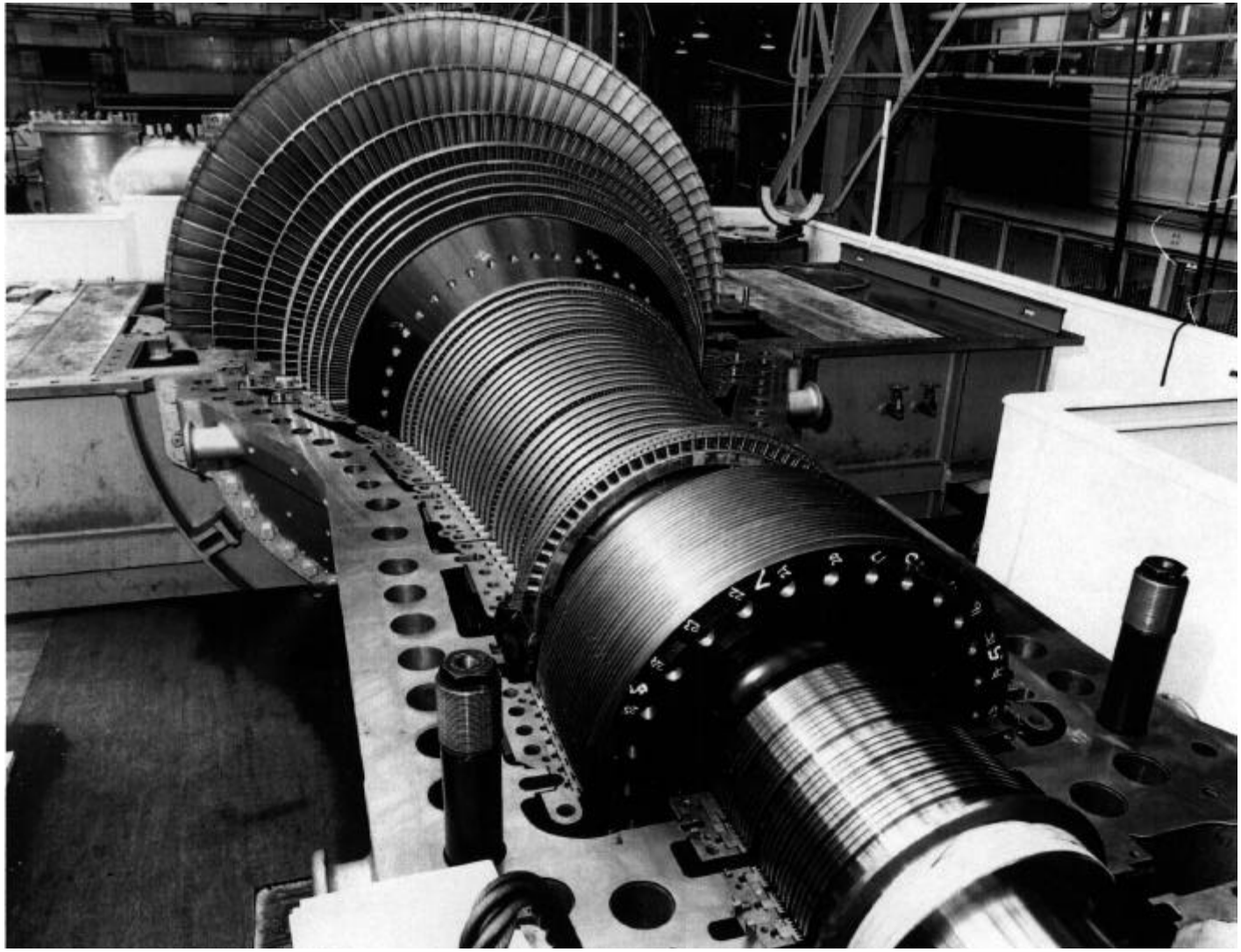

Figure 1-1
2%CrMoNiWV HP/LP combination rotor manufactured by Saarschmiede for Parsons TG Ltd at La Collette

2

OPTIMIZATION OF ROTOR COMPOSITION

Before manufacturing the EPRI-Europe Rotor, the extent to which optimization of the chemical composition could yield further improvements in toughness over the then existing version of the COST 505 2%CrMoNiWV alloy (particularly FATT) was investigated by testing 3 laboratory melts. A decrease of the trace elements P, As, Sb, Sn was examined together with a reduced silicon content; increases in the Mo content from 0.85% to 0.95% and W from 0.65% to 0.85% together with the effects of 0.03% to 0.04% Nb additions were also made. This clean steel composition whilst having low levels of embrittling elements and inclusions does not meet the so-called super clean quality because the manganese content was deliberately not reduced in order to maintain adequate toughness.

Five experimental heats with chemical compositions as shown in the table below were melted in a 150-kg high-frequency furnace and subsequently remelted in a vacuum-arc furnace to produce 200 mm diameter ingots. These ingots were subjected to upsetting followed by a draw-out forging process at a reduction ratio of 4.5 to produce a rectangular section of 210 x 70 mm (8" x 3"). These were subsequently stress relieved at 680°C. The samples taken from these bars were subjected to an austenitizing treatment at 950°C for 4 h, followed by heat treatments designed to simulate the microstructure and properties in various zones of a large rotor. The first heat treatment simulated the microstructure at the rim region corresponding to distances from the surface of 80 mm for oil quenched rotors or 120 mm for water quenched rotors, and the second corresponded to a diameter of 1300 and 1600 mm respectively.

Table 2-1
Chemical Composition of Laboratory Melts for optimization of the EPRI-Europe rotor

Steel#	C	Si	Mn	P	S	Cr	Mo	Ni	W	Al	Cu	Nb	V	N	As	Sb	Sn
1	0.21	0.035	0.63	0.004	0.004	2.14	0.85	0.74	0.67	0.006	0.015	-	0.28	0.012	0.006	0.0007	0.003
2	0.21	0.028	0.64	0.004	0.003	2.07	0.97	0.75	0.86	0.008	0.01	-	0.33	0.0104	0.007	0.0009	0.003
3	0.21	0.015	0.80	0.0045	0.003	2.07	0.975	0.78	0.94	0.006	0.012	-	0.265	0.0115	0.0063	0.0006	0.0036
4	0.21	0.025	0.68	0.004	0.003	2.11	0.84	0.74	0.66	0.007	0.015	0.029	0.32	0.012	0.007	0.0009	0.003
5	0.21	0.015	0.86	0.0054	0.0032	2.12	0.89	0.78	0.70	0.005	0.010	0.037	0.34	0.0098	0.0055	0.0004	0.003

Steel 1: Clean. Steel 2 and 3: Clean + Mo + W Steel 4 and 5: Clean + Nb

In the following tables, the results for test steels 1, 2 and 4 are shown in relation to the equivalent sample depth and tempering temperature in the range 660 to 690°C.

Table 2-2
Mechanical properties of Laboratory melts at simulated 120mm depth

Steel #	Heat Treatment	0.2%Y MPa	UTS MPa	EL %	RA %	Impact Energy, J (ISO-V)					FATT °C
						-40°C	-20°C	0°C	20°C	40°C	
1	From 650° → 950° (4h)										
	→ 2°/min +690° (16h)/air	621	747	19.3	73.7	12	74	86	165	206	0
	+670° (16h)/air	738	849	18.3	71.6	23	71	69	164	166	+7
	+660° (16h)/air	760	862	16.7	71.1	21	31	42	166	170	+8
2	From 650° → 25°/h → 950° (4h)										
	→2°/min +690° (16h)/air	607	730	20.3	71.1	39	72	172	170	197	-13
	+670° (16h)/air	736	855	17.3	69.3	34	51	149	168	171	-10
	+660° (16h)/air	778	873	17.3	68.7	13	31	54	154	168	+8
4	From 650° →25°/h →950° (4h)										
	→2°/min +690° (16h)/air	652	732	17.7	71.1	47	131	160	174	173	-25
	+670° (16h)/air	716	815	18.0	69.8	51	132	153	179	174	-27
	+660° (16h)/air	748	854	17.3	68.4	43	60	149	168	177	-12

Steel 1 - clean, Steel 2 - clean + Mo + W, Steel 4 - clean + Nb
Simulated rim heat treatment corresponding 80 mm distance from rim using oil quenching or 120 mm from rim with a water quench

Table 2-3
Mechanical properties of Laboratory melts at simulated 1.6m rotor core

Steel #	Heat Treatment	0.2%Y MPa	UTS MPa	EL %	RA %	Impact Energy, J (ISO-V)					FATT °C
						-40°C	-20°C	0°C	20°C	40°C	
1	From 650° → 25°/h → 950° (4h)										
	→2° min +690° (16h)/air	614	730	20.3	73.6	25	42	81	184	190	0
	+670° (16h)/air	699	812	17.3	67.3	48	24	81	177	121	+6
	+660° (16h)/air	770	862	17.3	69.4	23	27	49	51	151	+27
2	From 650° → 25°/h → 950° (4h)										
	→ 2°/min +690° (16h)/air	592	719	18.0	71.4	13	48	89	167	185	0
	+670° (16h)/air	705	827	17.7	69.8	42	50	66	150	171	+6
	+660° (16h)/air	740	841	17.7	67.2	7	7	21	66	154	+26
4	From 650° → 25°/h → 950° (4h)										
	→ 2° min +690° (16h)/air	625	722	18.7	70.4	42	159	150	167	175	-30
	+670° (16h)/air	688	802	17.0	70.2	52	68	178	183	174	-14
	+660° (16h)/air	744	844	17.0	69.3	10	62	153	155	158	-13

Steel 1 - clean, Steel 2 - clean + Mo + W, Steel 4 - clean + Nb
Simulated core heat treatment corresponding to core of rotor with diameter 1 300 mm using oil quenching or a diameter of 1 600mm with a water quench

Table 2-2 shows the properties for a cooling rate corresponding to a rotor rim, while table 2-3 shows the corresponding values for a simulated rotor core. From comparison of these values it is evident that the FATT value rises with increasing strength and sample depth, as had been anticipated. Whilst there are no significant differences between steel numbers 1 and 2, the excellent FATT values obtained for steel number 4, which contains 0.029% Nb, is particularly noteworthy. This is due to a very marked grain refinement to a size of ASTM 9-10, as a result of the niobium addition. The finer microstructure resulted in acceleration of transformation in the pearlite phase such that thermal treatment simulating the conditions in the core of a water-quenched 1600 mm diameter rotor gave unacceptable ferrite levels of 10 to 15%. Furthermore, the finer structures had much poorer creep properties. Figure 2-1 shows the creep behavior of the 3 steels at 550°C and a stress of 139 MPa for the simulated core of a 1 300 mm diameter rotor after oil quenching, showing not only the poorer creep-rupture properties of the Nb-doped heat number 4 but also the less favorable behavior of heat

number 2 which had increased Mo and W contents. It is assumed that higher levels of carbide forming elements either result in a larger amount of undissolved carbides during austenitizing or accelerate the re-crystallization occurring in the range of the secondary creep strain.

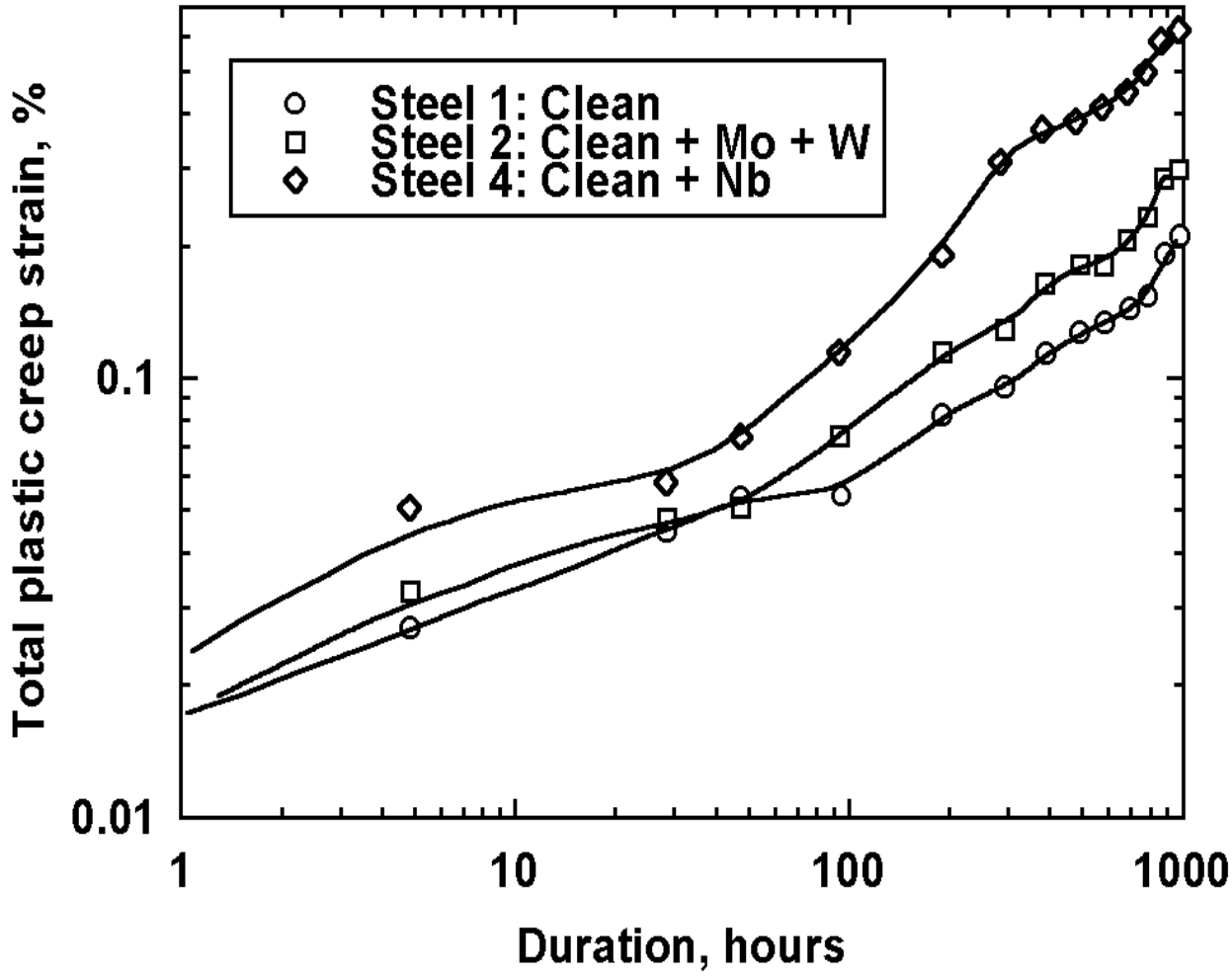

Figure 2-1
Creep Properties of the Trial Melts

The experimental heats were also used to investigate the susceptibility to long-term embrittlement at 480°C. This involved heat treating the samples to simulate the conditions 80 mm from the rim in the core of a 1 600 mm diameter rotor after water quenching to a 0.2% yield strength of 700 MPa and then artificially aging at 480°C for up to 10 000 h. This revealed no significant increase in FATT.

The results of the microstructural examinations show that, except for the Nb-alloyed heat, their structure is bainitic over the entire cross-section of a simulated 1300 mm diameter oil-quenched rotor or a 1 600 mm diameter water-quenched rotor. Even for

2000 mm diameter rotors the presence of ferrite in the core after water quenching would not be expected.

Comparison of all of the test results has shown that up to 0.2% yield strengths of 700 MPa, a decrease in the content of the embrittling elements Si, P, As, Sb and Sn in the 2%CrMoNiWV steel gives better FATT values and can also avoid long-term embrittlement. In the case of large turbine rotors manufactured from ESR steel, however, it is not possible to lower the silicon content to less than approximately 0.06% for metallurgical reasons. Increasing the Mo and W contents promises a better FATT only in the rim zone of the rotors. This advantage, however, is offset by poorer creep properties. While an addition of 0.04% Nb gives better toughness due to grain refinement, as already stated, it is also detrimental to the creep-rupture properties and results in an unacceptable formation of ferrite + carbide.

Consequently, the following mean chemical analysis was suggested for the manufacture of the EPRI-Europe rotor from an ESR-ingot of 2 300 mm diameter (Table 2-4):

Table 2-4
Target and actual chemical composition for the EPRI-Europe rotor compared to previous 2%CrMoNiWV rotors evaluated under COST 505

Steel Type	C	Si	Mn	P	S	Cr	Mo	Ni	W	V	Al	C	As	Sb	Sn
Aim: 2%CrMoNiWV	0.21 - 0.23	<0.1	0.65 - 0.75	<0.007	<0.005	2.05 - 0.15	0-8 - 0-9	0.7 - 0.8	0.6 - 0.7	0.3 - 0.35	<0.01				
COST 505 ESR	0.22	0.1	0.66	0.01	0.003	2.1	0.84	0.75	.67	0.32	<0.008	0.06	0.015	0.014	0.1
COST 505 VCD	0.23	0.075	0.68	0.006	0.004	2.08	0.83	0.74	0.65	0.3	<0.009	0.09	0.018	0.005	0.008
Aim: EPRI-Europe rotor	0.22	0.07	0.7	<0.005	0.002	2.1	0.85	0.75	0.65	0.32	0.008	<0.06	<0.008	<0.001	<0.006
Actual: EPRI-Europe rotor	0.22	0.06	0.7	0.005	0.001	2.13	0.86	0.76	0.65	0.32	0.008	0.06	0.007	0.0007	0.005

Further details have been reported in Reference [14].

3

MANUFACTURE AND PRELIMINARY TESTING OF THE EPRI-EUROPE ROTOR

The EPRI-Europe rotor was manufactured by Saarschmiedewerke by an electro-slag remelting route according to the sequence outlined in Table 3-1. The steel was melted in a 120 tonne electric arc furnace, cast into electrodes, and subsequently remelted into an ESR ingot 2300 mm in diameter and weighing 95 tonnes. The chemical composition of the ESR ingot is shown in Table 2-4. After heating to 1280°C in a forging furnace, the ingot was subjected to a sequence of forging operations on a 60 MN press including stretch forging to 1900 mm octagonal cross-section, two upsetting operations, and finally stretch forging to 1820 mm diameter in the LP section and 1355 mm diameter in the HP section (Figure 3-1) giving a total stretch reduction ratio of 8.2.

After the forging sequence, the rotor was isothermally transformed in the pearlite phase field at 690°C and, following machining to 1750 mm diameter in the LP section and 1250 mm diameter in the HP section, normalized at 950°C and tempered at 680°C.

Table 3-1
Manufacturing sequence of the 2%CrMoNiWV HP/LP rotor

Manufacturing Sequence
Steel melting and casting of electrodes
Electroslag remelting
Forging
Preliminary heat treatment
Ultrasonic examination
Machining for quality heat treatment
Vertical quality heat treatment with differential quenching of HP and LP parts and tempering for higher strength level
Ultrasonic examination

Manufacturing Sequence
Mechanical testing, tangential outside
Trepanning of radial cores diameter 395 mm of HP and LP parts (HD1 - ND1)
Second tempering for lower strength level
Mechanical testing, tangential outside
Trepanning of radial cores diameter 395 mm from HP and LP parts (HD2 - ND2)
Cutting of radial cores for further evaluation tests

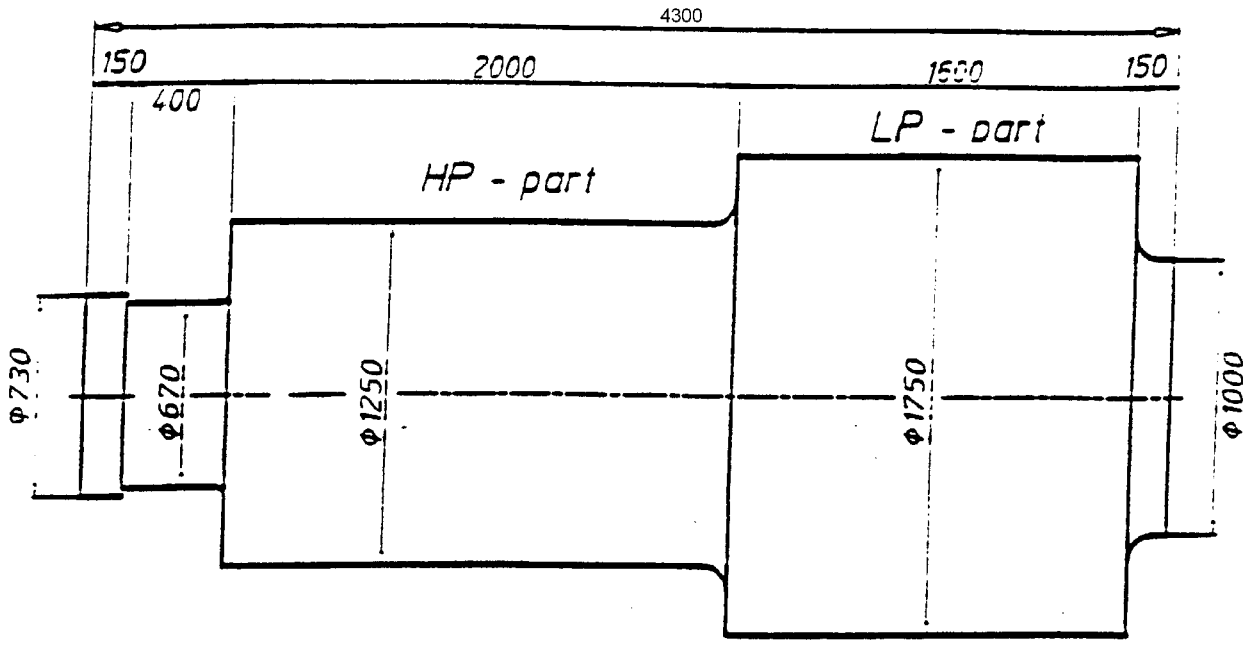

Figure 3-1
Quality heat treatment contour for the trial HP/LP forging

During quenching and tempering, the rotor was austenitized in a gas-heated vertical furnace for 31.5 hours at 950°C. Quenching was performed in a vertical air-hardening facility equipped with 3 series of water spray nozzles and 4 fans, with a total capacity of 40 000 m^3/hour (see Figure 3-2). Each nozzle series could be equipped with different nozzle types and separately controlled with respect to water pressure and flow rate. In this way, it was possible to simulate oil quenching in the upper, HP section, by selecting a specific water and air mix, while achieving drastic water cooling in the lower, LP, section. During the quenching operation, the forging was rotated at a speed of 8 rpm to ensure even cooling. Cooling times for the rotor were chosen to obtain 200°C maximum in the core of the HP section over a period of 660 min and 100°C

maximum in the core of the LP section with a 1200 min cooling time. Subsequently, the rotor was tempered for 35.5 hours at 655°C, slowly furnace-cooled to 250°C, and finally cooled in air.

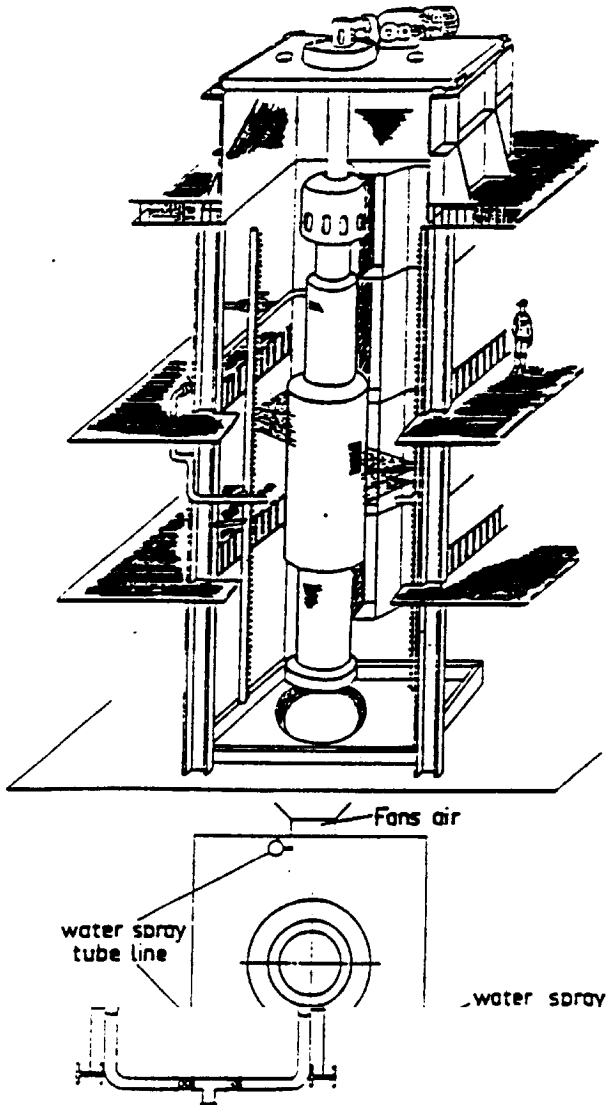

Figure 3-2
Schematic of rotor cooling system used to produce the trial rotor forging at Saarshmiede

Subsequent ultrasonic inspection at a defect detectability of 1.2 mm DGS in the thick LP section and 0.8 - 1 mm DGS in the HP section revealed no defects. Testing of tangential specimens from the rim locations A and B1 of the LP section and location C of the HP section gave the values shown below. As can be seen in Figure 3-3, the target 0.2% yield strength of 690 to 720 MPa was obtained, except for location C, which exhibited a 0.2% yield strength marginally below the target range.

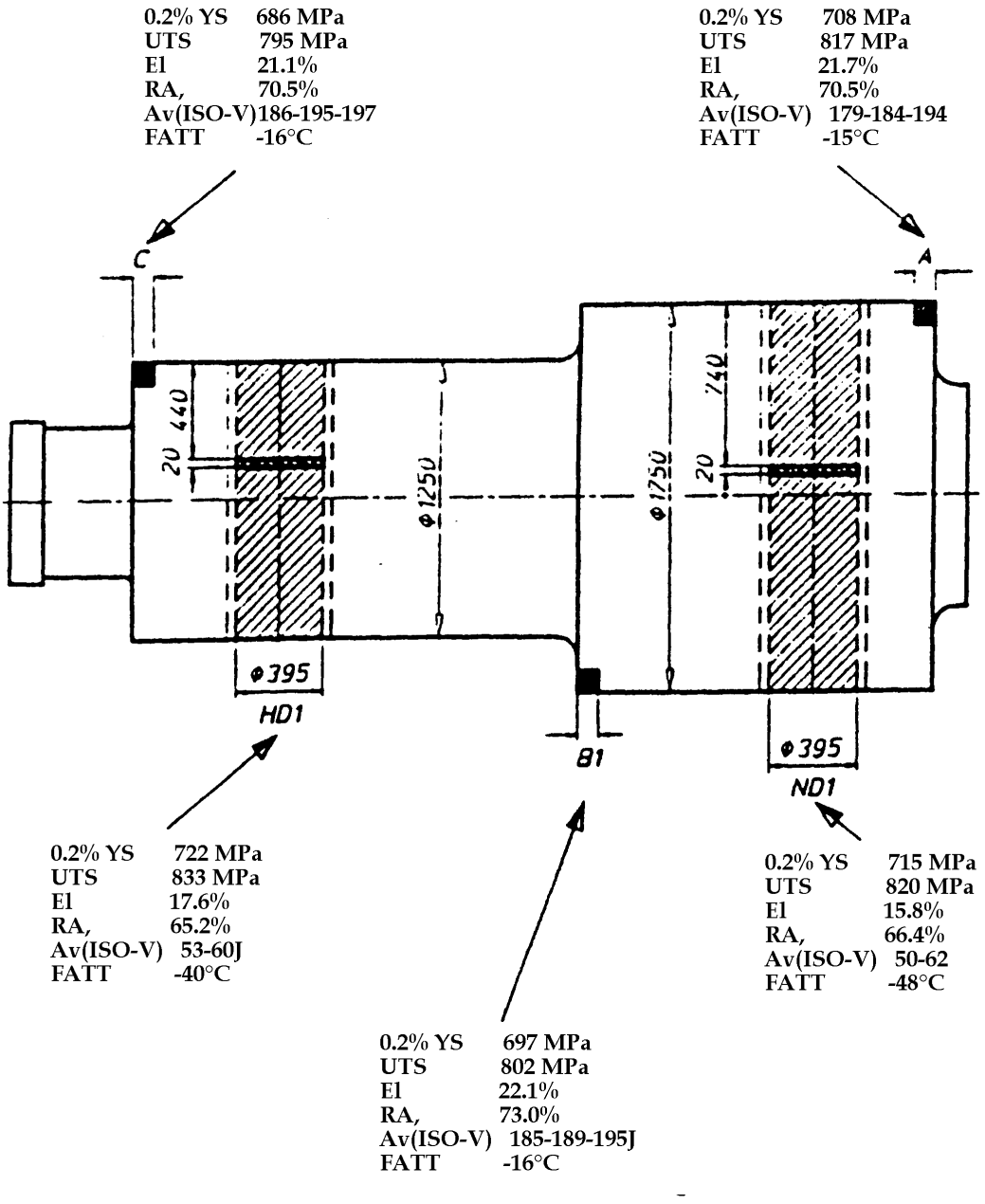

Figure 3-3
Mechanical properties of the higher yield strength section of the trial rotor

Following this testing, a through-section radial bore core LP1 (low pressure part core 1, higher yield strength) with 395 mm diameter was removed from the LP section and an identical radial core HP1 (high pressure part core 1, higher yield strength) was removed from the HP section. These cores were sectioned into samples, which were made available to the turbine manufacturers participating in the program for further examination.

Specimens for the determination of mechanical properties were taken from the sectioned cores, HP1 at a location 440 mm from the surface and LP1 at a location 740 mm from the surface. The results are compared to the near-surface tangential values in Figure 3-3.

Following the removal of the radial cores HP1 and LP1, the rotor was subjected to a second tempering treatment at 655°C for 32 hours followed by furnace cooling. This treatment was aimed at obtaining a lower 0.2% yield strength of approx. 625-650 MPa. The radial cores (HP2 and LP2) were then removed and samples taken tested in the same way as for the higher strength level. The results are shown in Fig. 3-4. Cores HP2 and LP2 were also sectioned and distributed to the turbine manufacturers participating in the project.

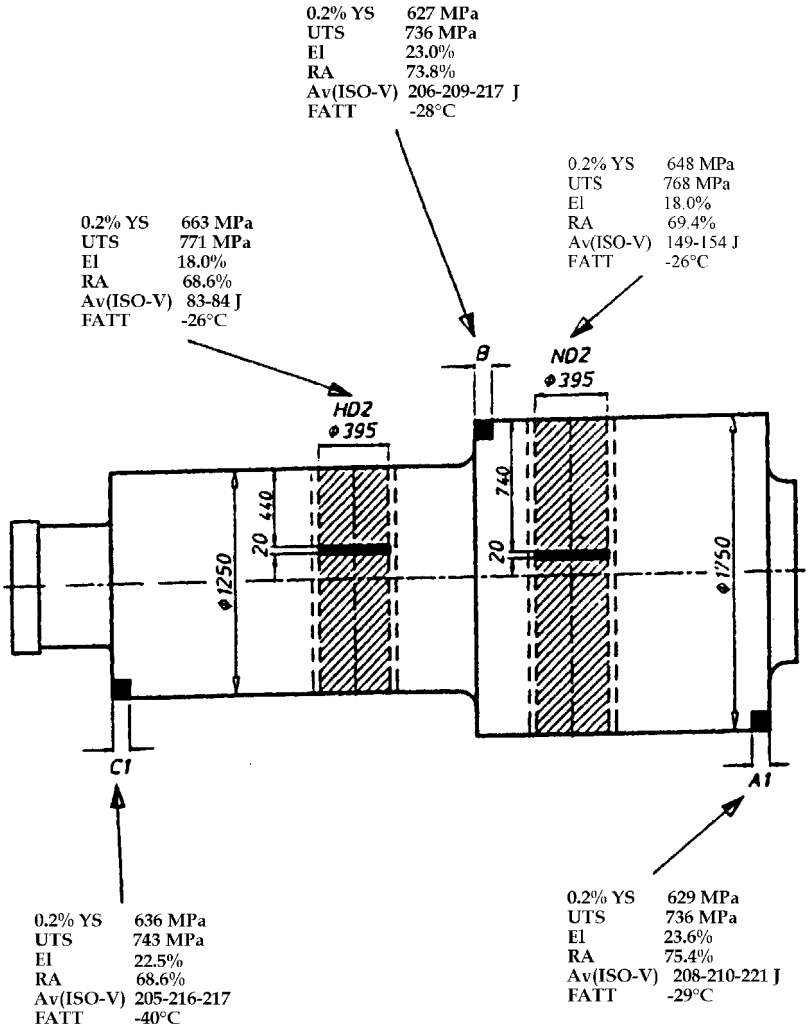

Figure 3-4
Mechanical properties of the lower yield strength section of the trial rotor

In addition to the mechanical properties, the product analysis as well as the structure and the grain size were determined for these sample locations. The results are given in Figure 3-5. These results fully met the specification for the rotor forging.

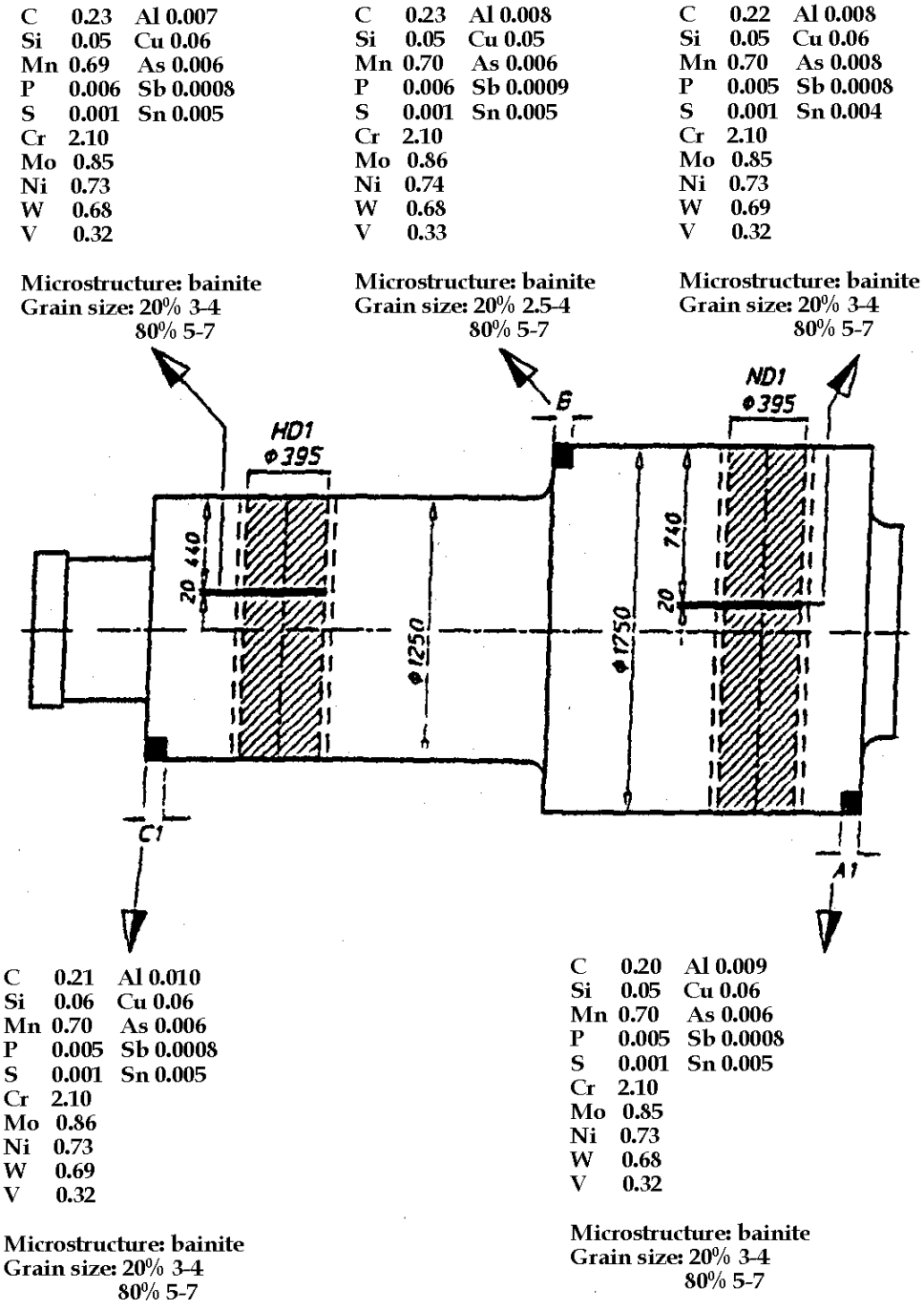

Figure 3-5
Chemical composition, grain size and microstructure of the trial rotor

4

MECHANICAL PROPERTY EVALUATION

The overall mechanical property investigative program for the EPRI-Europe rotor is given below. This encompasses all the key mechanical and metallurgical parameters thought necessary to design a HP/IP combination rotor. The results obtained from this program formed the basis for comparison with conventional 1%CrMoV and 3½%NiCrMoV rotor steels, and with two manufactured rotors that the consortium had previously evaluated [10]. One rotor was an ESR-rotor for SIEMENS/KWU which had been an integral test extension of the full representative diameter, which was then cut off for subsequent testing (referred to as the COST 505 ESR rotor). The other rotor was a VCD rotor made for GEC ALSTHOM Energie, which was completely sectioned for testing (referred to as the COST 505 VCD rotor). The overall program is given in Table 4-1: Detailed information on the partnership and rotor cutups are given in appendix C.

Table 4-1
Overall test program for the evaluation of the 2CrMoWV material

#	Task
1.1 1.2	Sectioning of the rotor Drawings for test material and specimen positions
2	Macro/microstructure
3	Chemical composition
4	Tensile properties - RT, > RT
5 5.1 5.2 5.3	Toughness properties - Impact energy at RT along the radius - FATT and uppershelf energy - Fracture toughness
6 6.1 6.4 6.5.2 6.6.3	Exposure Aging at 425°C, 480°C, 540°C, for 5000h, 10000h, 20000h followed by tasks - Tensile properties after all times - FATT after all times - Fracture toughness only after 20000h
7	Creep rupture 9-550°C; 600°C, each 9: 3 x), 3 x o, for target 1000, 3000, 10000h

#	Task
	and 1 x σ up to 20000h
8	Creep crack growth η- 550°C, t = 2000, 10000h
9 9.1 9.2	LCF Without dwell Ni-500, 3000, 10000, 30000, η = RT, 350°C (∅ 1750 mm) or 530°C (∅ 1250 mm) With dwell Ni-300, 600, 1300, 2000 ..... 2500, η = 530°C
10	Fatigue crack growth High frequency, η = RT, 530°C
11	SCC Smooth longest run aimed for 10000h, η = 95°C

5

RESULTS

Chemical composition

In Figure 3-5 the melt analysis from the ESR-ingot and the chemical position from different positions of the rotor are summarized. To compare the result of the EPRI-Europe rotor with the ESR and VCD COST 505 2%CrMoNiWV rotors, the results published in [10] are shown in Table 5-1. As pointed out in the introductory chapter, the aim was to decrease the content of the embrittling elements Si, P, As, Sb and Sn with the aim of improving the toughness. In the literature, different factors are defined to characterize the influence of the chemical composition on the long term stability of toughness. In Table 5.1, the J-factor [18], the Bruscato factor χ [19] and the K-factor [20], which is a combination of the other two factors, is calculated for the chemical composition of the melt analysis of the different rotors examined (See equations 5-1 to 5-3 below).

$$J=(Mn + + Si)\,(P+Sn) \qquad \text{(eq. 5-1)}$$

$$\chi=\frac{10P + 5Sb + 4Sn + As}{10} \qquad \text{(eq. 5-2)}$$

$$K=(Mn + Si)\,(10P + 5Sb + 4Sn + As) \qquad \text{(eq. 5-3)}$$

Further reductions of the Mn-content, which is necessary to achieve the so-called "super-clean" condition is not possible due to hardenability reasons. Therefore, the calculated J-factor and K- factor in this table are given to show the improvement that can be achieved by producing a "clean steel" in this type of steel. From Table 5-1 the improvement in the cleanliness of the EPRI-Europe rotor in comparison with the first rotors of the COST 505-project can be seen.

Table 5-1
Cleanliness factors for EPRI-Europe rotor

f	χ	J	K
COST 505 ESR	22.5	152	0.171
COST 505 VCD	13.5	106	0.102
Aim EPRI-Europe rotor	8.7	86	0.068
Actual EPRI-Europe rotor	8.05	76	0.061

Microstructure

The bainitic microstructure of the center portion of the HP- and LP-part of the rotor is typical for this type of steel and heat treatment (Figure 3-5), consisting of a grain size of 20% ASTM 3-5 and 80% ASTM 5-7 in the HP section, and 20% ASTM 3-4 and 80% ASTM 5-7 in the LP section.

Tensile properties

Mechanical properties have been determined on the rim and center portion of the rotor for both yield strength conditions, with a tangential orientation of the specimen, see Figures 5-1 to 5-4. Additionally, in the LP-part a long radial tensile specimen covering the entire radius was tested to obtain information about the properties over the cross section, [21]. In Table 5-2 the test results for the higher yield strength condition are shown whilst Table 5-3 shows those for the lower yield strength condition. For the rim position the reported value is an average of two specimens. For the center position the quoted value is an average result from various laboratories and test positions of the inner section. The results are plotted as a function of the normalized distance from the center of the rotor (x/R); (x/R = 1 indicates a position at the surface of the rotor, x/ R = 0 indicates a position at the core of the Rotor).

Table 5-2
Tensile Properties of the high yield strength part

Position	x/R	0.2% yield MPa	UTS MPa	A %	Z %
		LP Part			
A: tangential / outside		708	817	21.7	70.5
rim position	0.9	741	846	19.5	72.5
center position	<0.14	716	822	18.3	68.8
B1: tangential / outside		697	802	22.1	73.0
		HP- part			
rim position	0.9	748	851	20	71.5
center position	<0.29	723	835	19	67
C: tangential / outside		686	795	21.1	70.5

Table 5-3
Mechanical Properties of the low yield strength part

Position	x/R	0.2% yield MPa	UTS MPa	A %	Z %
		LP-part			
Al :tangential / outside		629	736	23.6	75.4
rim position	0.9	649	776	20.3	75.0
center position*	< 0.14	640	768	19.5	71.5
B: tangential / outside		627	736	23.0	73.8
		HP-part			
rim position	0.9	649	777	20	74
center position*	< 0.29	653	774	20.4	71.7
C1: tangential / outside		636	743	22.5	73.8

In Figures 5-1 and 5-2 the results of long radial tensile specimens from the LP-part are shown for both strength levels. The excellent homogeneity of the mechanical properties over the cross section of the rotor can be seen, even from the 1750 mm diameter segment in the LP-part. The mechanical properties for the higher strength level condition at room temperature and elevated temperatures are shown for the LP-part in Figures 5-3 and for the HP-part in Figure 5-4.

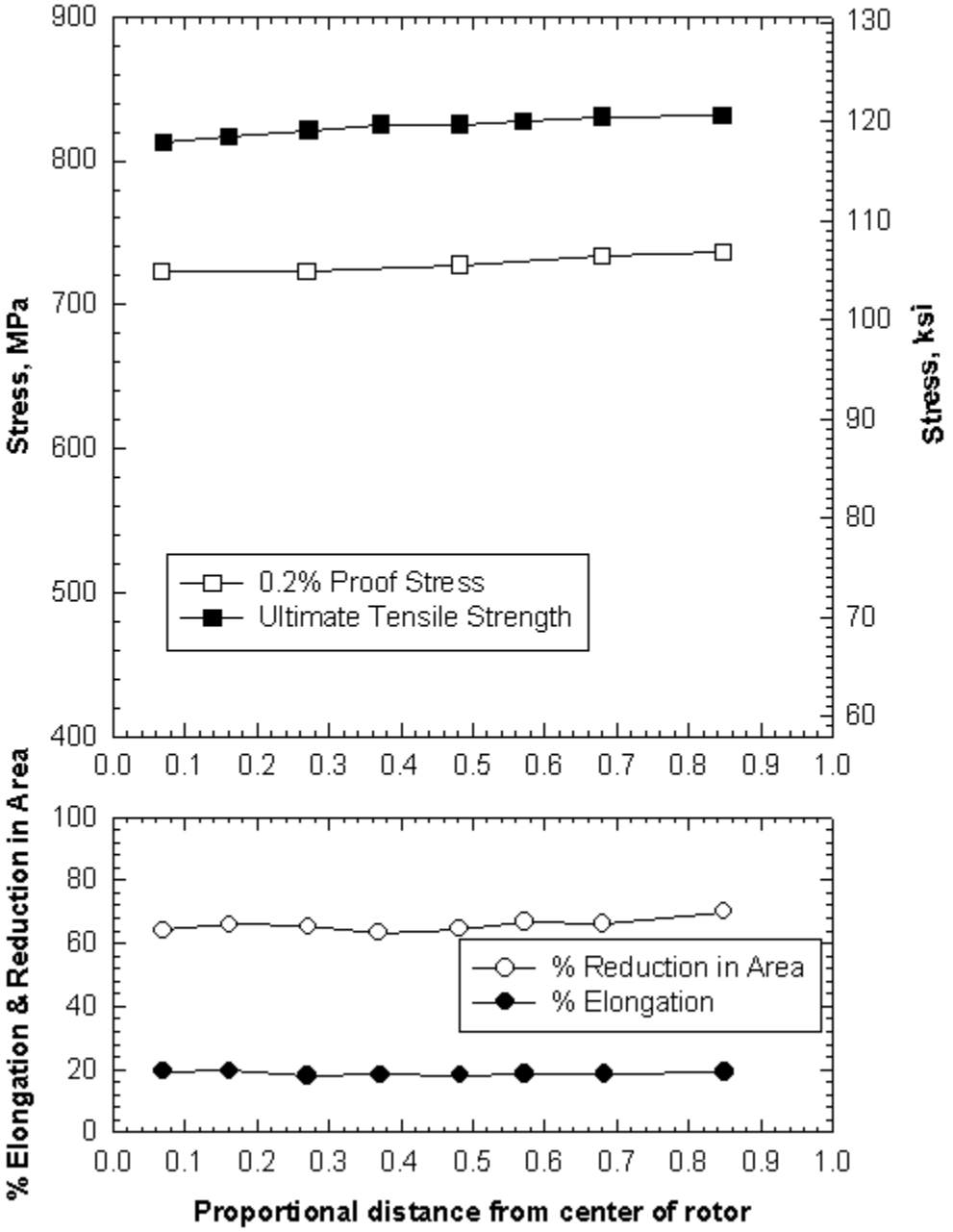

Figure 5-1
0.2% yield strength and ductility as a function of location for the trial rotor section heat treated to the lower yield strength level

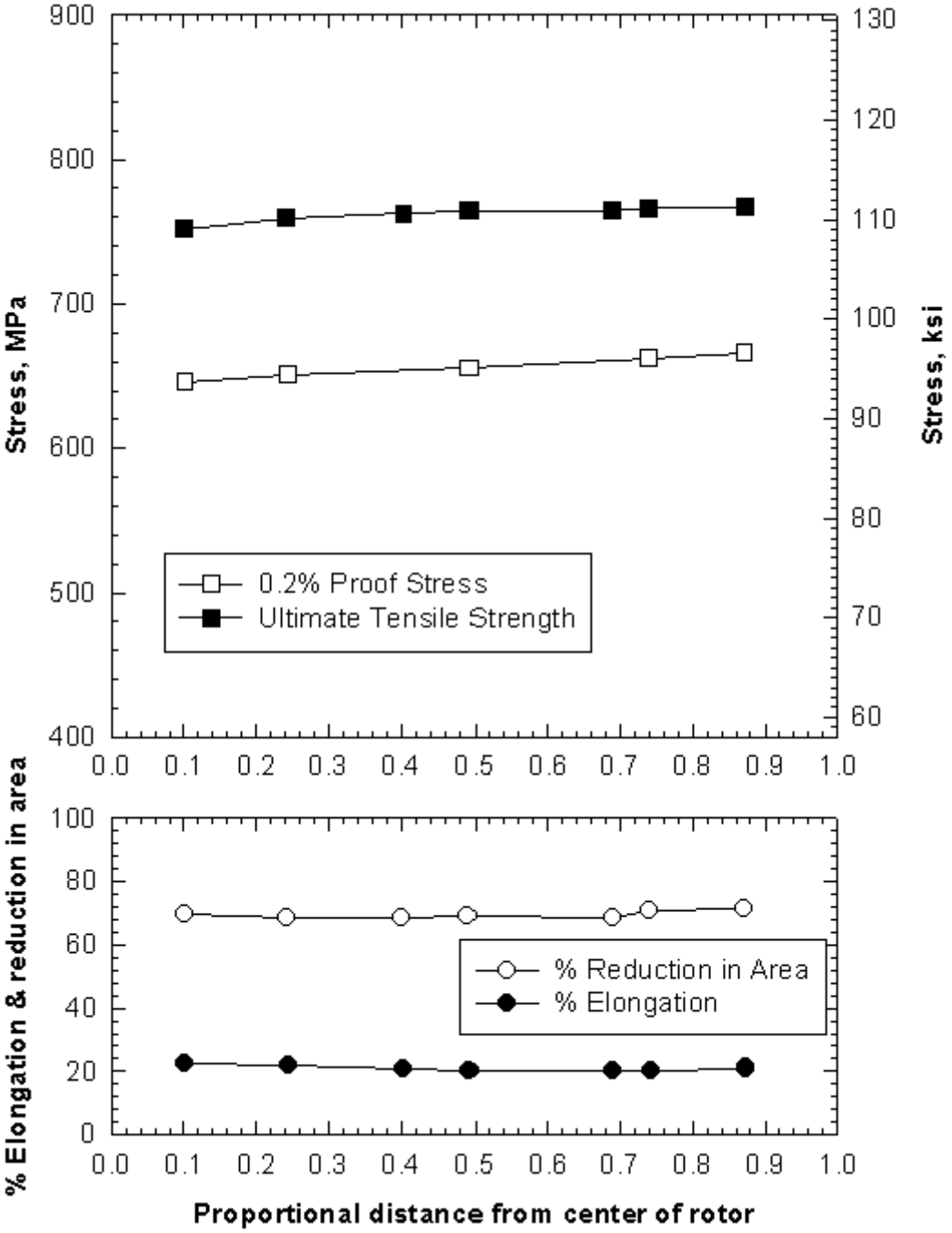

Figure 5-2
0.2% yield strength and ductility as a function of location for the trial rotor section heat treated to the higher yield strength level

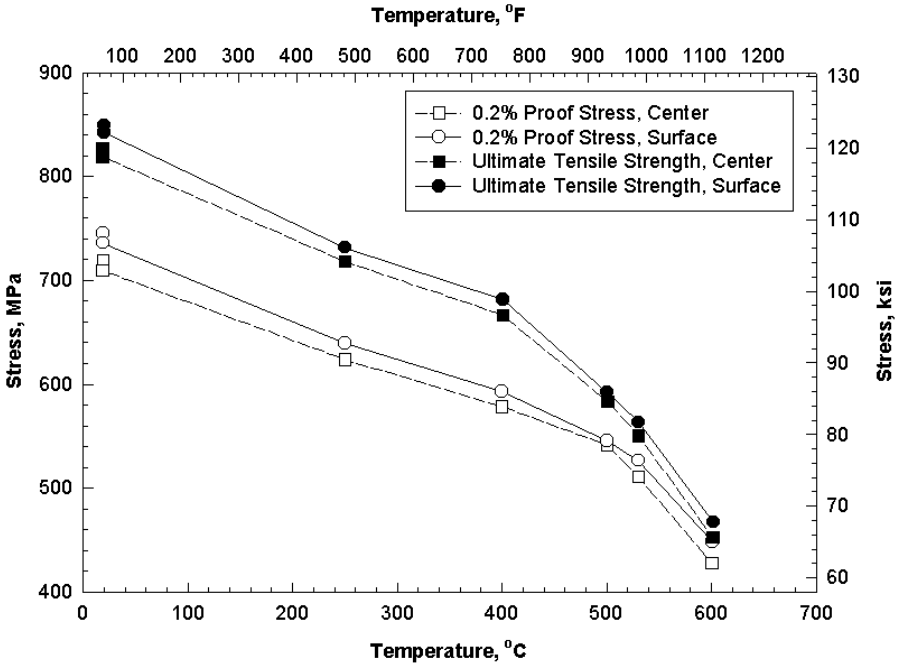

Figure 5-3
Elevated temperature tensile properties for the trial rotor section LP part heat treated to the higher yield strength level

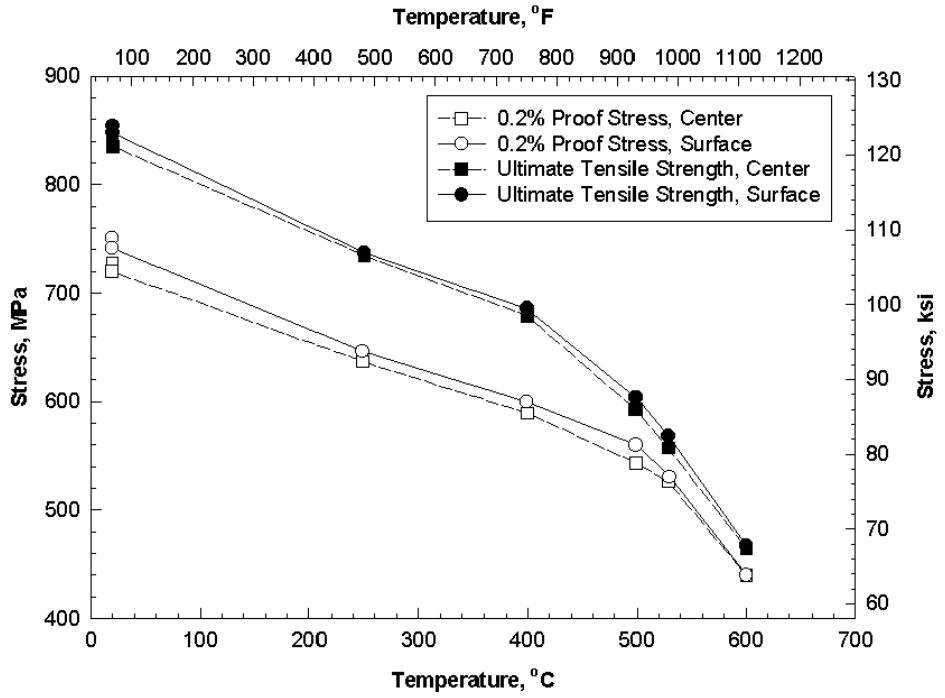

Figure 5-4
Elevated temperature tensile properties for the trial rotor section HP part heat treated to the higher yield strength level

Impact energy and FATT

The impact energy was also tested at rim and center positions and over the cross section of the rotor. The orientation of the specimen was tangential/radial and radial/tangential, see (Figure 5-5 to 5-8). The radial/tangential specimen orientation was additionally used for testing the impact energy at 20°C over the cross section of the rotor.

FATT

The notch impact transition temperature FATT was determined in the as-received condition in the rim and center portion of the rotor for both strength levels, see below (Table 5-4).

Table 5-4
Notch Impact Values for the trial EPRI-Europe rotor

0.2% yield>690 MPa	FATT °C	0.2% yield>620 MPa	FATT °C
HP part		**HP part**	
Rim	45	Rim	15
Center	51	Center	14
LP part		**LP part**	
rim	15	rim	0
center	53	center	18

An increase of the FATT over the cross section from rim to the center of the rotor can be clearly seen for the LP part of the rotor. In the HP segment the center and rim FATT's are comparable although the FATT in the higher yield strength condition is much higher as expected.

Impact energy

In the Table below (5-5) the impact energy at 20°C at different positions are summarized for both strength levels.

Table 5-5
Impact Energy Values at different positions of the Forging

Rotor location	x/R	Kv20°C J
High yield strength		
	HP part	
rim	0.9	39
center†	<0.29	41
	LP part	
rim	0.9	87
center	0.14	54
Low yield strength		
	HP part	
rim	0.9	154
center†	<0.29	70
	LP part	
rim	0.9	175
center	0.14	106

† average from various laboratories and test positions

The different toughness levels between these two strength levels can be clearly seen. Figures 5-5 and 5-6 show the impact energy results at room temperature over the cross section of the rotor for the higher yield strength condition of the LP-part and HP-part respectively. The impact energy levels of the LP-and HP-parts are similar in the higher yield strength condition at both surface and center.

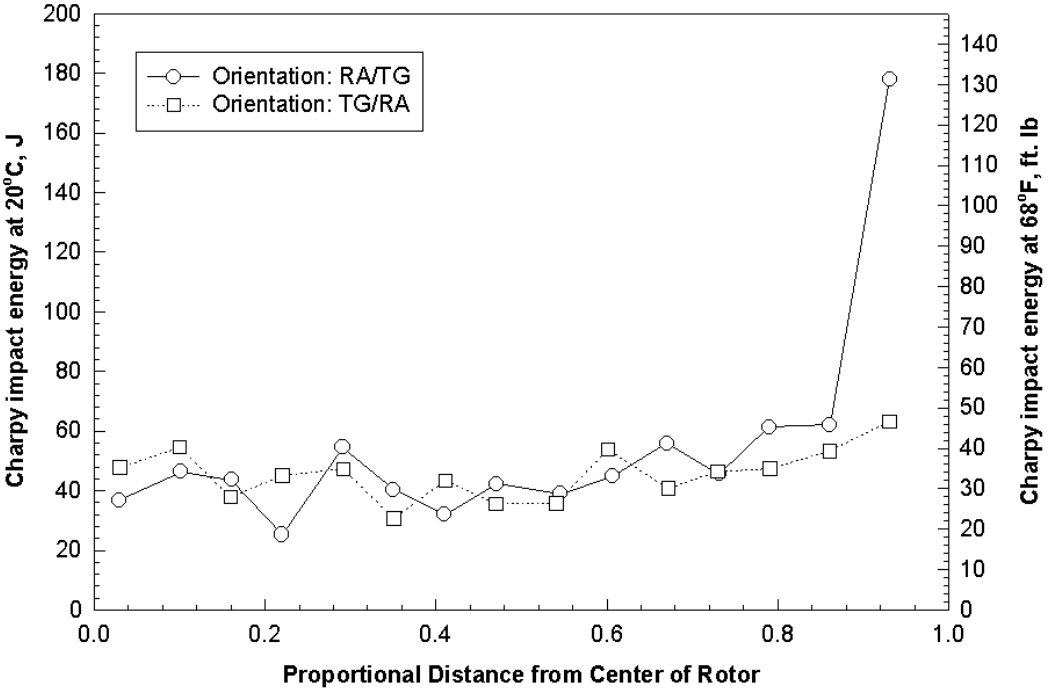

Figure 5-5
Impact energy values for high yield strength LP section of the trial rotor

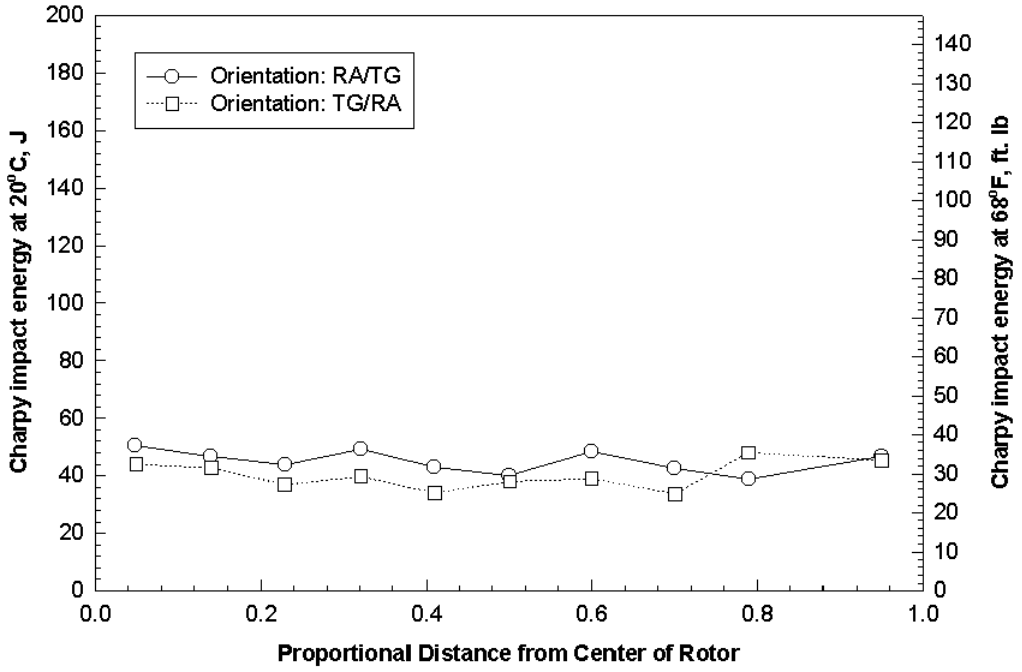

Figure 5-6
Impact energy values for high yield strength HP section of the trial rotor

For the lower yield strength condition the impact energy results over the cross section are shown for the LP-part and for the HP-part in Figure 5-7 and Figure 5-8 respectively. At a depth of about 250 mm - 300 mm from the surface the values approach those towards the core of the rotor. This corresponds to the results observed for the two COST 505 rotors, which had comparable strength levels to the EPRI-Europe rotor in the 0.2% yield >620 MPa strength condition, see (Figures 5-9 and 5-10). Impact energies are plotted as a function of temperature for the inner section of the LP-and HP-Part in the higher yield strength conditions (Figures 5-11) and in the lower yield strength condition in (Fig 5-12). As observed in earlier work [10], there is considerable scatter in the data at temperatures close to the FAT temperature. To evaluate the scatter, the relationship between impact energy and percentage ductile fracture is shown in figure 5-13 for all specimens and conditions. This figure indicates that some data points should be excluded from the determination of the FAT-temperature.

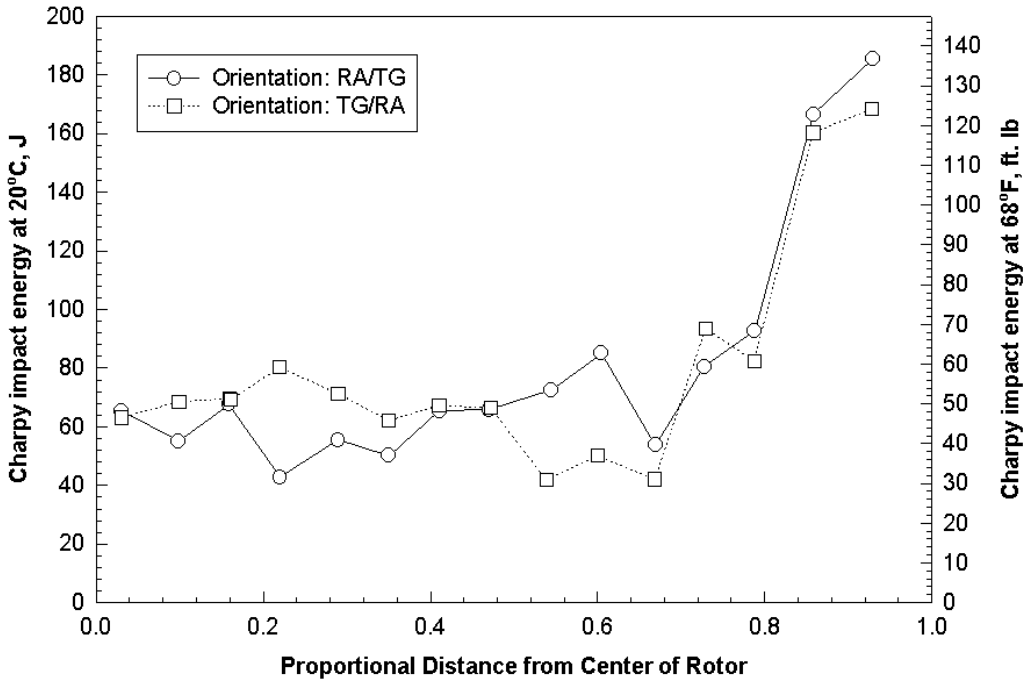

Figure 5-7
Charpy Impact values for the LP low yield strength section of the trial rotor

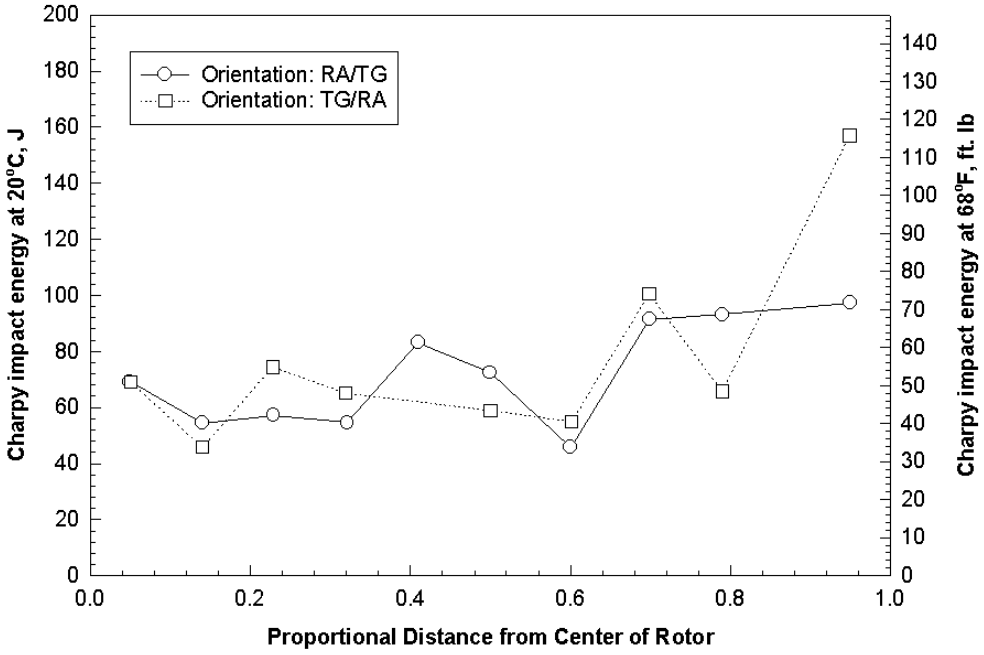

Figure 5-8
Charpy Impact values for the HP low yield strength section of the trial rotor

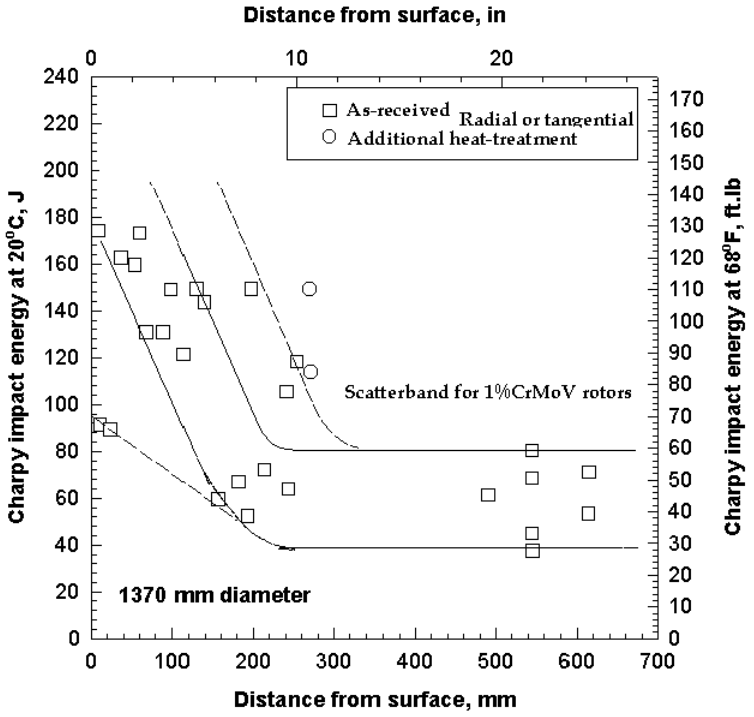

Figure 5-9
Room temperature impact energy values in the as-received and additional heat-treatment condition for the COST 505 ESR rotor

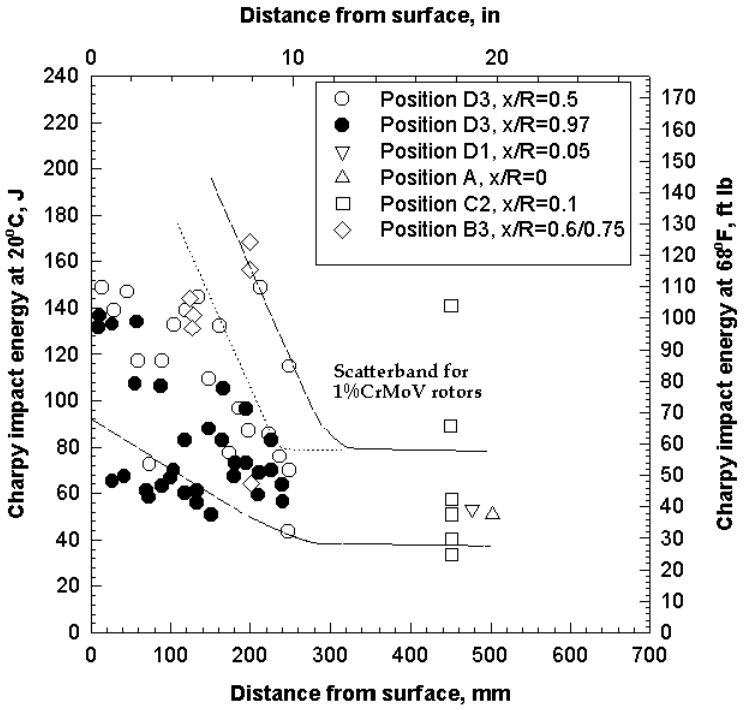

Figure 5-10
Room temperature impact energy in as-received and aged condition for the COST 505 VCD rotor

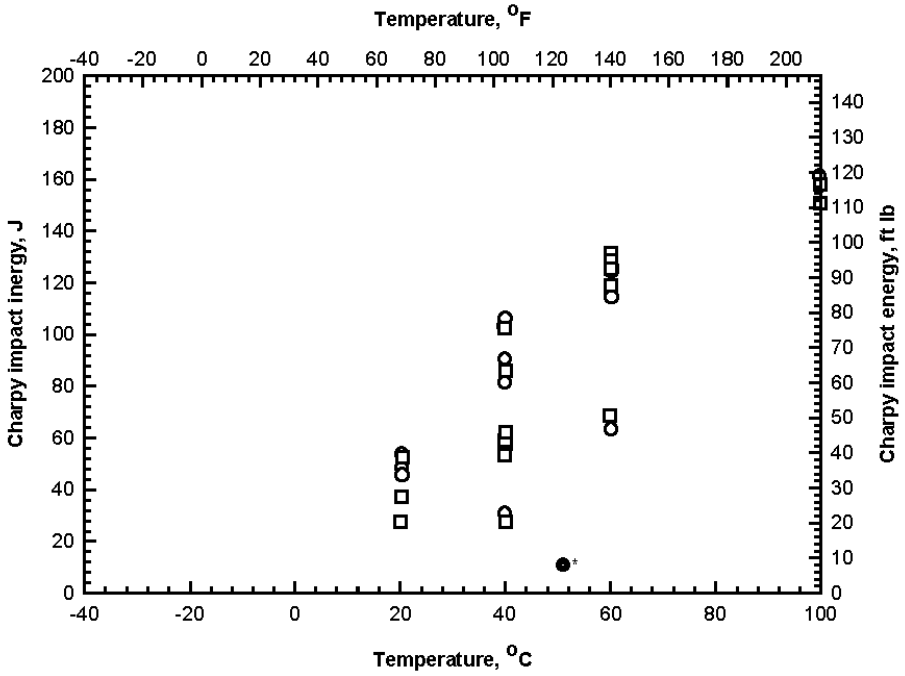

Figure 5-11
FATT curves for the high yield strength LP and HP parts of the EPRI-Europe trial rotor

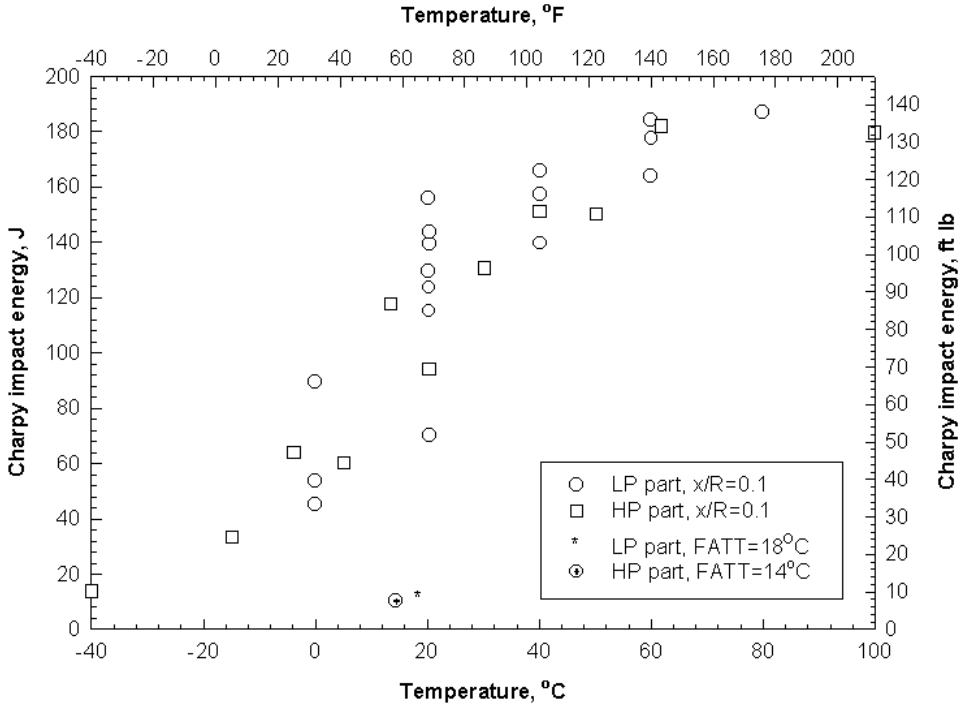

Figure 5-12
FATT curves for the low yield strength LP and HP parts of the EPRI-Europe trial rotor

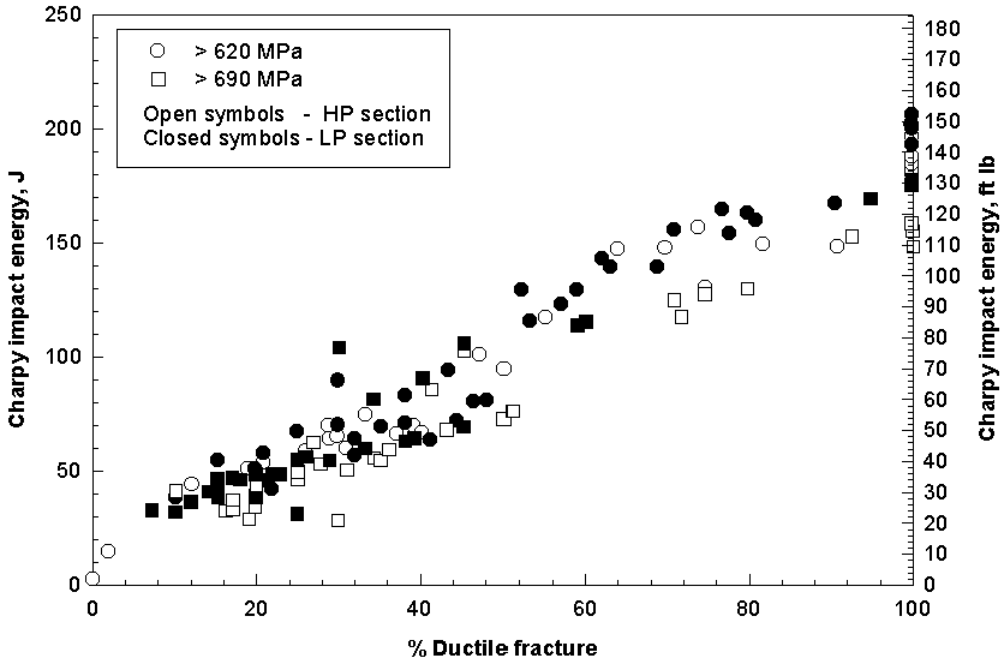

Figure 5-13
Ductile fracture in the EPRI-Europe trial rotor

A comparison of the basic mechanical properties of the EPRI-Europe rotor and the COST 505 rotors are summarized in Table 5-6.

Table 5-6
Comparison between EPRI-Europe and COST 505 rotors

Part	Position	Diameter, mm	0.2% yield, MPa	UTS, MPa	A, %	Z, %	Av, J	FATT, °C
COST 505-ESR	Center	1370	635	745	19	62	60	40
COST 505-VCD	Center	1000	625	740	17	64	42	25/40
Low strength EPRI-Europe HP section	Center	1200	723	835	19	67	41	14
Low strength EPRI-Europe LP section	Center	1750	716	822	18.3	68.8	54	18
High strength EPRI-Europe HP section	Center	1200	640	768	19.5	71.5	70	51
High strength EPRI-Europe LP section	Center	1750	653	774	20.4	71.7	106	53

Values are an average from the various laboratories and test positions

The most significant differences between the properties of the EPRI-Europe rotor and the COST 505 rotors are in relation to the toughness levels observed for the low yield strength (0.2% yield>620MPa) condition. The LP-part of the EPRI-Europe rotor with a diameter of 1750 mm exhibits excellent toughness levels compared with the results of the COST 505 rotors with a lower diameter but comparable yield strength. For the higher yield strength condition of the EPRI-Europe rotor (0.2% yield >690 MPa) it was possible to attain the toughness level of the COST 505 rotors with an increased diameter and a higher yield strength. The values shown are for the as received condition, which demonstrates good toughness properties for this type of steel, even for the high yield strength condition up to a diameter of 1750 mm.

Fracture Toughness

Fracture toughness testing using CT-specimens was carried out on the inner section of the LP- and HP-part of the rotor for both strength level conditions. Additional fracture toughness tests were also carried out on the rim section of the LP- and HP-part for the higher yield strength condition. Valid fracture toughness values according to ASTM E 399 and ASTM E 813 could not be achieved in every case and other recognized toughness parameters were sometimes used. The relationship between fracture toughness and temperature is shown for all tests carried out in Figure 5-14. Fracture toughness results are shown for the higher yield strength condition in Fig 5-15 whilst Fig. 5-16 shows toughness observed for the lower yield strength condition.

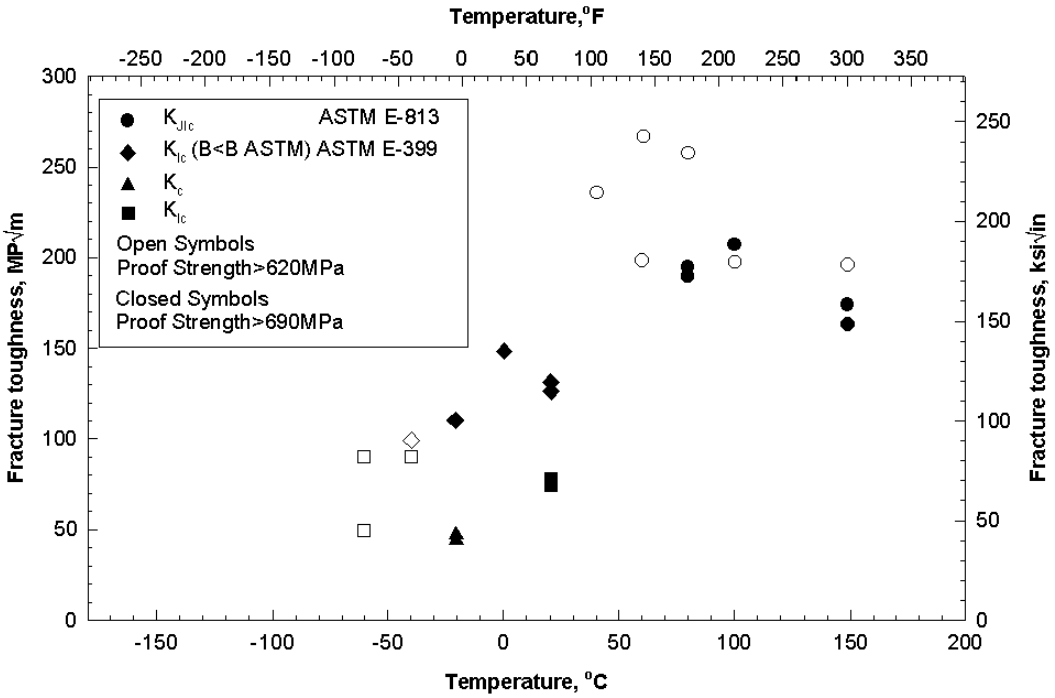

Figure 5-14
Fracture toughness for all sections of the EPRI-Europe trial rotor

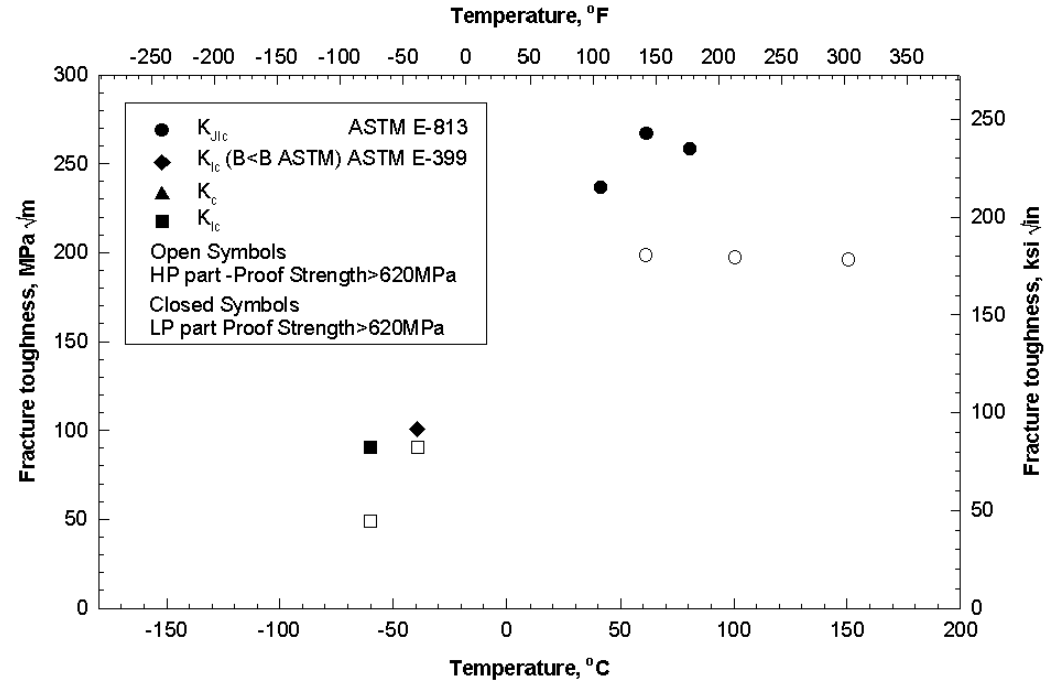

Figure 5-15
Fracture toughness for the high yield strength section of the EPRI-Europe trial rotor

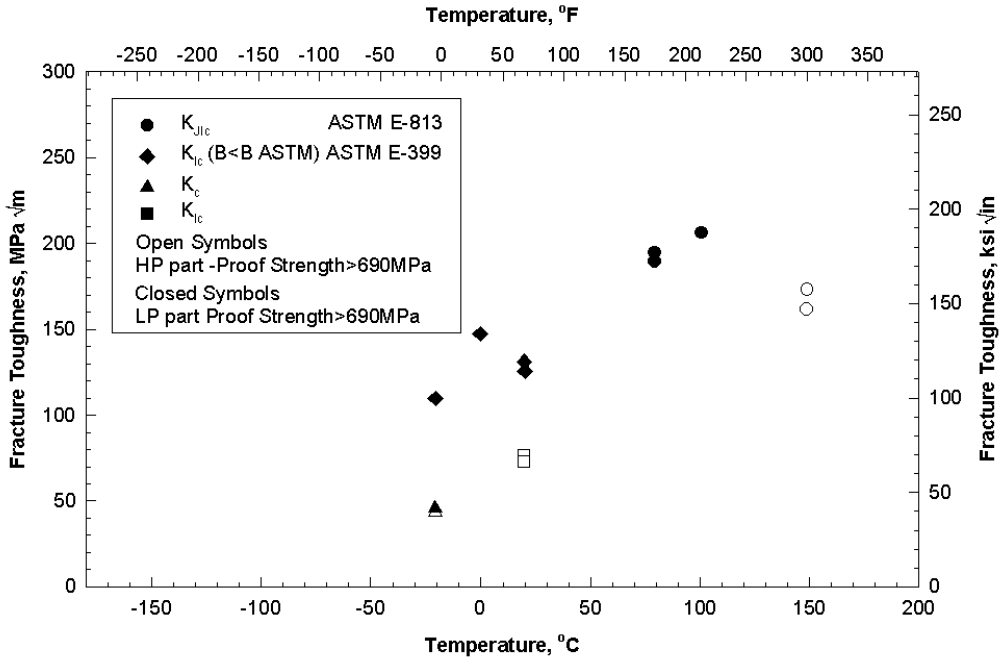

Figure 5-16
Fracture toughness for the low yield strength section of the EPRI-Europe trial rotor

The fracture toughness results for the two strength level conditions can be summarized as follows:

(i) High Yield Strength Condition.

Valid K_{IC} values according to ASTM E-399 were determined at -20°C and +20°C for the HP segments. However valid K_{IC} values could not be determined at 0°C and 20°C for the LP segment. A difference in toughness behavior was observed between the HP and LP segments when tested according to ASTM E813. Thus, valid fracture toughness values were only possible for the LP segment at test temperatures of 80°C or above since below this temperature insufficient slow stable crack growth could be achieved. For the HP segment, valid toughness values were only possible at test temperatures of 150°C and above for the same reasons. Toughness values in the rim and core sections were comparable which is in accordance with the Charpy impact test results at 20°C over the cross section of the radial cores.

(ii) Low Yield Strength Condition.

Valid K_{IC} values according to ASTM E399 could only be achieved at temperatures of -40°C and below for both the LP and HP segments. Valid K_{JIC} values according to ASTM E 813 could only be determined on the LP segment at temperatures of 40°C and above. For the HP segment two tests were carried out at 60°C , only one of which

exhibited sufficient stable crack growth to allow a valid K_{JIC} to be determined. The notable feature of the toughness results is the differences observed between the different yield strength conditions. The improved toughness of the low yield strength condition over the high yield strength condition is also reflected in the Charpy Impact test results. Fig 5-17 shows a comparison of the toughness values of the EPRI-Europe Rotor with those of the earlier COST 505 Rotor work and for ASTM A470 - Class 8 steel, and clearly shows that the COST 505 data lay within the scatter band of the EPRI-Europe rotor. Only the high yield strength condition (0.2% yield>690MPa) of the HP segment of the EPRI-Europe rotor exhibited lower toughness levels than those of the COST 505 and American rotors which is presumably a consequence of the yield strength differences between the materials.

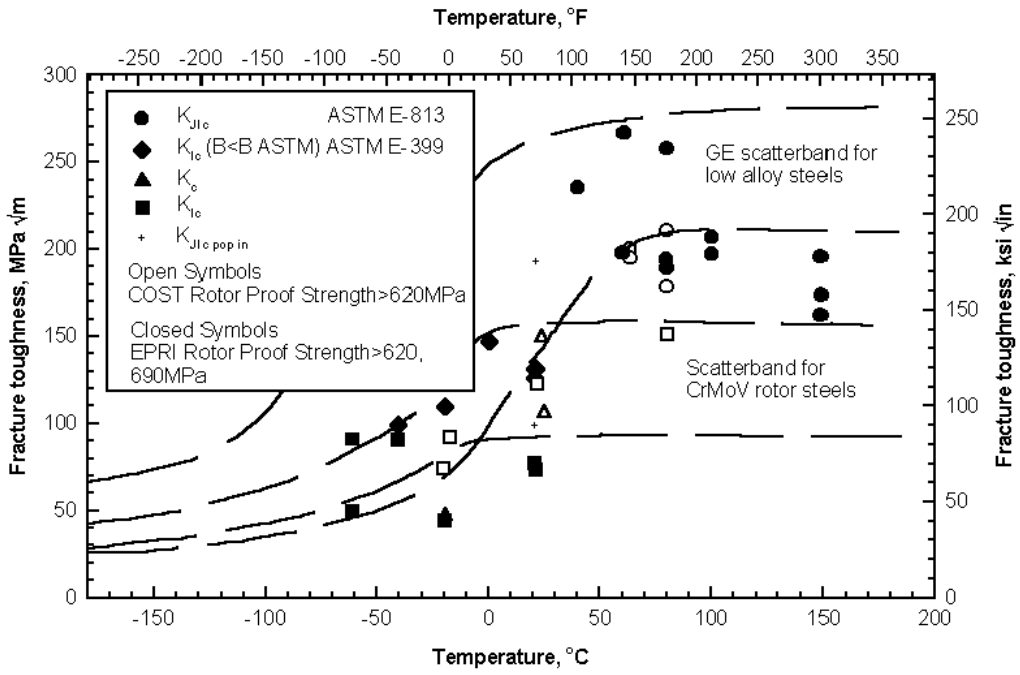

Figure 5-17
Fracture toughness of EPRI-Europe and COST 505 rotors

Fatigue Crack Growth

To determine fatigue crack growth rates, CT-specimen were taken from the inner portion of the rotor and tested at 20°C and 530°C. The fatigue crack growth results are summarized in Figs. 5-18 and 5-19 and show only small scatter. No difference between HP- and LP-part results can be seen. This corresponds to the fact that the strength level of both parts of the rotor is similar. For both temperatures the results fit quite well with the upper limit of the results for 1%CrMoV rotor steels.

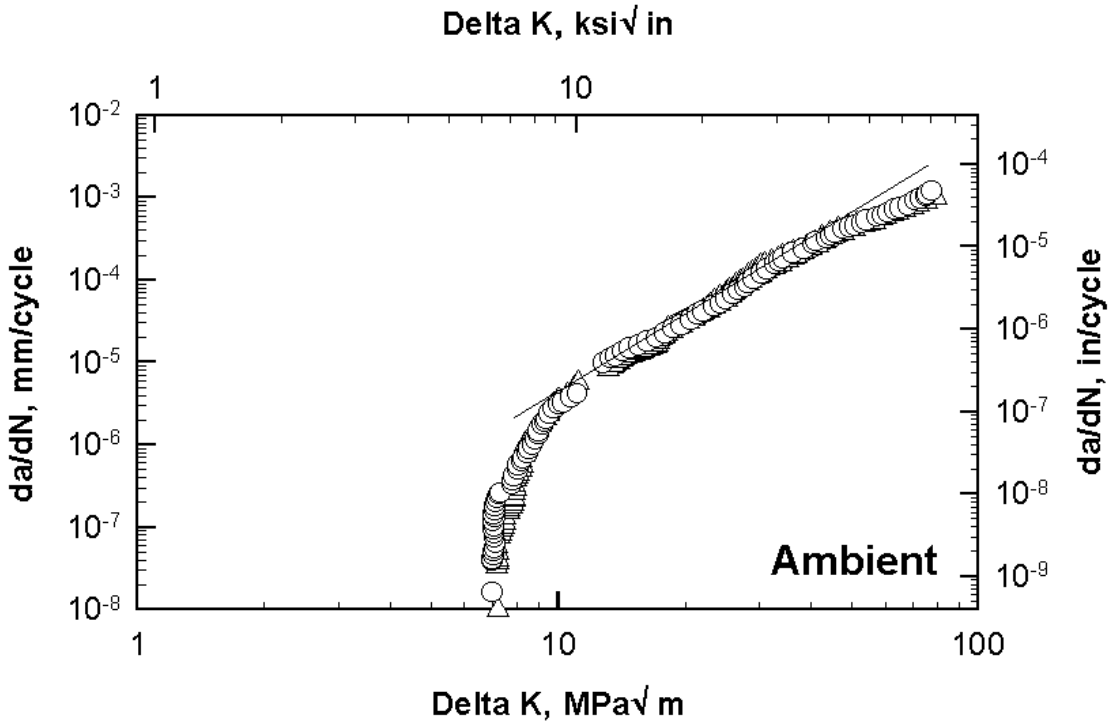

Figure 5-18
Fatigue crack growth rate for the high yield strength section of the EPRI-Europe trial rotor at room temperature

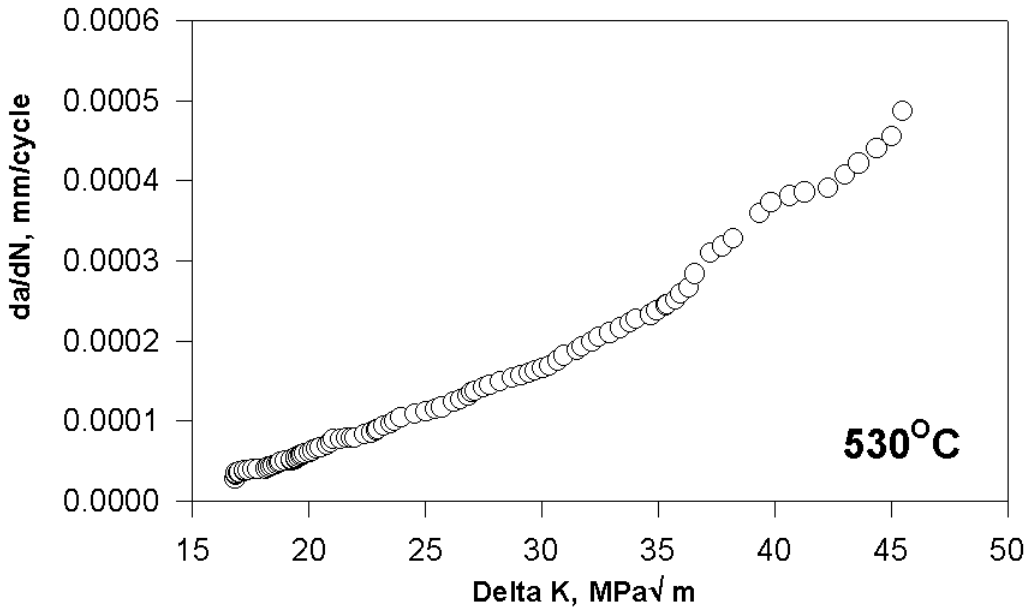

Figure 5-19
Fatigue crack growth rate for the high yield strength section of the EPRI-Europe trial rotor at 530°C

Exposure tests

Investigations were also carried out to determine the effect of aging exposures at 425°C, 480°C and 540°C for 5 000 and 10 000 h on the variations in notch impact toughness and in the tensile properties at room temperature. Further specimens will be checked after 20 000 exposure. The specimens used for the exposure tests originated from the inner zone (x / r = 0.05 - 0.075) of the 395 mm diameter radial cores extracted from the HP and LP sections of the pilot shaft (Positions: HP 1.4.1, LP 1.4.1, HP 2.4.1 and LP 2.4.1), and for both the high yield strength condition (0.2% yield>690MPa, HP1 and LP1) and the low yield strength condition (0.2% yield> 620 MPa, HP2 and LP2). The specimen positions in the drilled core for test conditions HP1, LPI, HP2 and LP2 are documented in appendix 3. Two tensile test specimens were tested for each test condition. The notch impact transition temperature, FATT, was determined in the initial condition by means of 18 ISO notch-impact bending specimens with a selection of specimens from several specimen levels (A - E, see appendix 3) in order to obtain an overview of the influence of specimen position on the test results. After exposure the notch impact toughness versus test temperature was again determined with 12 ISO-V notch impact bending specimens.

Electrically heated laboratory furnaces with air circulation to reduce temperature scatter in the furnace chamber were used for specimen exposure. Several thermocouples per furnace, fastened to the specimens., were used to record the temperature of the specimens. The maximum temperature deviation in the furnace chamber was ± 3°C.

The mechanical properties determined for the initial material condition are shown in the following table (5-7) along with tests carried out by Saarschmiede directly after heat treatment.

The results obtained by Saarschmiede and the turbine manufacturers are in close agreement. The lowest 0. 2% Proof Stress for the lower tempered condition (HP1 / LP1) is 715 MPa whereas in the higher tempered condition (HP2 / LP2) it is 648 MPa. Accordingly the transition temperatures of the notch impact toughness $FATT_{50}$ reach a maximum of +53°C and +26°C respectively.

Table 5-7
Initial mechanical properties for the EPRI-Europe rotor

Condition	Company	0.2% yield, MPa	UTS, MPa	A, %	Z, %	FATT50, °C
HP1	Forgemaster	722	833	17.6	65	+40
HP1	Turbinemaker	727	845	17.6	68	+51
LP1	Forgemaster	715	820	15.8	66	+48
LP1	Turbinemaker	717	834	18.2	66	+53
HP2	Forgemaster	663	771	18.0	69	+26
HP2	Turbinemaker	648	770	22.0	73	+14
LP2	Forgemaster	648	768	18.0	69	+15
LP2	Turbinemaker	649	772	18.7	70	+18

The results determined after exposure for 5 000 and 10 000 h at 425°C , 480°C and 540°C are summarized in Figures 5-20 to 5-31.

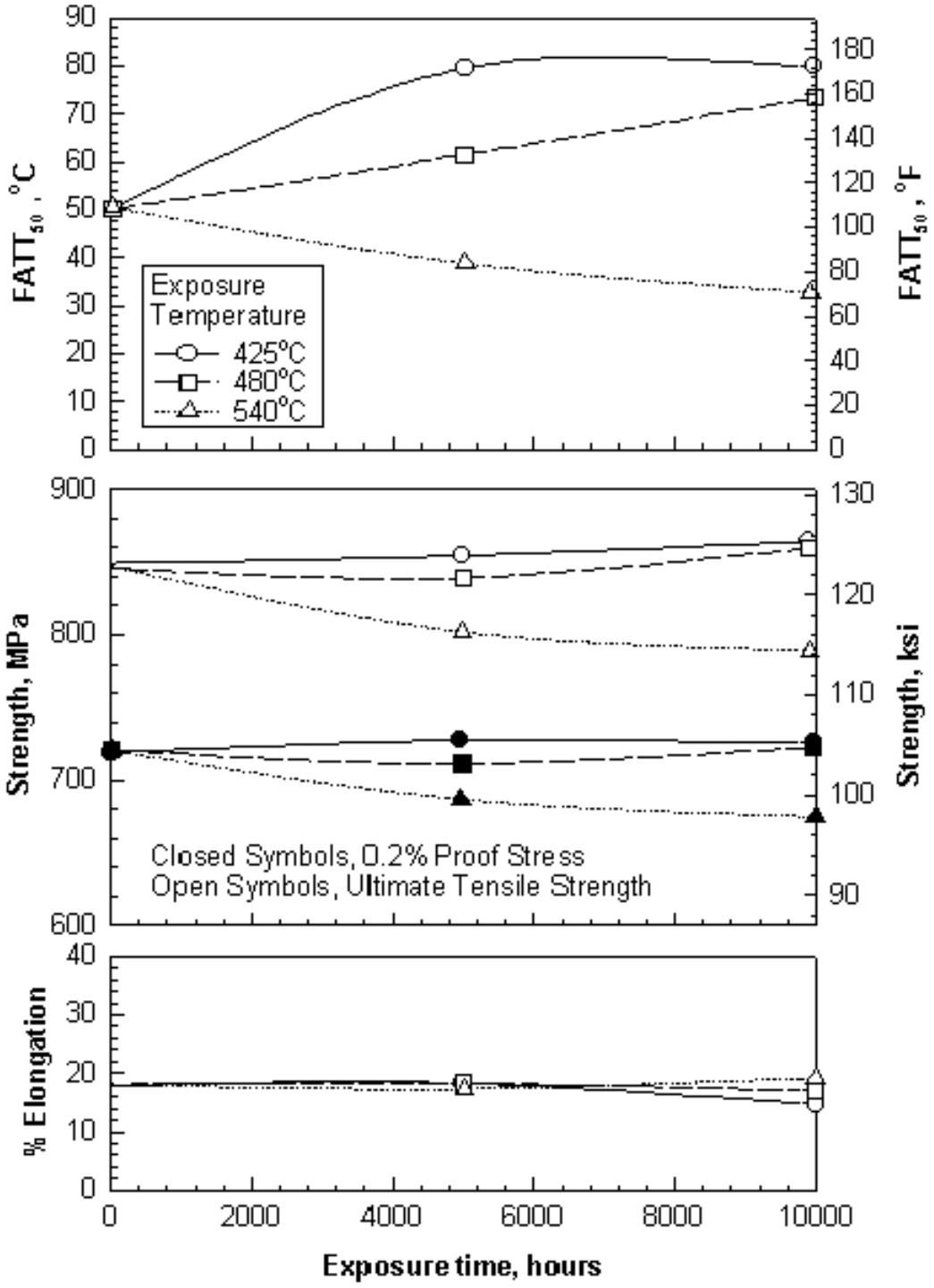

Figure 5-20
Variation of FATT and tensile properties with time of exposure due to temper embrittlement for the high strength section of HP portion of the trial rotor

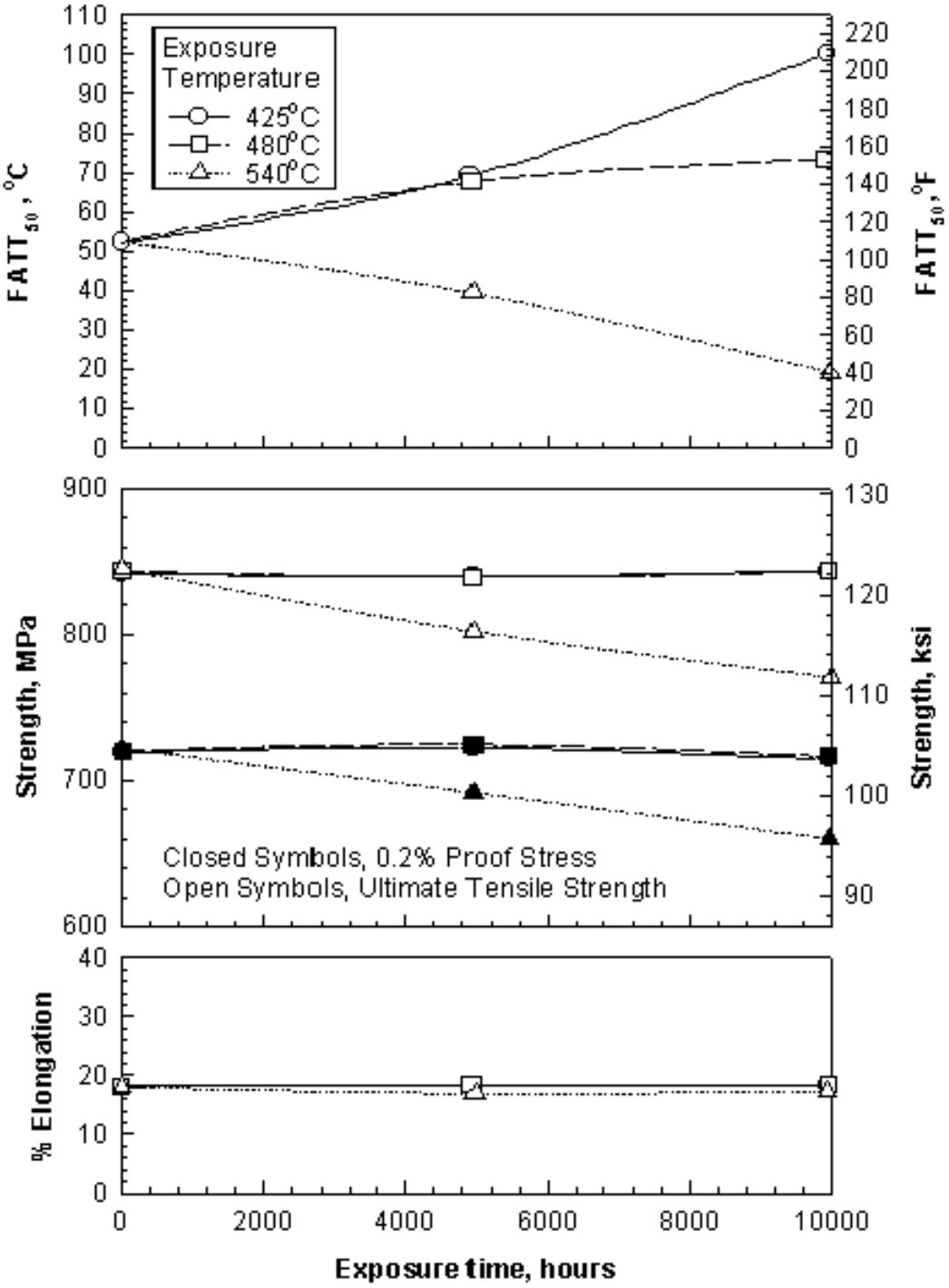

Figure 5-21
Variation of FATT and tensile properties with time of exposure due to temper embrittlement for the high strength section of LP portion of the trial rotor

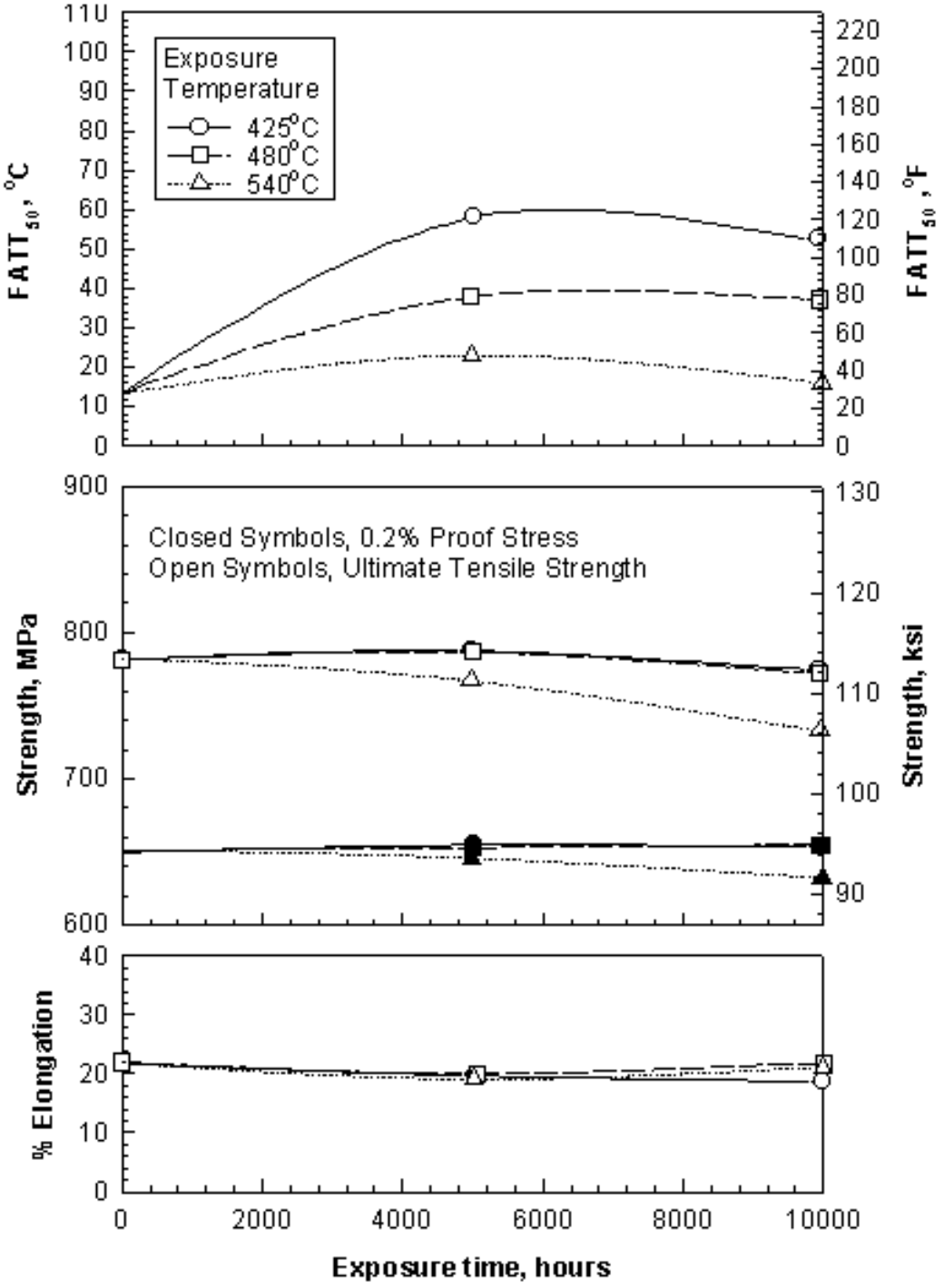

Figure 5-22
Variation of FATT and tensile properties with time of exposure due to temper embrittlement for the low strength section of HP portion of the trial rotor

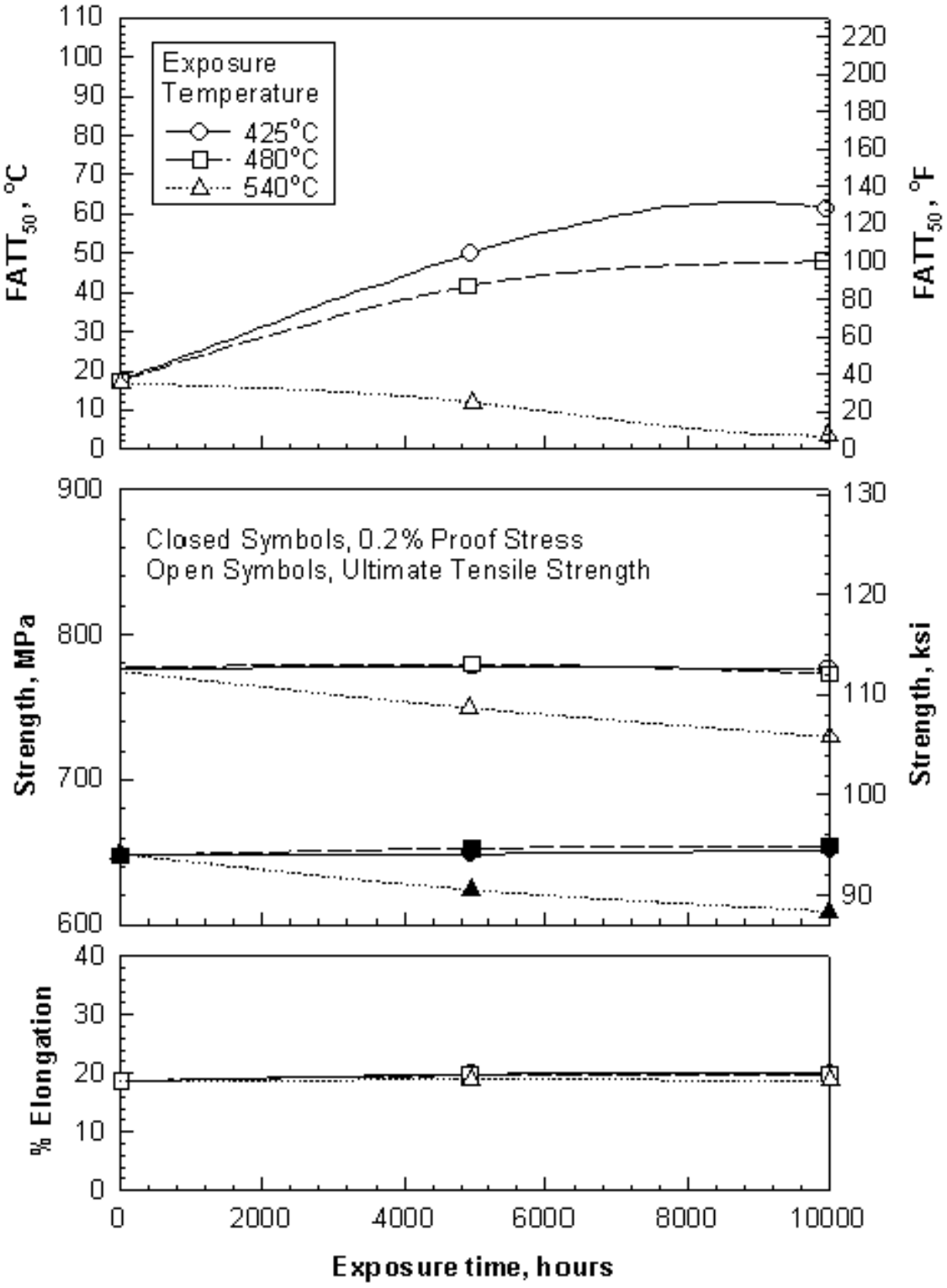

Figure 5-23
Variation of FATT and tensile properties with time of exposure due to temper embrittlement for the low strength section of LP portion of the trial rotor

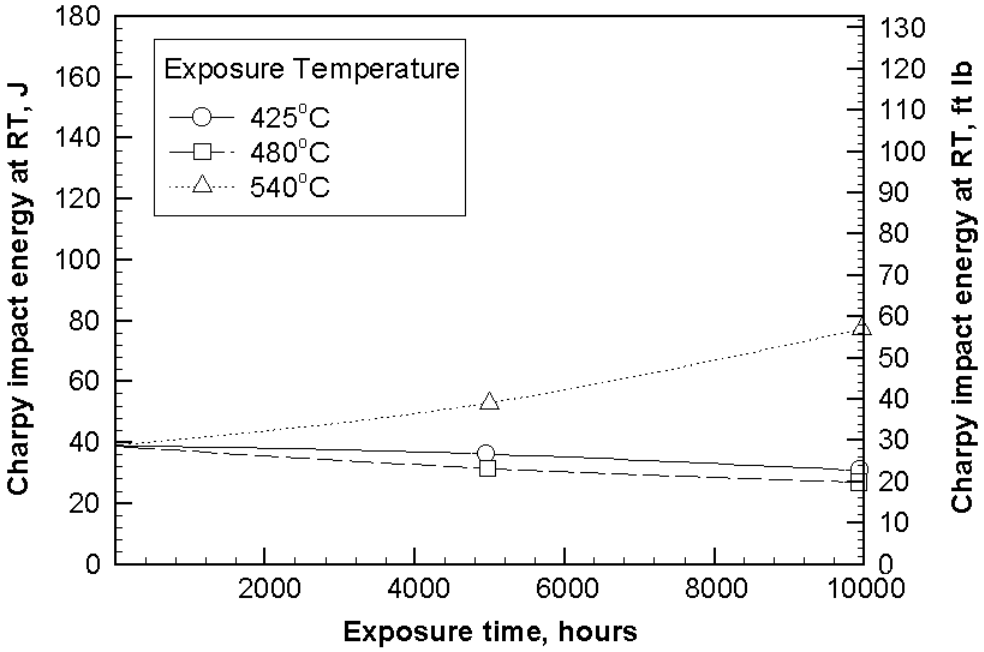

Figure 5-24
Variation of impact properties with time of exposure due to temper embrittlement for the high strength section of the LP portion of the trial rotor

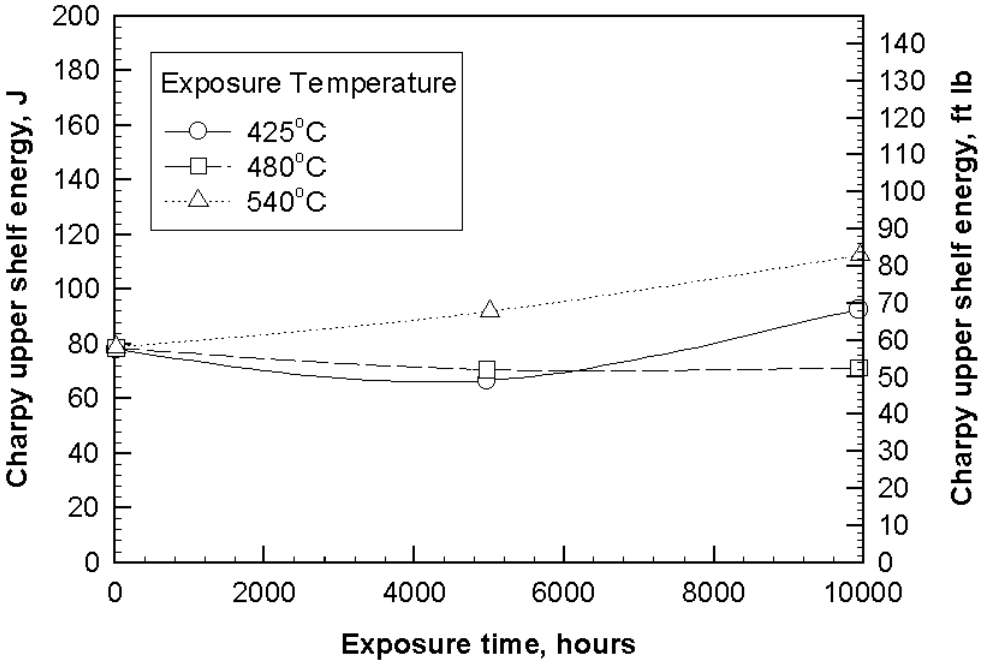

Figure 5-25
Variation of upper shelf properties with time of exposure due to temper embrittlement for the high strength section of the LP portion of the trial rotor

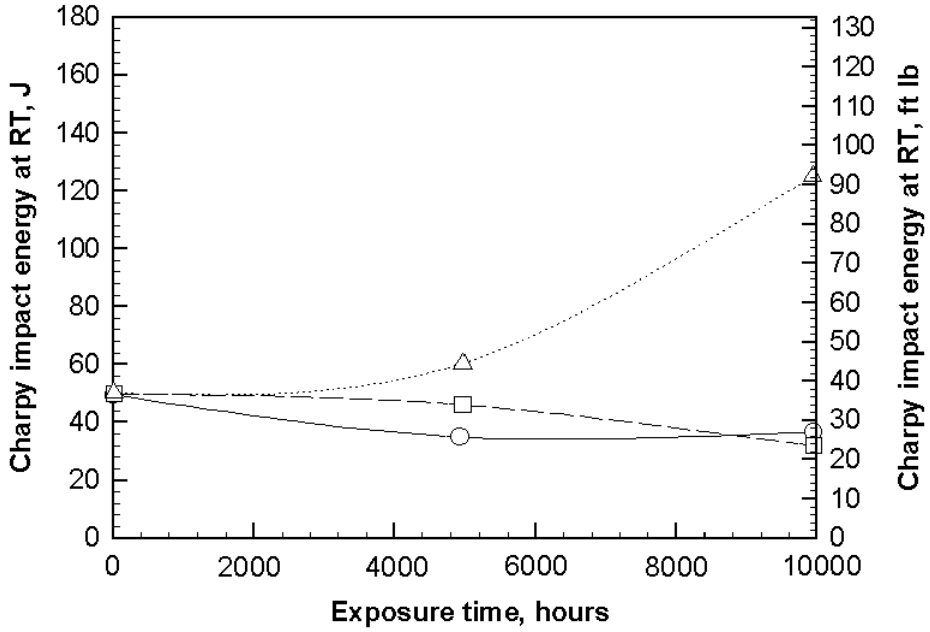

Figure 5-26
Variation of impact properties with time of exposure due to temper embrittlement for the high strength section of HP portion of the trial rotor

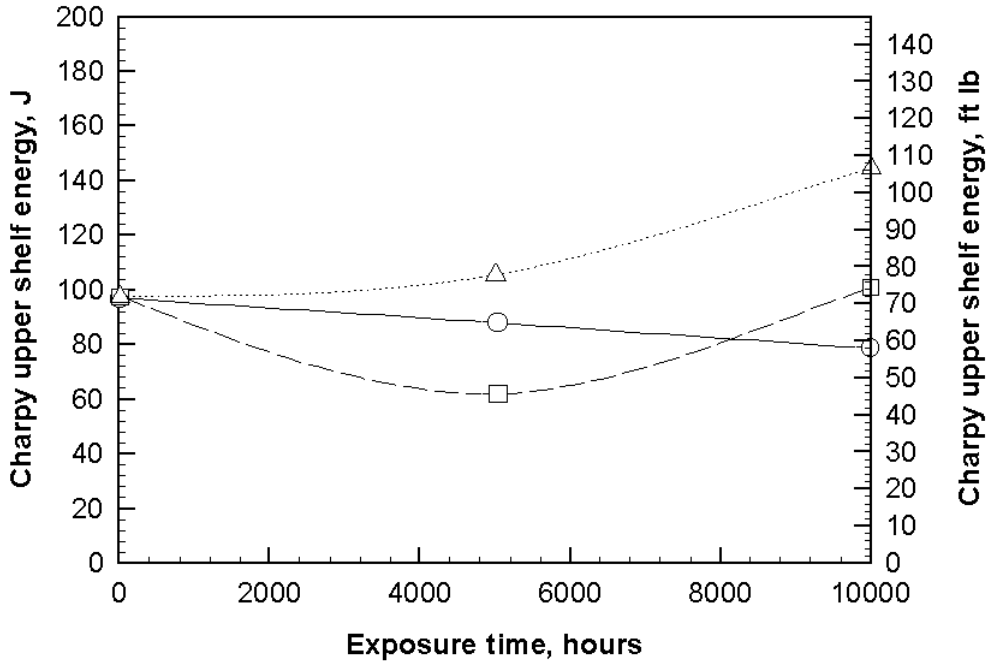

Figure 5-27
Variation of upper shelf properties with time of exposure due to temper embrittlement for the high strength section of HP portion of the trial rotor

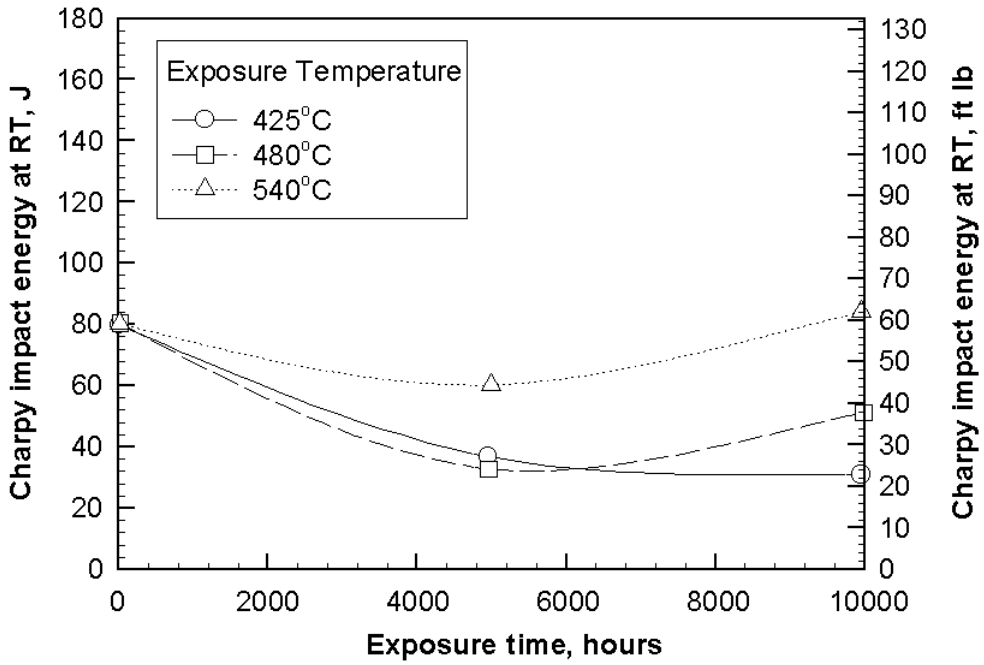

Figure 5-28
Variation of impact energy properties with time of exposure due to temper embrittlement for the low strength section of the HP portion of the trial rotor

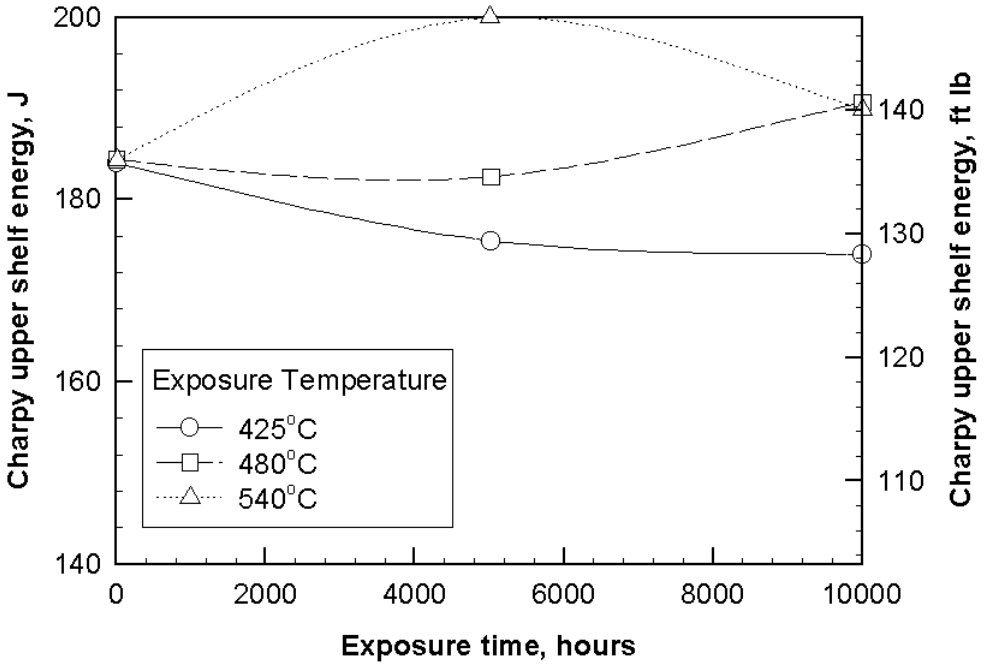

Figure 5-29
Variation of upper shelf properties with time of exposure due to temper embrittlement for the low strength section of the HP portion of the trial rotor

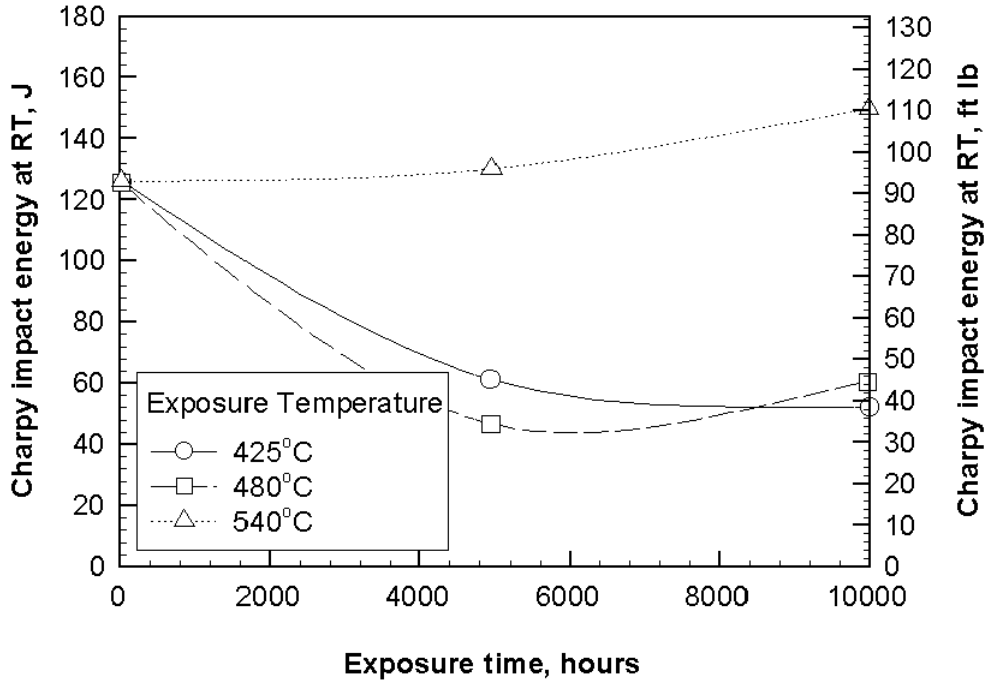

Figure 5-30
Variation of impact energy properties with time of exposure due to temper embrittlement for the low strength section of the LP portion of the trial rotor

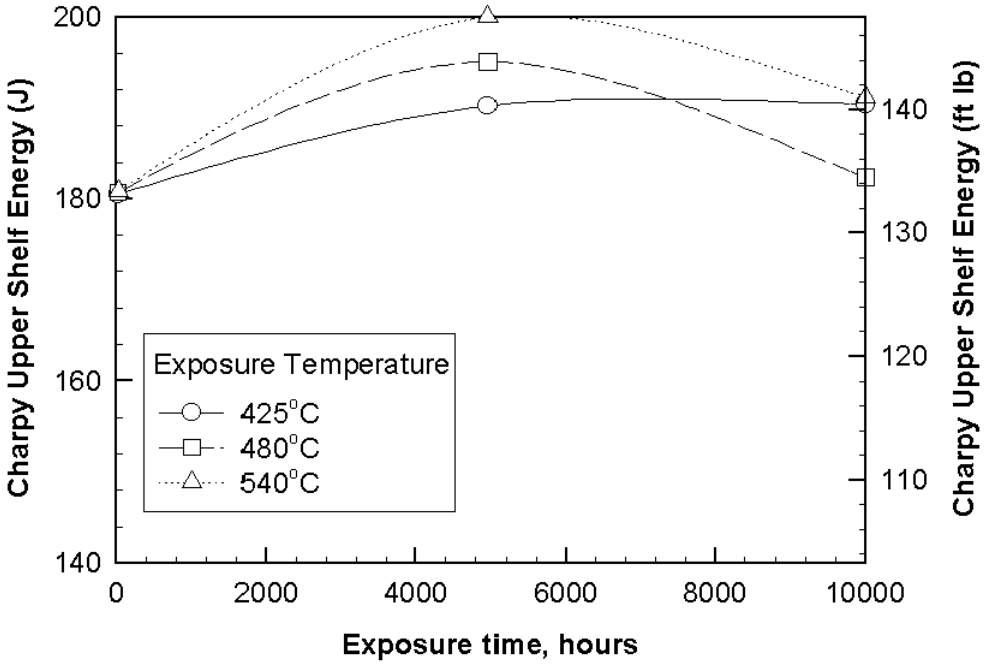

Figure 5-31
Variation of upper shelf properties with time of exposure due to temper embrittlement for the low strength section of the LP portion of the trial rotor

Long-term exposure at the aforementioned temperatures was found to result in the following main changes:

- 425°C exposure led to the most severe embrittlement
- Exposure at 540°C leads to softening and a reduced embrittlement
- A maximum FATT of 100°C was reached after 10 000 hours at 425°C in the LP portion of the trial rotor

Corresponding with a reduction in the 0.2% Proof Strength, exposure at 540°C resulted in an improvement in toughness indicated by a maximum reduction of 30°C in the $FATT_{50}$. The following $FATT_{50}$ values were recorded after 10 000 h exposure:

The change in $FATT_{50}$ ($\Delta FATT_{50}$), which is very similar to published results for the 1%CrMoV rotor steel [22], is plotted in Figure 5-32 as a function of the exposure temperature. The graph also shows the results which were determined in the COST 505 program on specimens from two rotors [10]. The smaller of the two rotors was a VCD melt and the larger rotor - same as the EPRI-Europe rotor - was an ESR melt For all three rotors the exposure at 480°C resulted in very similar changes in the FATT50. At 425°C the smaller VCD rotor of the COST 505 program was about 20°C better. However, the test results of the COST 505 VCD rotor also show that at 350°C it is still possible for slight embrittlement - even if on a much smaller scale - to occur. In consideration of the larger changes determined for the specimens of the EPRI-Europe rotor after exposure at 425°C a further investigation after exposure at 350°C would be meaningful.

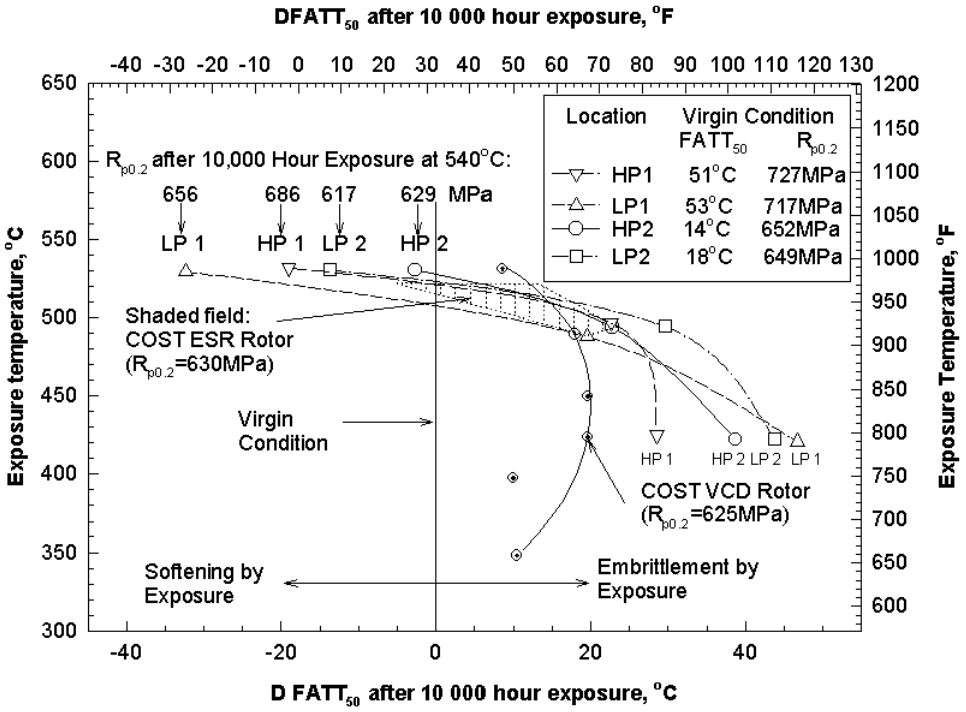

Figure 5-32
Change in FATT after 10 000 exposure for the COST 505 and EPRI-Europe rotors

For three positions of the EPRI-Europe rotor toughness improvements are exhibited following exposure at 540°C which is more evident than in the COST 505 rotors. This is presumably attributable to the lower tempering temperature and to the different grain structure since, in the first instance, the higher 0.2%Proof strength condition (LP1 and HP1) exhibits the largest changes and, secondly, the HP positions (HPI and HP2) exhibit a lower reduction than the coarser cooled LP positions. To facilitate a discussion of the influence of the chemical composition on the recorded changes in toughness the chemical compositions of the rotors are compared in the Table below:

Table 5-8
Comparison of chemical composition between EPRI-Europe and COST 505 steels

Element	Melt	HP Location[1]	LP Location[2]	ESR	VCD
C	0.22	0.23	0.22	0.22	0.23
Si	0.06	0.05	0.05	0.10	0.075
Mn	0.70	0.69	0.70	0.66	0.68
P	0.005	0.006	0.005	0.010	0.006
S	0.001	0.001	0.001	0.003	0.004
Cr	2.13	2.10	2.10	2.1	2.08
Mo	0.86	0.85	0.85	0.84	0.83
Ni	0.76	0.73	0.73	0.75	0.74
W	0.65	0.68	0.69	0.67	0.65
V	0.32	0.32	0.32	0.32	0.30
Al	0.008	0.007	0.008	< 0.008	0.009
Cu	0.06	0.06	0.06	0.06	0.09
As	0.007	0.006	0.006	0.015	0.01)1)
Sb	0.0007	0.0008	0.0009	0.014	0.005
Sn	0.005	0.005	0.004	0.010	0.007

[1] Center location [2] Melt analysis

The comparison shows that the chemical compositions - with the exception of the trace elements - of the EPRI- Europe and the COST 505 rotors are very similar. During the COST 505 investigation, Auger analysis of failed specimens revealed that the increase in $FATT_{50}$ is associated with an increase in intercrystalline cracking of the notch impact specimens with the exposure period due to increased enrichment of phosphorus at the grain boundaries [10], see Figure 5-33, i.e. a similar type of embrittlement to that found in the 3½%NiCrMoV steels in the investigated temperature range, [23]. Figure 5-34 shows the variations of ΔFATT of the 425 and 480°C tests of the EPRI- Europe rotor and those of the two COST 505 rotors as a function of the phosphorus content. The scatter in the results is relatively large, presumably as a result of the different and superimposed influencing variables, such as rotor size, microstructure, grain size, initial strength and melting method. Bearing in mind the relatively high phosphorus content (0.010%) of the COST 505 ESR rotor the increase in D FATT50 observed for this

rotor following a 480°C exposure is relatively low, being roughly of the same order of magnitude as that established for the two other rotors which only exhibited phosphorus contents of 0.005 - 0.006%. Regrettably, no results are available from the 425°C exposure tests on the COST 505 ESR rotor.

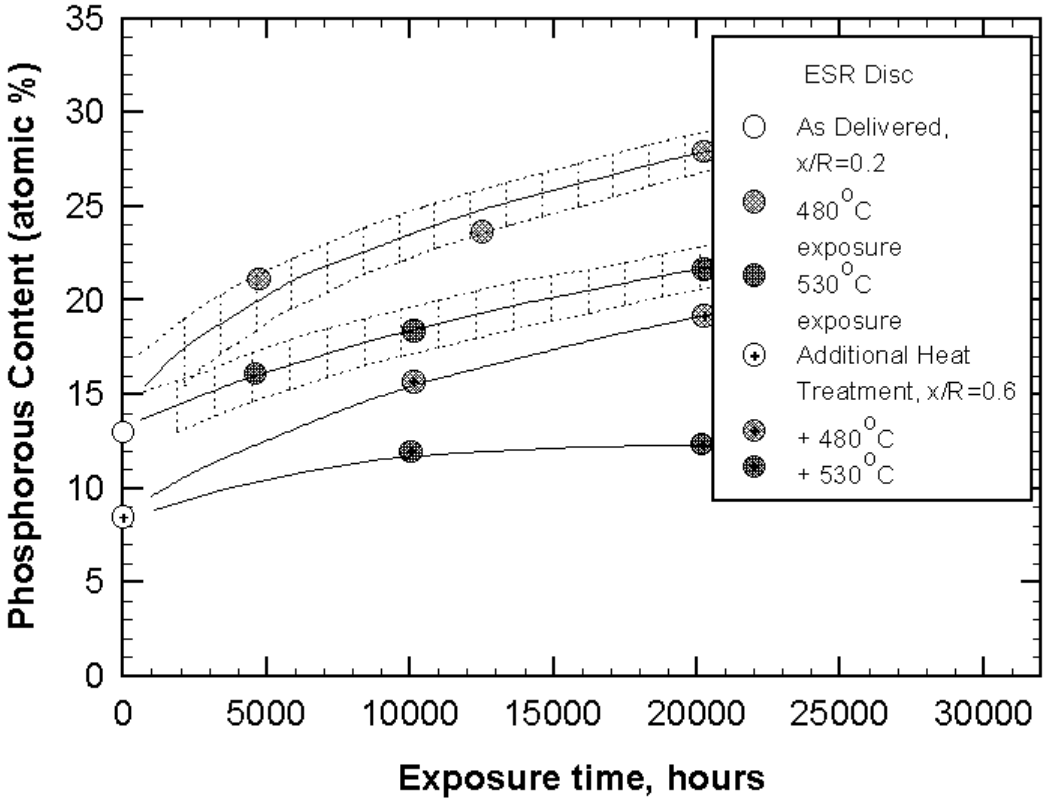

Figure 5-33
Grain boundary concentration of phosphorus as a function of exposure time in the COST 505 VCD rotor

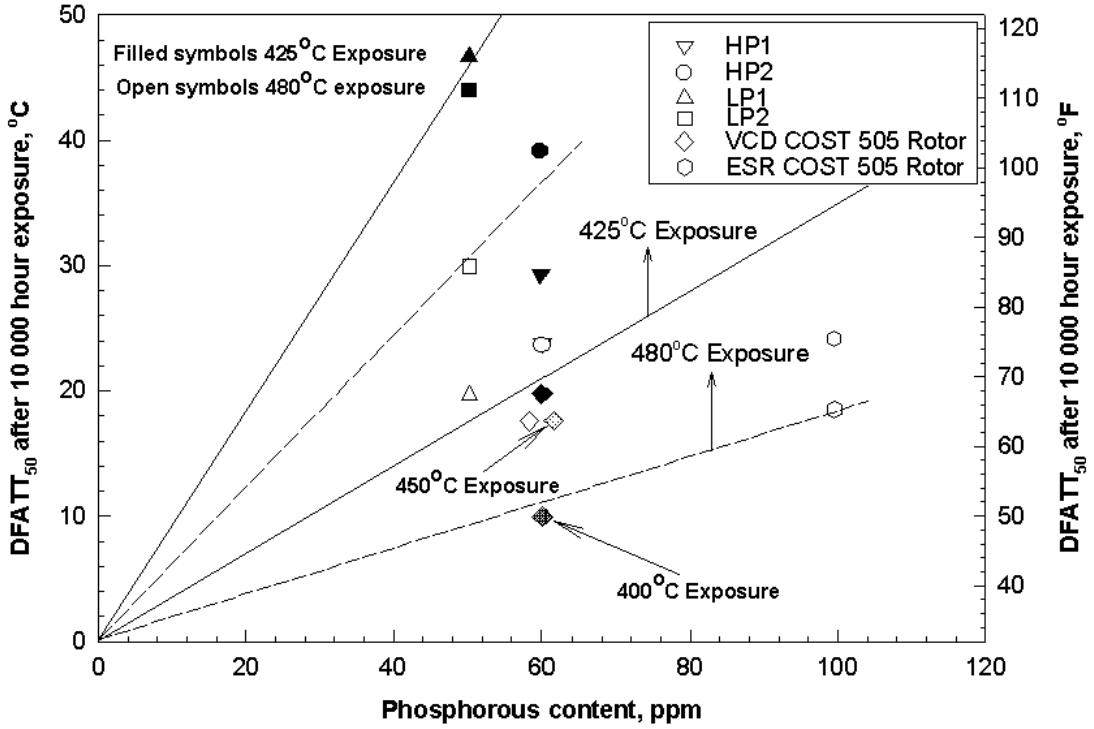

Figure 5-34
Change in FATT of the EPRI-Europe rotor with respect to phosphorus content after 10 000 hours exposure at various temperatures compared to the COST 505 rotors

The linear relationship between the $\Delta FATT_{50}$ and the phosphorus content suggested by figure 5-35 is presumably nonexistent. For example, for 3½%NiCrMoV steels, the results in Figure 5-35, indicate that a substantial rise in $\Delta FATT_{50}$ was only observed between 10 and 30 ppm phosphorus and was also dependent on the manganese content.

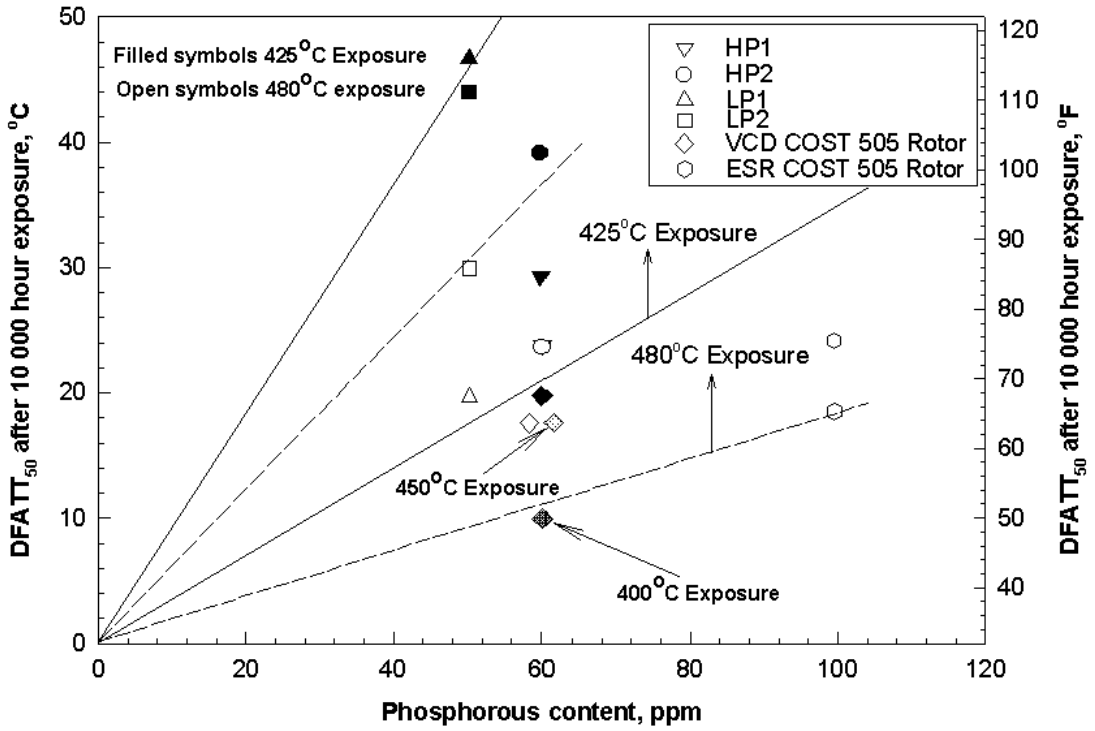

Figure 5-35
Change in FATT with respect to Phosphorus for 3.5%NiCrMoV steels

In general terms, the results show that further work would be required in order to determine the influence of the phosphorus content of the 2% CrMoNiVW steel on the long-term embrittlement behavior. In view of the experience already gained with the 3½%NiCrMoV steel it would also be logical to investigate the long-term embrittlement behavior of this steel after "superclean melting", based on an approach with very low phosphorus contents of around 20 - 30 ppm. Lowering the Mn content to levels below 0.08% will presumably result in the disadvantage of inadequate through hardening of larger rotor cross sections.

Conclusions

1. 425°C leads to the maximum embrittlement.

2. higher yield strengths led to greater embrittlement.

3. The high strength and 425°C combination led to a FATT of 100°C.

4. At 540°C, the embrittlement decreases due to softening.

5. At 480°C exposure, the ΔFATT for the EPRI-Europe rotor and COST 505 rotors are comparable. AT 425°C the EPRI-Europe rotor ΔFATT is 25°C more than the COST 505 VCD rotor.

6. The reason for the above is not clear, and cannot be explained by phosphorus embrittlement alone.

Low Strain Fatigue Properties

Low strain high cycle fatigue data were produced under continuous cycling at ambient temperature and 350°C on 1750 mm diameter rim material and at 530°C on 1250 mm diameter rim material in both the low (620 - 650 MPa) and high (690 - 720 MPa) yield strength conditions. In addition, data with 0.5 hour tensile dwells at 540°C on 1250 mm diameter rim materials in both the low (620 - 650 MPa) and high (690 - 720 MPa) yield strength conditions were also generated.

All testing was carried out in push-pull strain control and using fully reversed load cycling. Two test laboratories were employed for these tasks: RR IRD carried out their tests at a constant cyclic frequency of 0.0083 Hz which results in strain rates typically between 0.5 and 1.0% / min. ABB carried out their tests at a constant strain rate of 6% / min. Details of the test specimens used are given in figures 5-36 and 5-37.

The ABB and RR IRD specimen details are shown below.

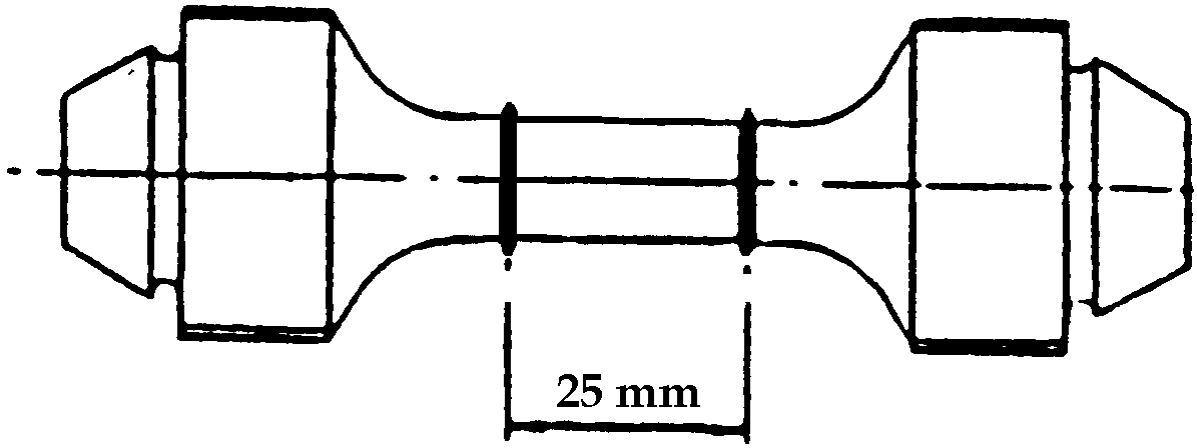

Figure 5-36
RR IRD high temperature high strain fatigue specimen details

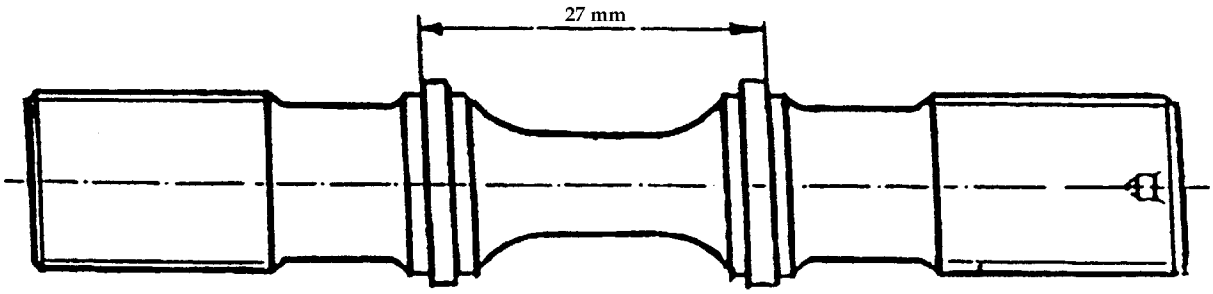

Figure 5-37
ABB high temperature high strain fatigue specimen details

The complete data are available in tabular form in Appendix D, and are plotted in Figure 5-38 to 5-41 as total strain range versus cycles to crack initiation.

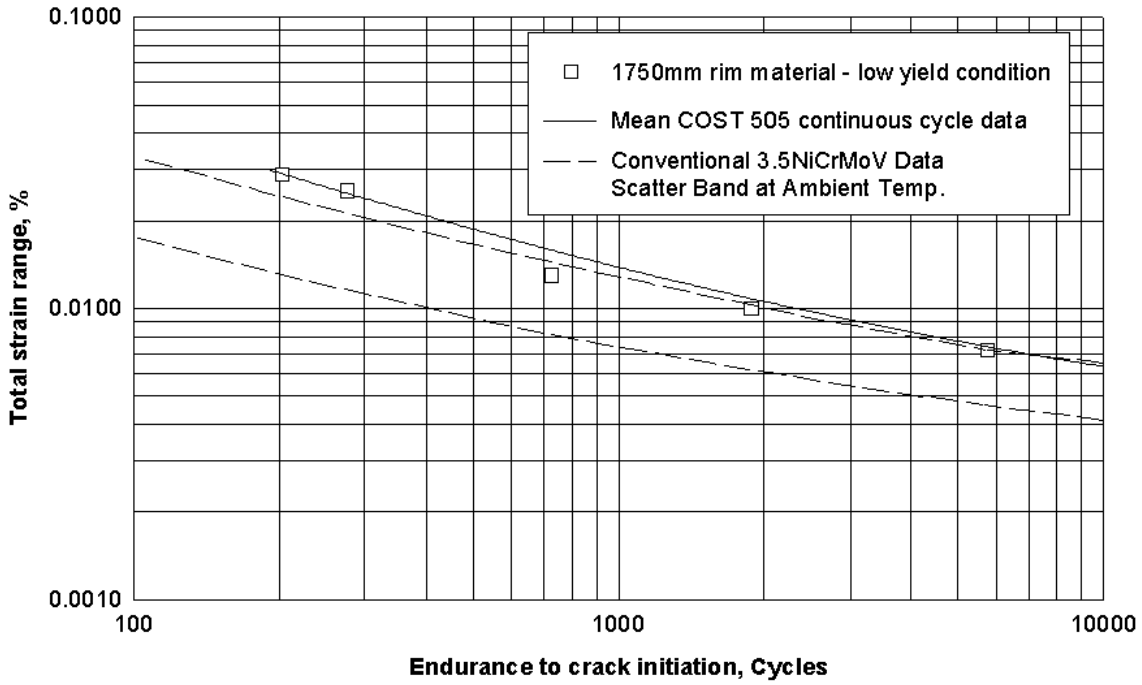

Figure 5-38
High strain fatigue resistance of the LP section of the EPRI-Europe rotor at room temperature in the low yield strength condition

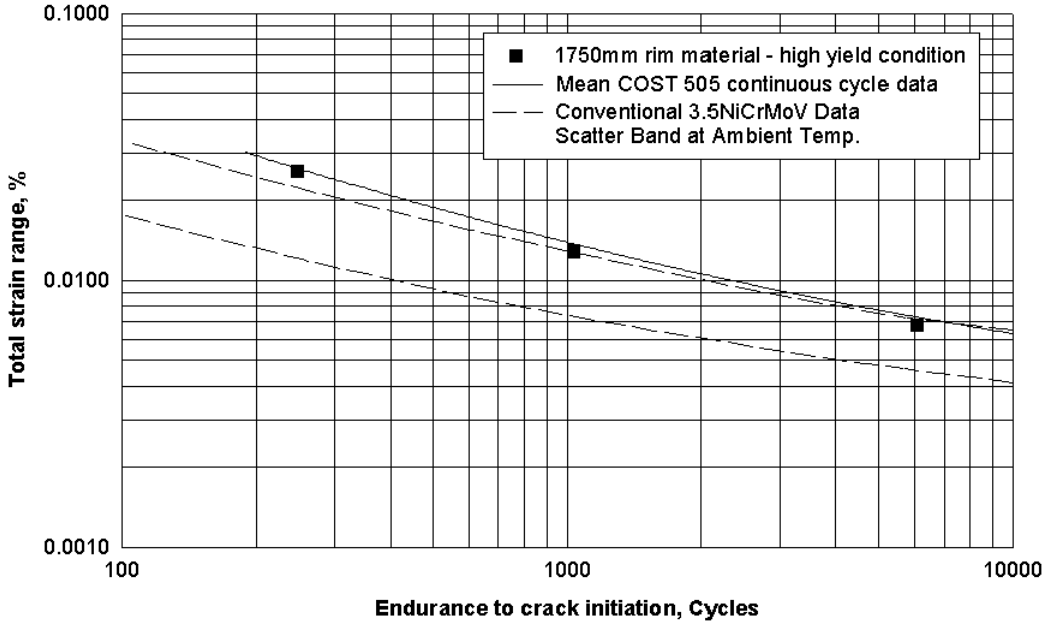

Figure 5-39
High strain fatigue resistance of the LP section of the EPRI-Europe rotor at room temperature in the high yield strength condition

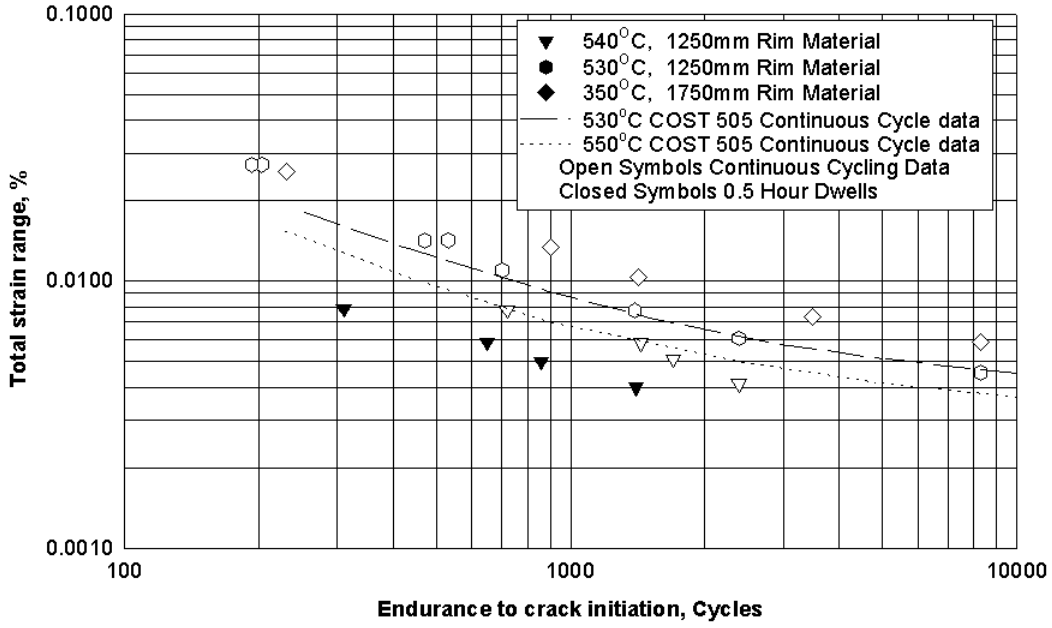

Figure 5-40
High strain fatigue resistance of the EPRI-Europe rotor HP and LP sections at elevated temperature

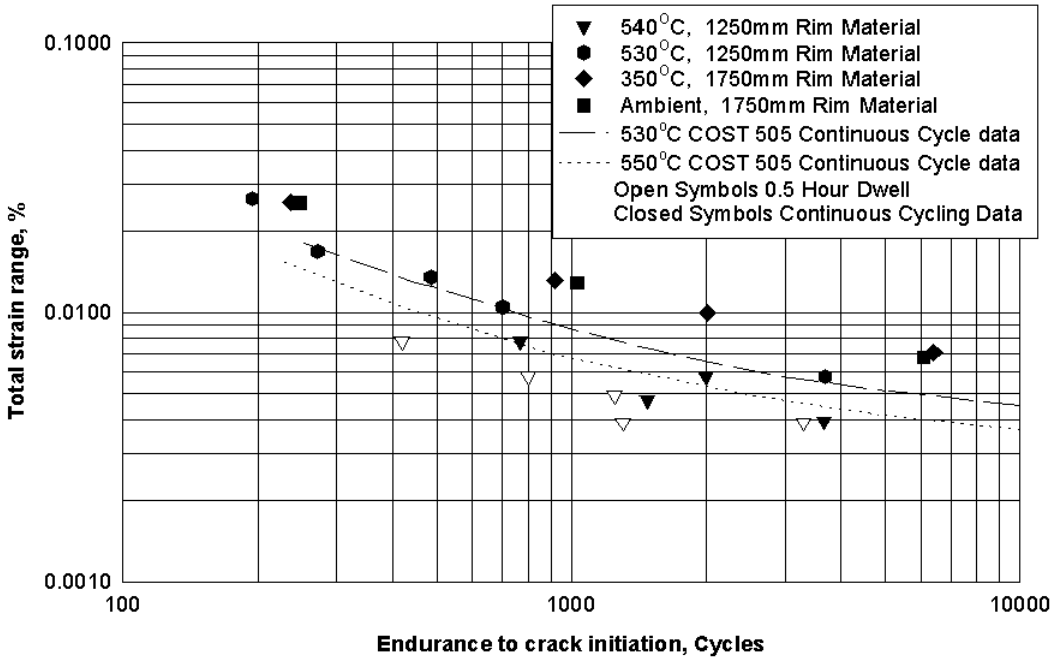

Figure 5-41
High strain fatigue resistance of the EPRI-Europe rotor HP and LP sections at elevated temperature

It seems clear from the these figures that the low cycle fatigue properties of 2%CrMoNiWV at 350°C are similar to those at ambient temperature. However at temperatures above 350°C there is a degradation in the low cycle fatigue properties. The difference in fatigue response between the 530°C and 540°C data can probably be explained by a combination of the small difference in test temperature, differences in testing strain rates between the two laboratories or more probably by the difference in specimen type employed between the two test laboratories. The 540°C specimens were invariably observed to fail from the radius of one of the extensometer ridges. It is believed that the local stress concentrating feature of the extensometer ridge may have contributed to the shorter lives of these tests. However, as Figures 5-40 and 5-41 indicate the 540°C data in the current work is similar to that determined at 550°C in the COST 505 test program for this material and the 530°C data in the current test program was very similar to the data determined at 530°C in the COST 505 program.

Notwithstanding the possible effect of specimen geometry the data incorporating 0.5 hour dwells at the maximum tensile stress indicate that this material appears to show a creep-fatigue interaction at 540°C which is manifest in a reduction in fatigue life of about 50% in comparison with the continuous cycling data at the same test temperature. There seems to be no distinguishable difference in fatigue response between the materials in the high or low yield strength conditions although the cyclic stress strain response between the two heat treatment conditions was different (see below). Figures 5-40 and 5-41 also shows ambient low cycle fatigue data for

3½%NiCrMoV rotor steel The LCF properties of the EPRI-Europe rotor steel at ambient temperature appears to lie just above the upper scatter band limit for 3½%NiCrMoV.

Figure 5-42 shows the cyclic stress strain data for the EPRI-Europe rotor steel showing the influence of test temperature. As might have been expected the data shows that the cyclic stress strain response of this steel decreases noticeably with test temperature and that material in the high yield strength condition exhibits a higher cyclic stress strain response than material in the lower yield strength condition.

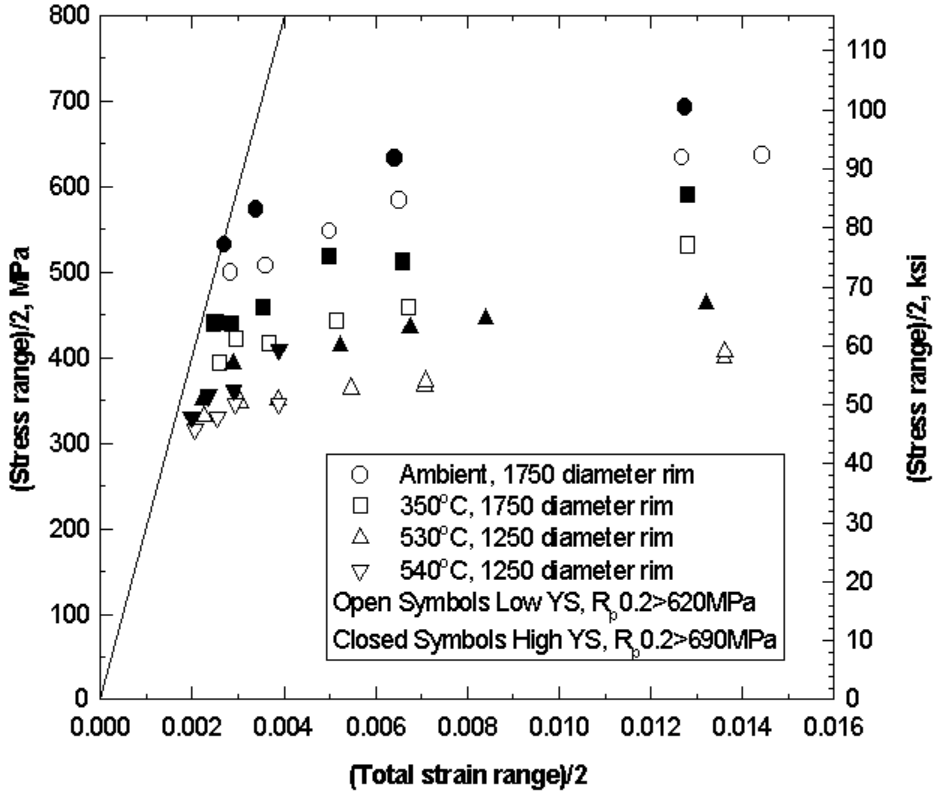

Figure 5-42
Cyclic stress-strain data for the EPRI-Europe rotor HP and LP sections

Conclusions

The low cycle fatigue properties of the EPRI-Europe rotor steel at ambient temperature appears to lie just above the upper scatter band limit for 3½%NiCrMoV and this was true up to 350°C, and at 540°C, the results are similar to conventional 1%CrMo¼V. Additionally, the fatigue properties of the material in the high and low yield strength conditions were indistinguishable at all test temperatures. A creep-fatigue interaction was observed at 540°C for the 2% CrMoNiWV steel. This is similar to the findings for

the COST 505 rotors, and adds to the confidence in the use of this material for combi rotors.

Creep behavior

Creep tests have been carried out for the core material of the high pressure part of the EPRI-Europe rotor (see appendix E). Isothermal tests at 550°C and 600°C were performed for the high yield strength (0.2% yield >690 MPa) and the low yield strength (0.2% yield >620 MPa) conditions respectively. Smooth and notched specimens were taken from sections HP1.6.1 and HP2.6.1 in the tangential directions (see Figures C-2 to C-5). Creep rupture tests during the work had durations out to 14000 hours.

The current status of the creep tests is shown in Appendix E.

Creep rupture strength

In Figures 5-43 and 5-44 the creep rupture strength results are given for both yield strength conditions at 550°C and 600°C. Additional short term tests at 500°C have been carried out for the high yield strength condition. The results from the EPRI-Europe rotor are compared with the scatterband of US air cooled 1%CrMoV steels.

Both yield strength conditions of the EPRI-Europe rotor show rupture strength in the range of the upper bound of this scatterband for 1%CrMoV steels (Change if not true or as appropriate).

If the two yield strength conditions of the EPRI-Europe rotor are compared, the high yield strength condition shows at 550°C longer time to rupture due to its higher initial strength at the test temperature. This strength effect is still observed up to the current test duration of 14 000 (Change as appropriate) hours. At 600°C this influence of initial strength on the creep rupture strength seems to be significant up to approx. 10 000 hours only.

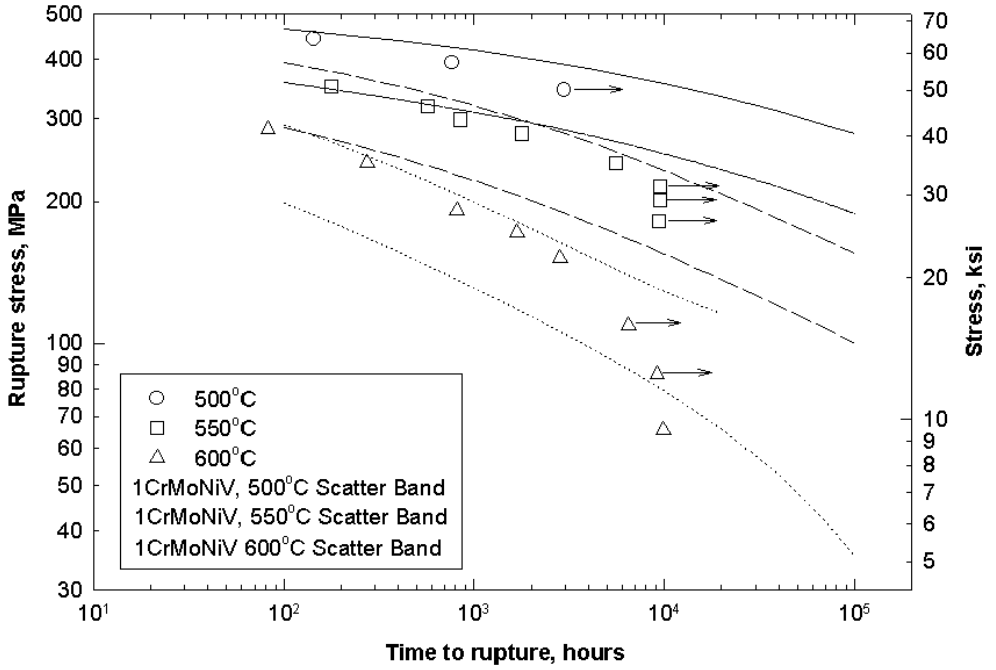

Figure 5-43
Creep rupture strength at the core of the high yield strength HP section of the EPRI-Europe rotor

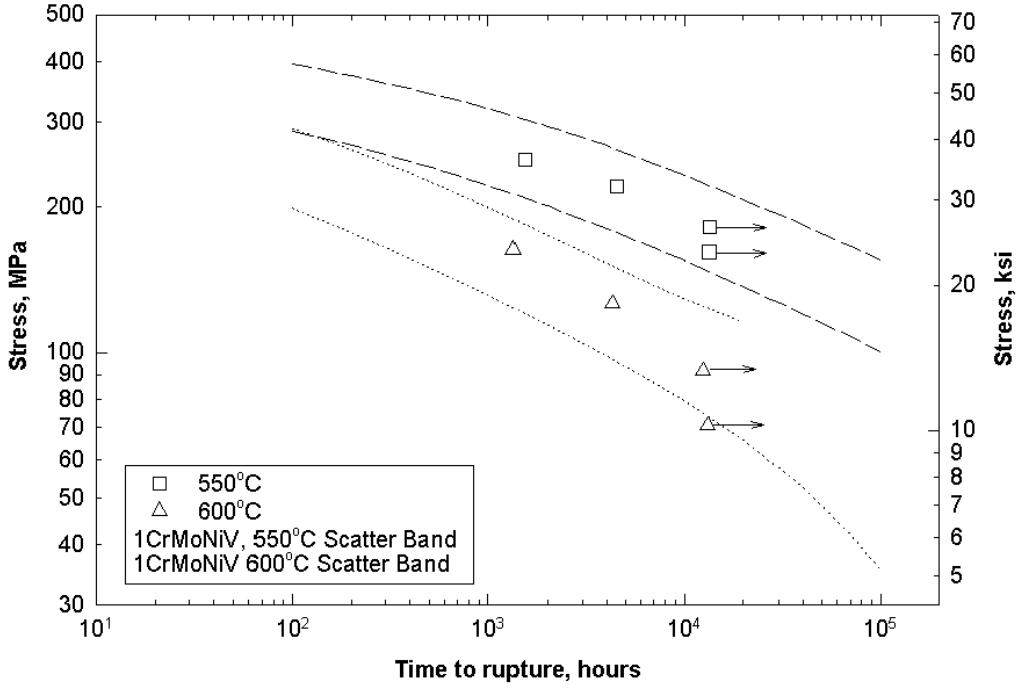

Figure 5-44
Creep rupture strength in the core of the low yield strength HP section of the EPRI-Europe rotor

Creep rupture ductility

Creep rupture ductility, i.e. elongation and reduction of area, is shown in Figs. 5-45 and 5-46. At 600°C the ductility is slightly higher than at 500 °C and 550°C as expected. No significant difference in ductility was observed, due to the difference in yield strengths. The values for rupture elongation at 500°C, 550°C and 600°C are above 20% and reduction of area is seen to be above 75% in the completed creep tests.

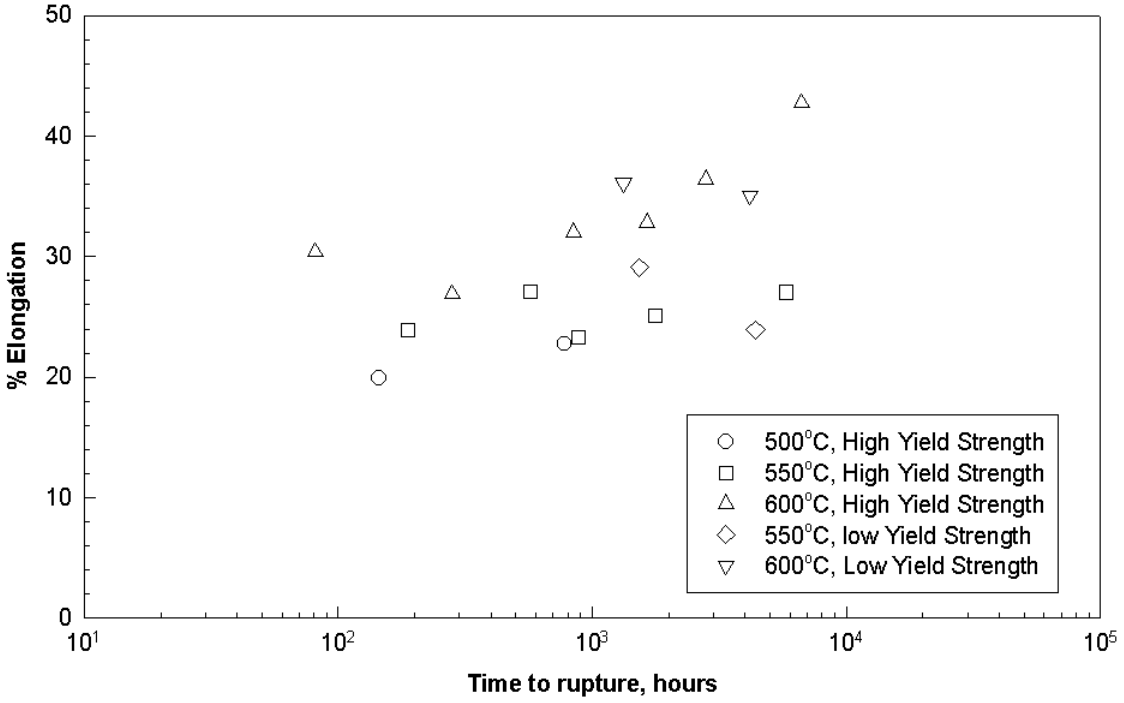

Figure 5-45
Creep ductility of the HP section EPRI-Europe rotor in both high and low yield strength conditions

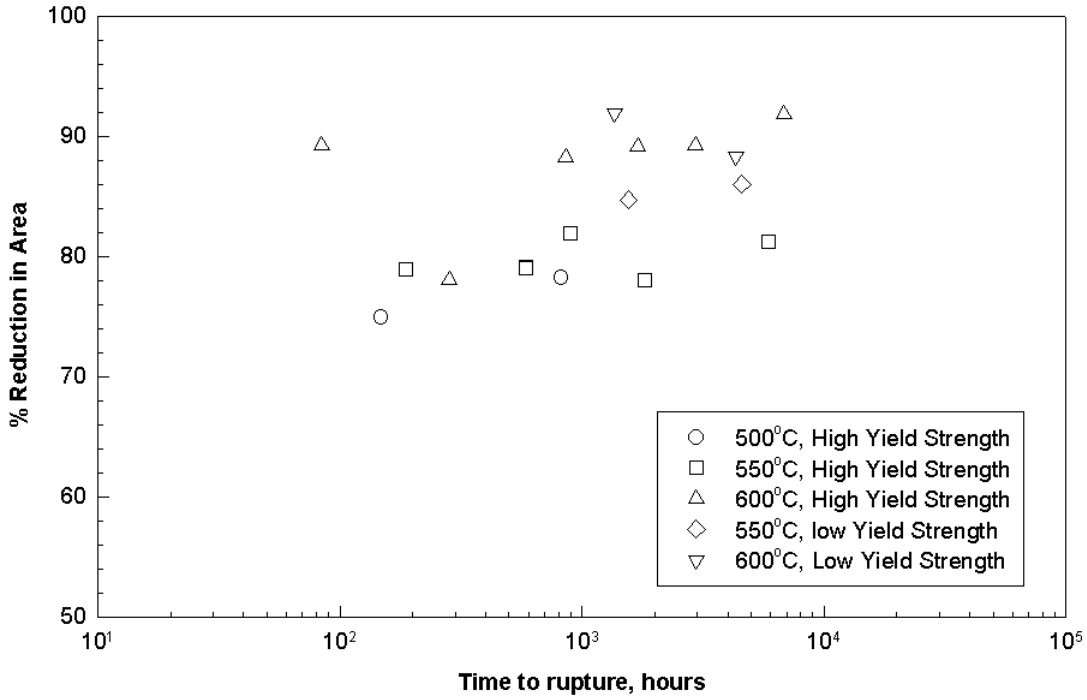

Figure 5-46
Creep ductility of the HP section EPRI-Europe rotor in both high and low yield strength conditions

Comparison with results from the COST 505 program

Creep properties for 2%CrMoNiWV steels have also been determined within the COST 505 program. A Larson-Miller parametric comparison for creep rupture strength is shown in Fig.5-47. Both yield strength conditions of the EPRI-Europe rotor are plotted together with the mean value from the different locations within the two rotors tested in COST 505 and together with the scatterband for 1%CrMoV steels mentioned above.

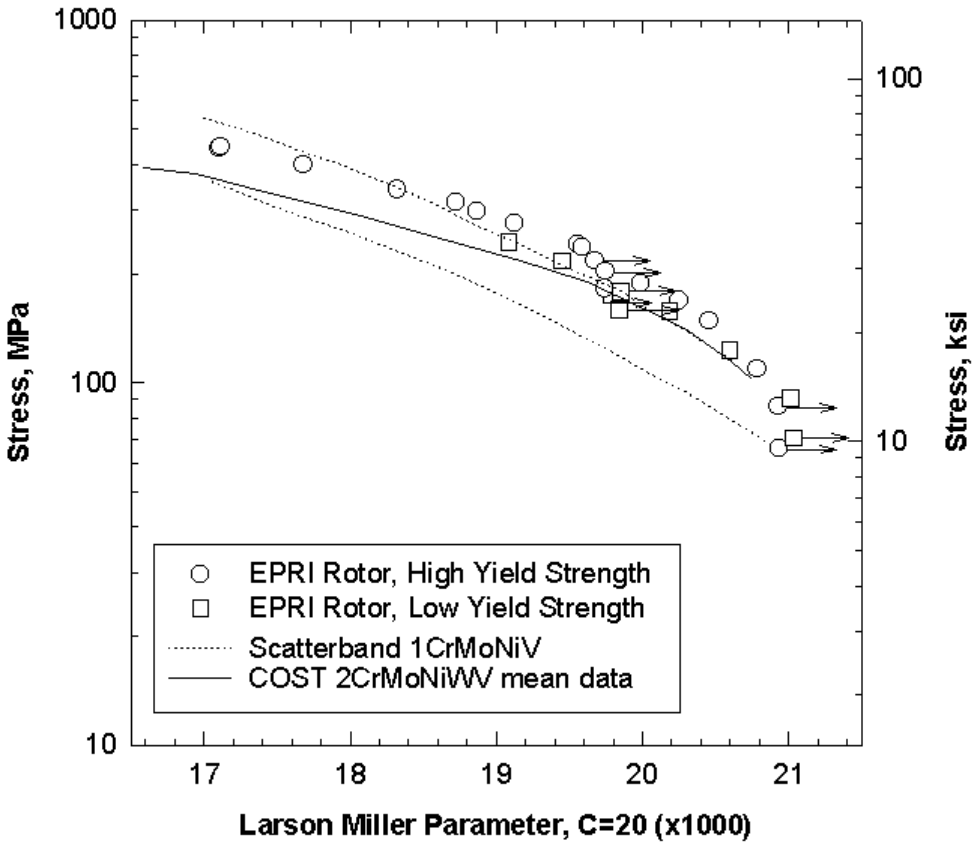

Figure 5-47
Parametric rupture data for the EPRI-Europe rotor HP core in both high and low yield strength conditions

The low yield strength material of the EPRI-Europe rotor shows similar creep rupture strength to that determined for the two rotors in the COST 505 program while the creep strength of the high yield strength material is above the COST 505 mean value. This may be explained by the yield strength levels of the COST 505 rotor materials which correspond to the low yield strength condition of the EPRI-Europe rotor.

With increasing Larson-Miller parameter, the mean value for creep rupture strength of the 2%CrMoNiWV rotor steel as tested in the COST 505 program, is approaching the upper bound of the scatterband of 1%CrMoV rotor steel(Change if necessary).

The low yield strength material of the EPRI-Europe rotor shows the same behavior, while the high yield strength material of the EPRI-Europe rotor is even exceeding this upper band curve. From the COST 505 investigations, lower bound values for creep elongation and reduction of area have been established. As shown in Fig. 5-48 these limits are also valid for both yield strength conditions and all the temperatures that the EPRI-Europe rotor was tested at. In particular, no decrease in reduction of area was

observed for the 2%CrMoNiWV rotor material as it is reported for 1%CrMoV rotor steels [8,10].

There are real concerns however that it will be necessary to await the results of long term creep testing, particularly in steels with higher nickel contents, since high nickel usually has a detrimental effects on the creep rupture strength, of steels, to establish whether these new steels will exhibit adequate long term properties.

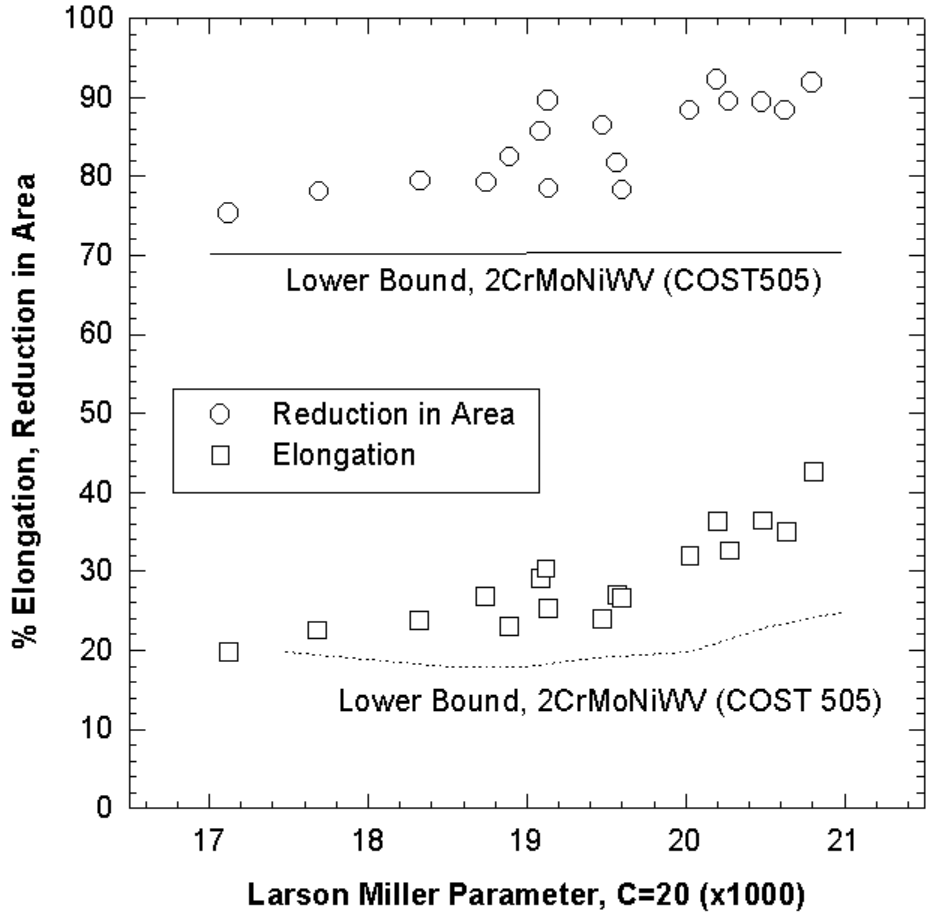

Figure 5-48
Larson-Miller ductility values for the EPRI-Europe rotor HP section in both high and low yield strength conditions

Notch sensitivity

Smooth and notched specimens have been tested under the same nominal stresses. No failure of a notched specimen was observed earlier than the corresponding smooth one. Some notched specimens from the low yield strength material were tested to failure and show significantly longer time to rupture than the smooth specimens. The notched

specimens from the high yield strength material were removed unbroken after the failure of the corresponding smooth specimen. This behavior confirms the lack of notch sensitivity seen in the COST 505 program.

Creep strain properties

Creep strain was determined by continuous measurement of the elongation or by using an interrupted strain measurement technique where the creep test is interrupted and the specimen removed to determine the current elongation.

In the Figs. 5-49 to 5-52 strain / time plots for both yield strength conditions and both test temperatures are presented. Discrete strain limits at 0.2%, 0.5% and 1% creep strain were read from these curves and summarized in Appendix C.

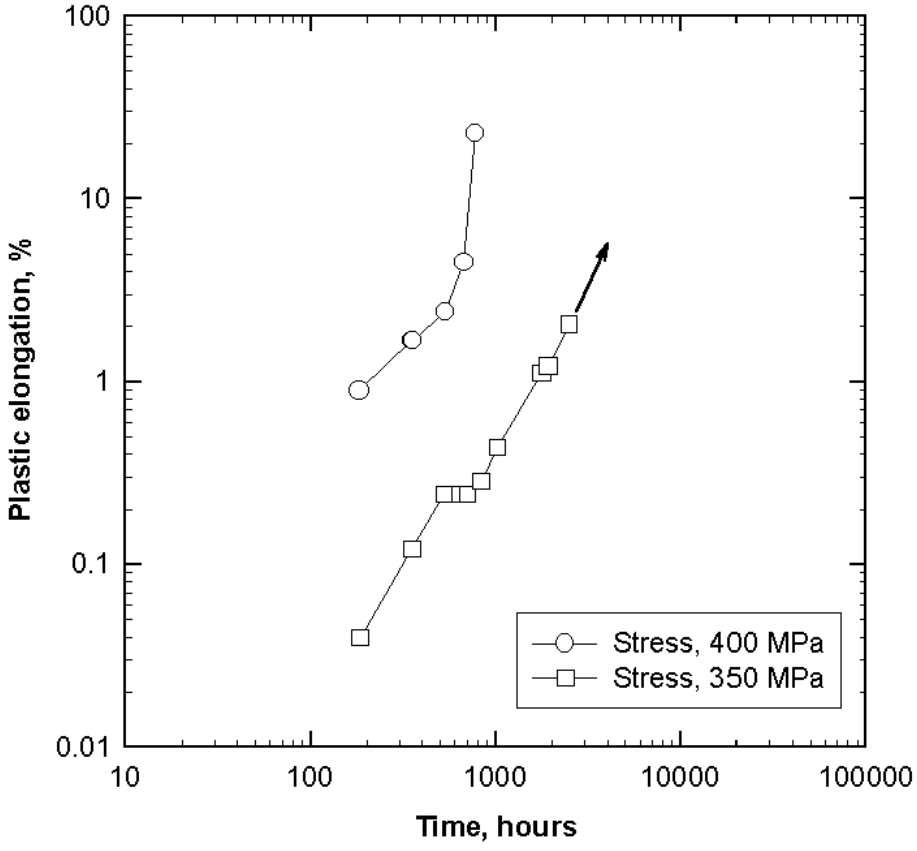

Figure 5-49
Creep strain data for the high yield strength HP section of the EPRI-Europe rotor at 500°C

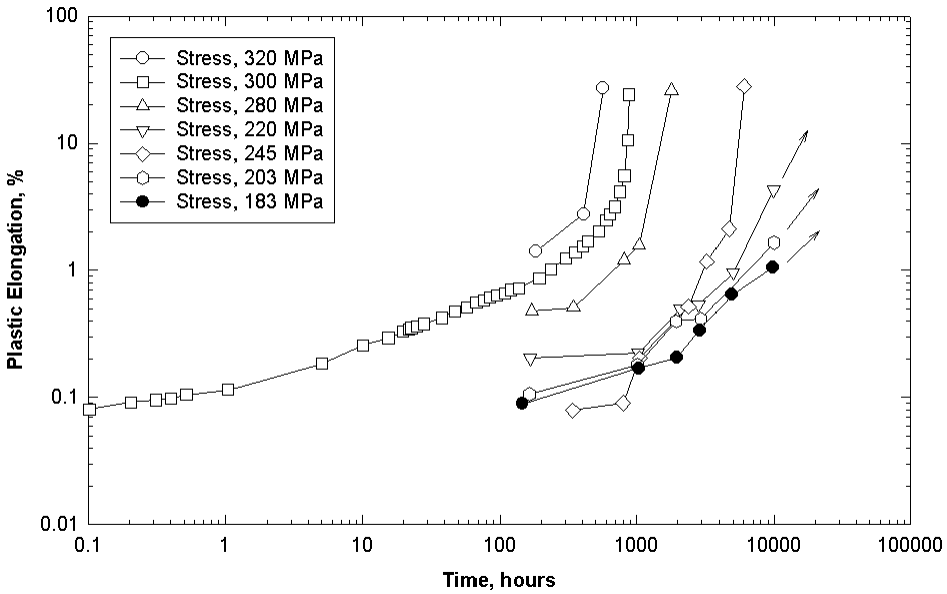

Figure 5-50
Creep strain data for the high yield strength HP section of the EPRI-Europe rotor at 550°C

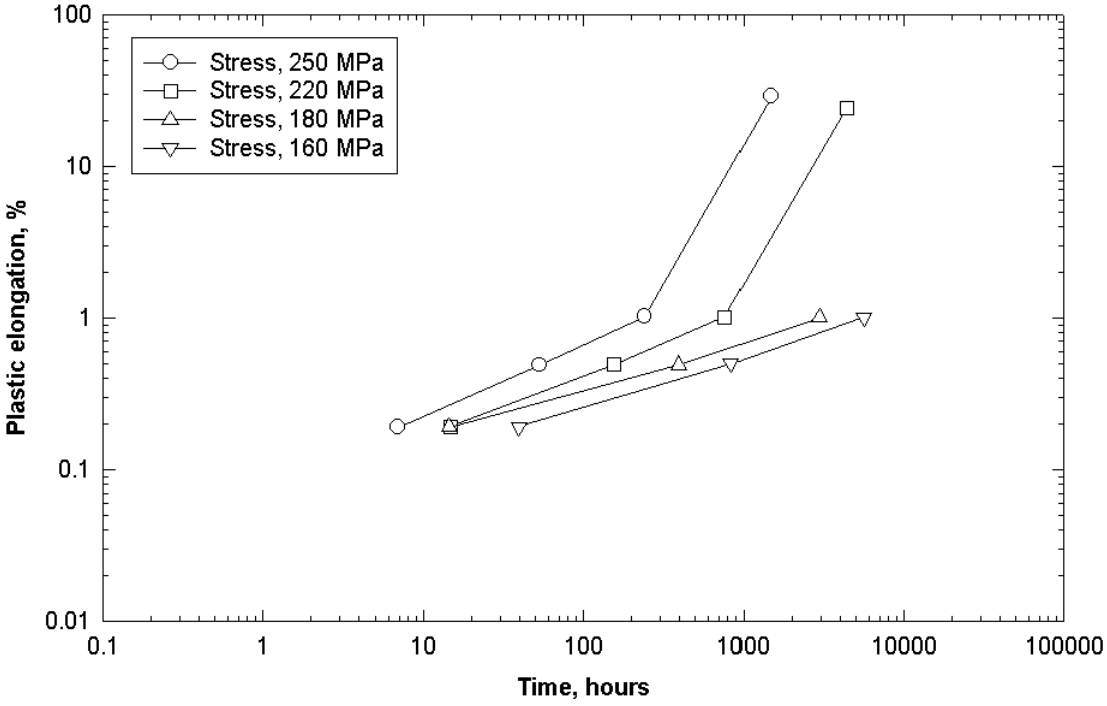

Figure 5-51
Creep strain data for the low yield strength HP section of the EPRI-Europe rotor at 550°C

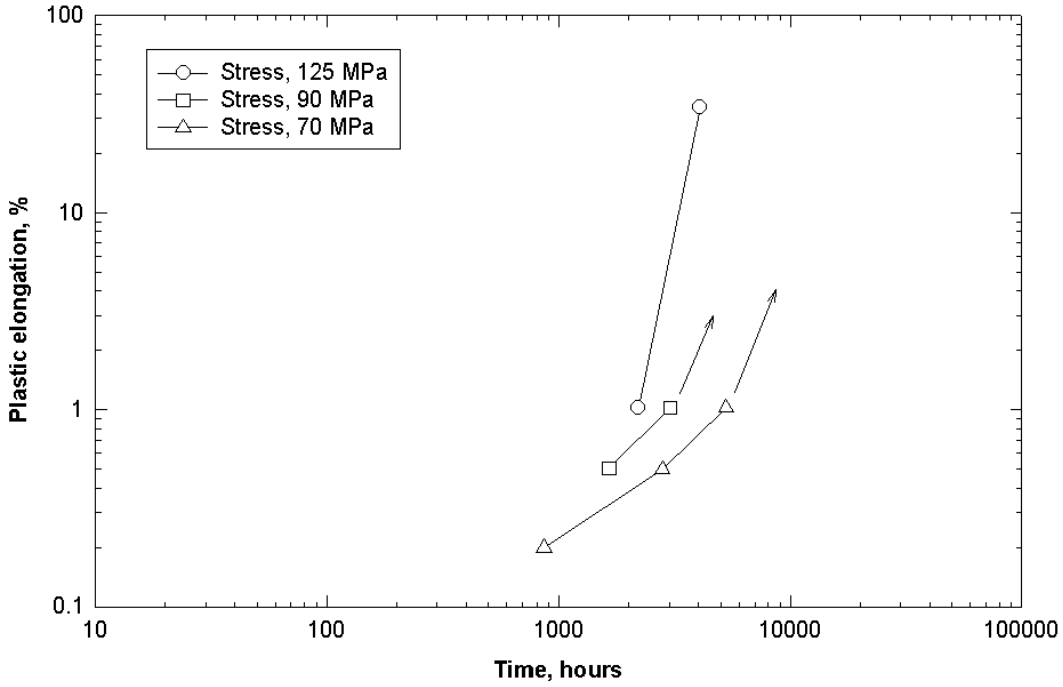

Figure 5-52
Creep strain data for the high yield strength HP section of the EPRI-Europe rotor at 600°C

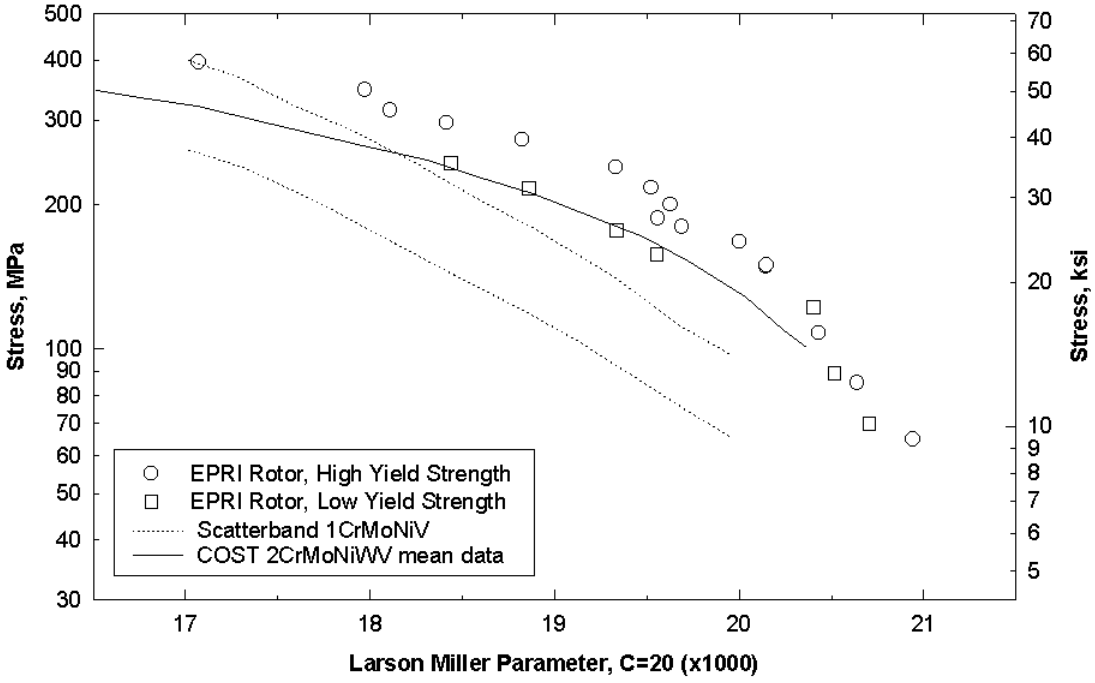

Figure 5-53
Time to 1% creep for the core HP section of the EPRI-Europe rotor

The 1% strain limits of both yield strength conditions of the EPRI-Europe rotor are compared to the mean value from the two COST 505 rotors and to the scatterband for 1%CrMoV steels in Fig 5-53. This Larson-Miller type comparison shows similar behavior for the 1% strain limit to that already shown for the rupture strength.

Creep Crack Growth

A series of creep crack growth tests have been performed on material from an axial location in the HP2 radial core through the 1250 mm diameter section of the EPRI-Europe rotor (see appendix C). The HP2 core was removed from the Saarschmiede forging after receiving a second tempering treatment to place the material in the 0.2% yield 625/650 MPa condition.

The tests were performed at 550°C in accordance with standard practice [24] using 10% side grooved Y-Z CT25 specimens, fatigue pre-cracked to a depth of 18 mm. Details of the test program are summarized in Table 5-9.

Table 5-9
CCG Test Program on EPRI-Europe rotor Steel at 550°C

Specimen Reference	σ_d, MPa	C^*li0.5mm), MPa, m/h	δ_i(0.5mm), mm	t_i(0.5mm), h	Δa, mm	t_r(tf†), h
MV235	240	5.9×10^{-5}	0.19	502	11.66	1388
MV234	200	1.0×10^{-5}	0.11	1869	8.26	6714
MV236	200	1.1×10^{-5}	0.10	1557	4.20	4244†
MV237	200	1.4×10^{-5}	0.08	1337	3.82	3496†
MV238	200	1.0×10^{-5}	0.09	1266	2.15	2297†
MV239	200					690‡

† test interrupted ‡ test continuing to interruption at 1 000 hours

The target rupture durations were ~2 000 and ~10 000h, and these were estimated by basing test loads on a reference stress (σ_d) calculation [25]. The use of σ_d, with reference to uniaxial creep rupture data, has previously been shown to provide a reasonable guide to failure times (tr) for CCG testpieces manufactured from rotor steels with a high rupture ductility. Ultimately, this approach resulted in rupture times for the trial forging which were shorter than the aim by approximately 30% (Fig.5-54).

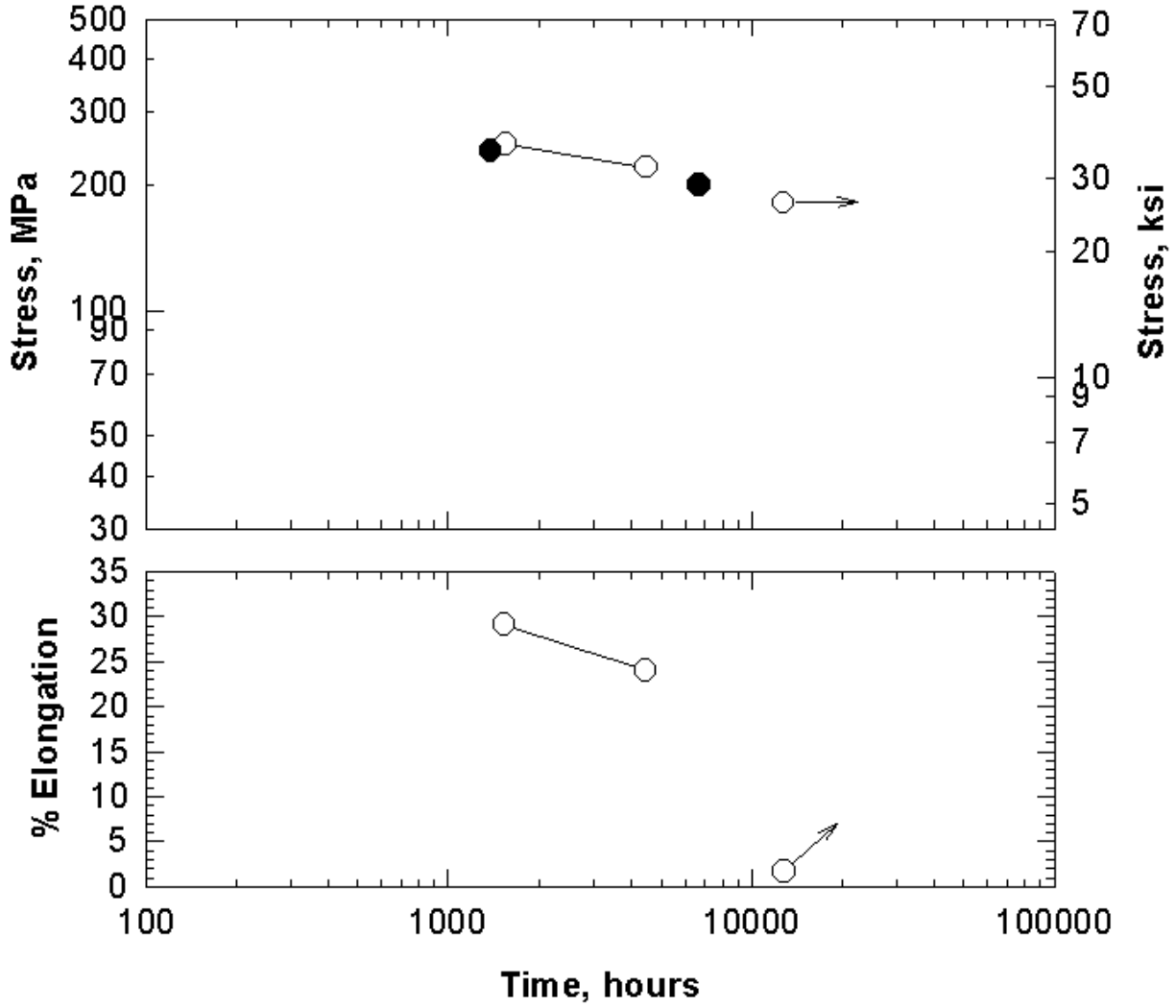

Figure 5-54
Comparison of uniaxial and creep crack growth testpiece rupture data for the EPRI-Europe rotor at 550°C

During the course of each test, load point displacement due to creep (LPDC) and crack development were continuously monitored. The test records for MV235 (σ= 240 MPa) and MV234 (σ =200 MPa) are shown in Figures. 5-55 to 5-58 respectively. Critical crack tip opening displacements ($\delta\{\chi c\}$) were derived from the LPDC records, at crack initiation, on the basis of a deformation hinge point determined by the physical measurement of displacement changes during test between a series of hardness indent pairs positioned along the length and either side of the pre-crack (χc defines the initiation criterion in terms of an increment of crack extension in mm).

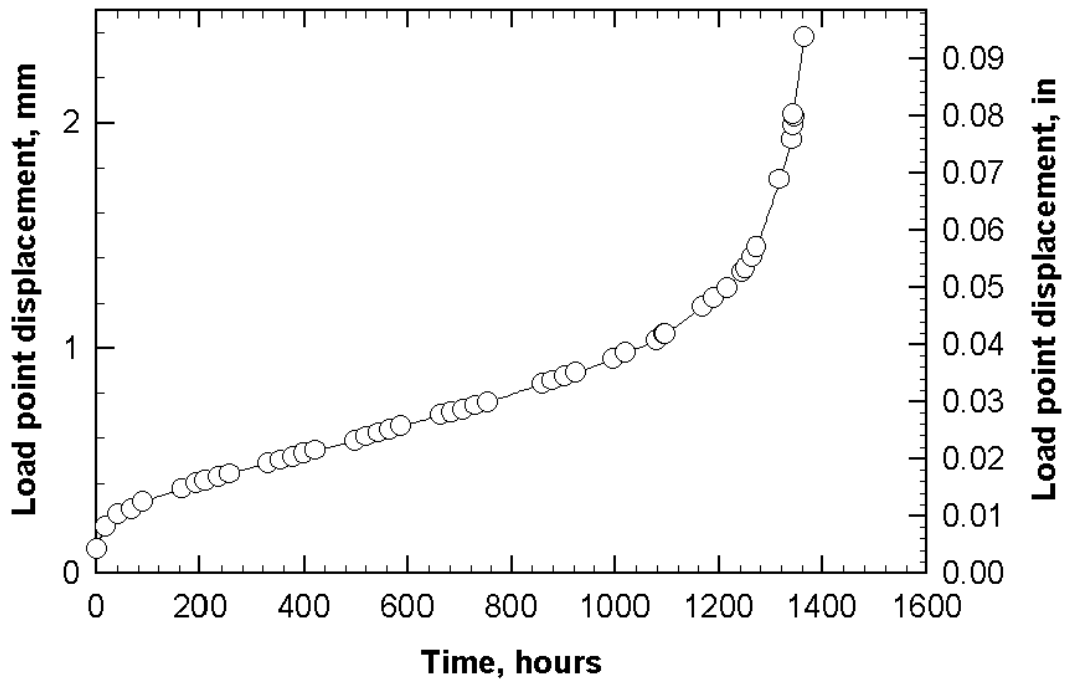

Figure 5-55
Load point displacement test records for the low yield strength HP section of the EPRI-Europe rotor (sd =240MPa) at 550°C

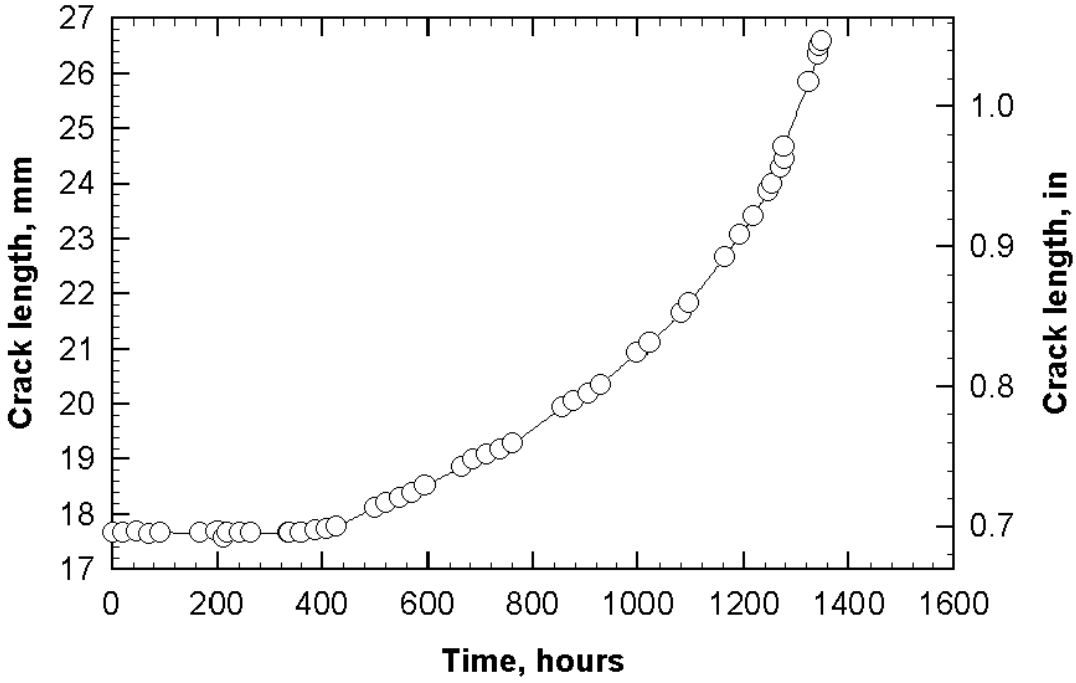

Figure 5-56
Crack length test records for the low yield strength HP section of the EPRI-Europe rotor (sd =240MPa) at 550°C

The time to rupture for creep crack growth testpieces (or components containing pre-existing defects) comprises elements of initiation time and propagation time. In high temperature defect assessments, initiation time - the creep crack initiation time (ti[xc]) is the time to the onset of creep crack propagation from a preexisting defect [26] - may be estimated using calculations involving C*i[χc], or δi[χc] [26], and values of these parameters for the EPRI-Europe rotor steel are listed in Table 5-9 (for χc = 0.5 mm). Creep crack initiation times are plotted against $C^{*}_{i[0.5mm]}$ in Fig 5-59: Propagation time is determined from data on creep crack propagation rates.

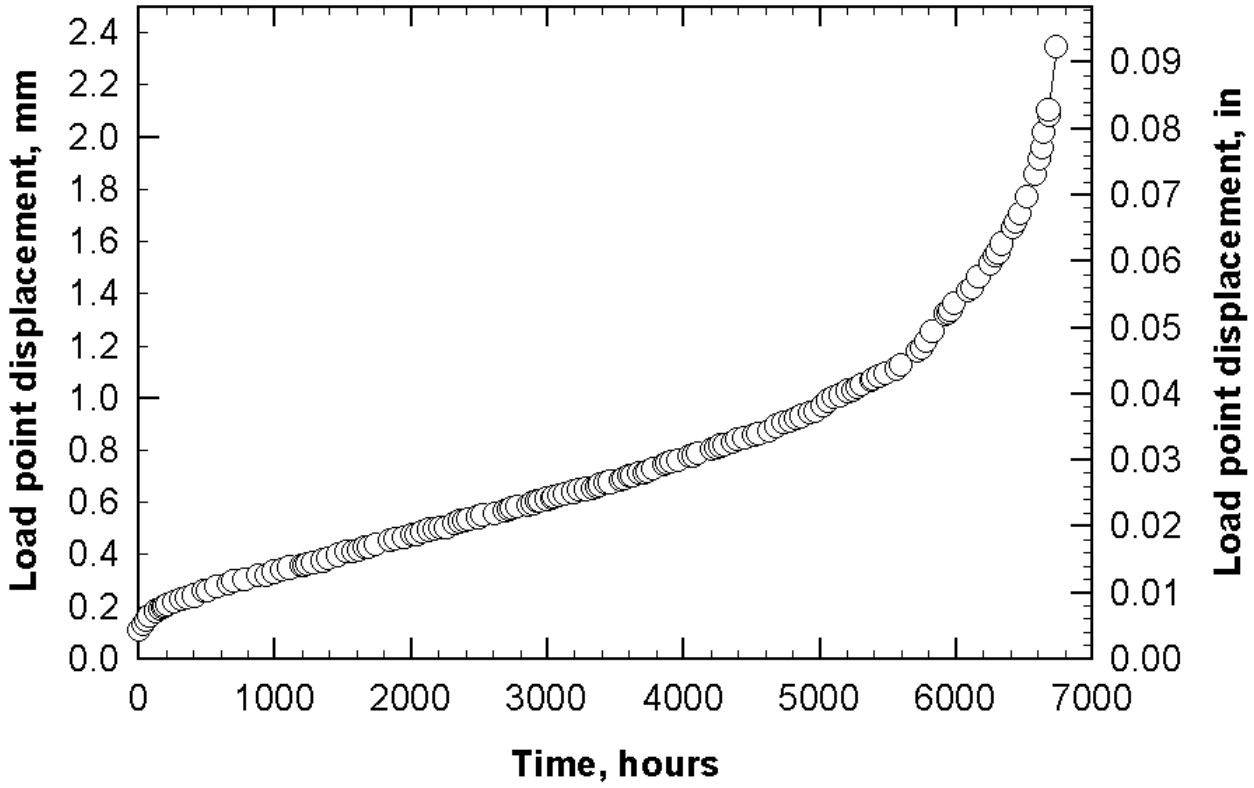

Figure 5-57
Load point displacement test records for the low yield strength HP section of the EPRI-Europe rotor (sd =200MPa) at 550°C

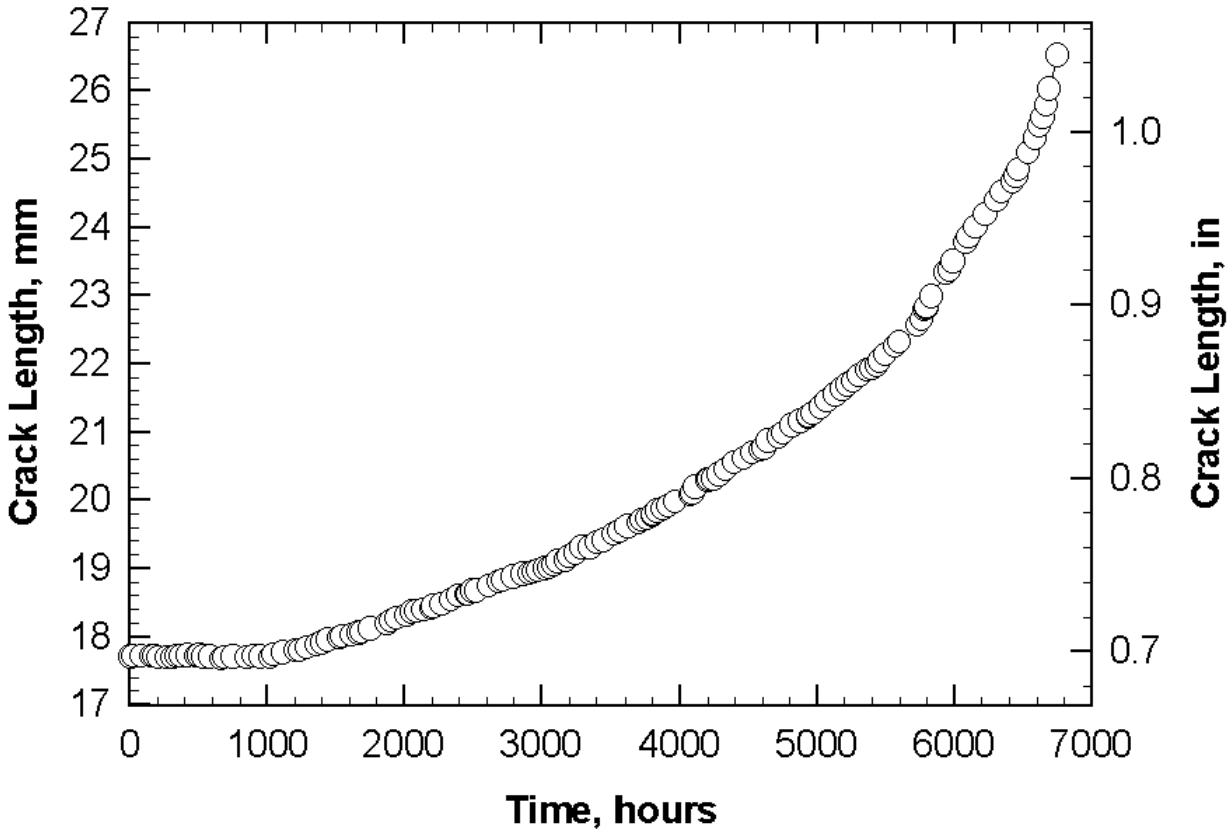

Figure 5-58
Crack length test records for the low yield strength HP section of the EPRI-Europe rotor (sd =200MPa) at 550°C

Creep crack propagation rates for the EPRI-Europe rotor steel are plotted as a function of C^* in Fig. 5-60. The evidence from this investigation indicates that the transition between Stage I and Stage II crack growth occurs between 1 and 2 mm for this alloy at 550°C. In Fig.5-60, there is a high intensity of data points in the Stage I to Stage II da/dt transition region for the σ_d = 200 MPa condition. This is due to the contribution of the results from the interrupted tests (refer to Table 5-9 for individual δ_a values).

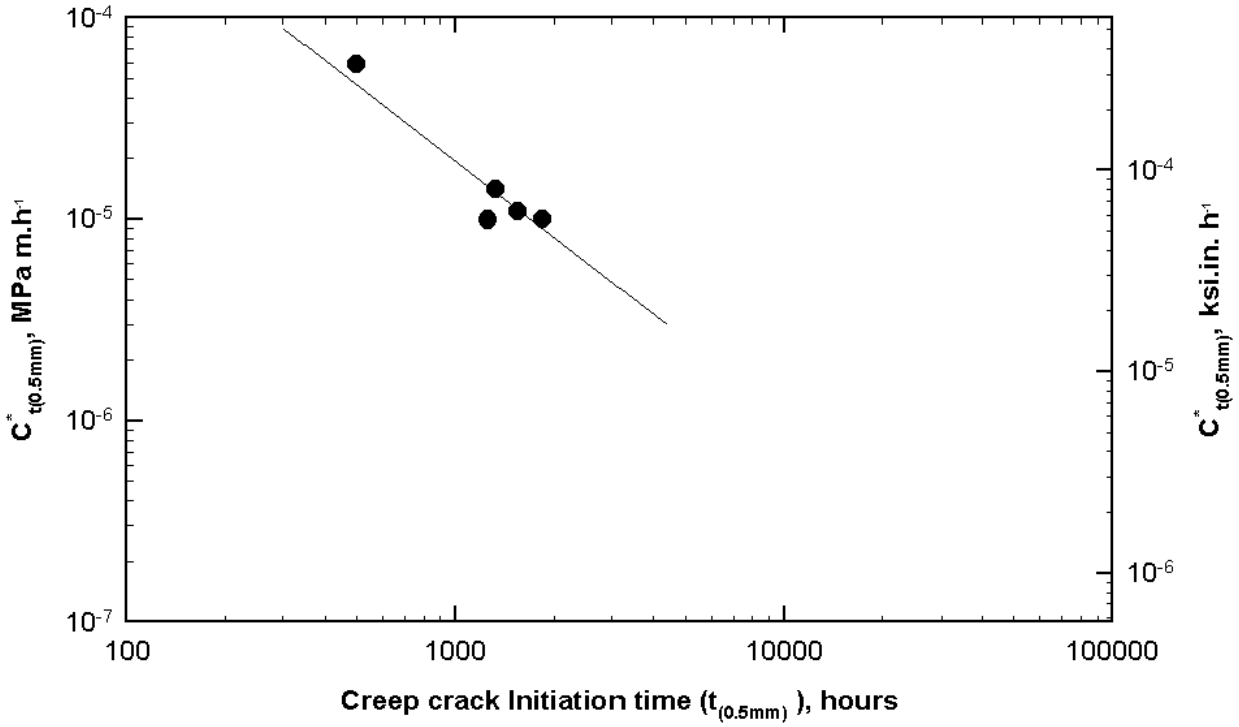

Figure 5-59
Summary of creep crack initiation results for the low yield strength HP section of the EPRI-Europe rotor at 550°C

Creep crack growth rates for the EPRI-Europe steel are well within the databand of the COST 505 ESR and VCD 2%CrMoNiWV steels.

Post test metallographic inspection indicated that creep crack growth was by a mixed ductile transgranular / intergranular fracture mechanism at 550°C.

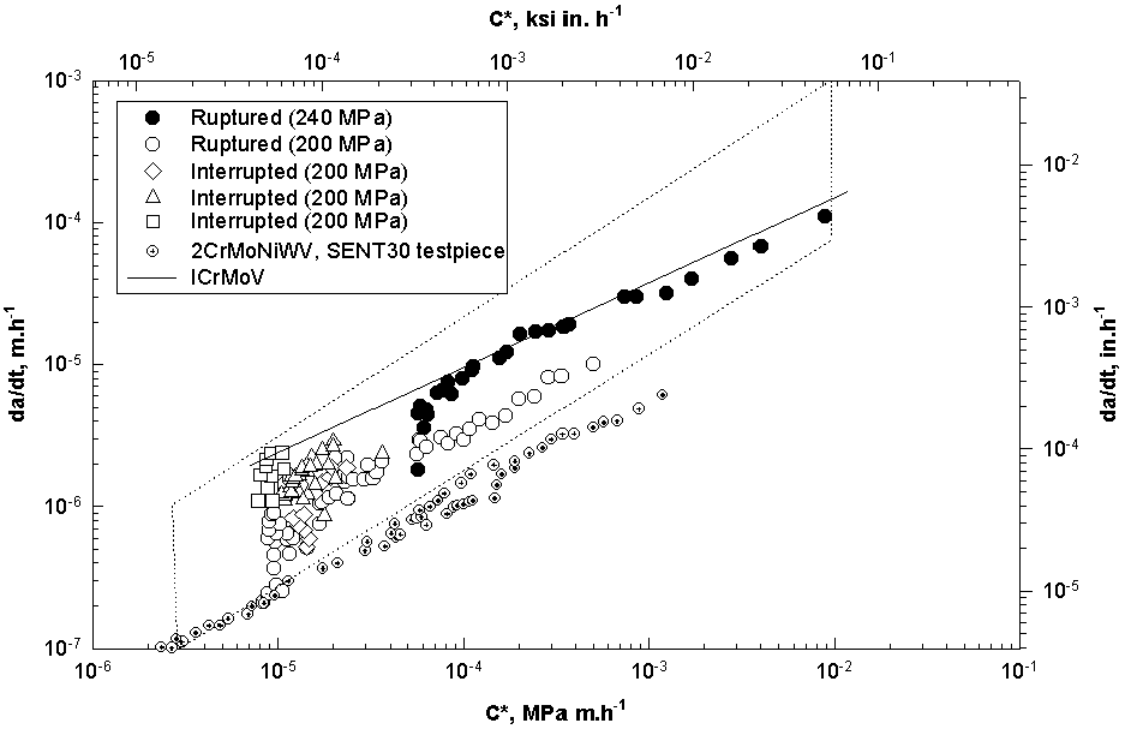

Figure 5-60
Summary of creep crack propagation results for the low yield strength HP section of the EPRI-Europe rotor at 550°C

Conclusions

The creep strength of the HP portion of the trial rotor lies in the upper scatterband of 1%CrMo¼V rotor steel out to 14 000 hours, with a comparable initial creep rupture strength. Material heat treated to the higher yield strength had higher rupture strength, such that the creep strength lies above the COST 505 data: no notch weakening was observed at either yield strength condition. The 1% creep strain limit of 2%CrMoNiWV rotor steel tended to exceed the scatterband of 1%CrMoV rotor steels with comparable initial strength, and the creep rupture ductility of the 2%CrMoNiWV rotor steel was consistently high and superior to that of 1%CrMo¼V rotors. With increasing Larson-Miller parameter, the 1% creep strain limit of the 2%CrMoNiWV rotor steel exceeds the upper bound of the scatterband for 1%CrMoV rotor steels.

Stress Corrosion Cracking and Pitting Tests

During normal operation, single-cylinder rotors should not see conditions that would lead to stress corrosion cracking, and during off-load periods, nitrogen blanketing is used to reduce the propensity of cracking. However, there have been instances of mainly LP rotors that have suffered pitting damage which could have led to cracking,

and potentially catastrophic fast fracture. It is for this reason that a series of tests on the new material was carried out in order to determine whether the new EPRI-Europe material would suffer environmental assisted cracking in service.

Constant load tests

Stress Corrosion Cracking (SCC) and Pitting tests were carried out on 1750 mm diameter rim material in the unaged condition in both the low (620 - 650 MPa) and high (690 720 MPa) yield strength conditions. The tests were exposed to low O_2 (<10 ppb) high purity condensing steam at 9 - 100°C. The test cell environment was not recirculated; the condensing steam exiting the cell being passed directly to drain. The SCC tests were performed under constant loading conditions on Denison T47E modified creep testing machines. The SCC specimen details are shown below.

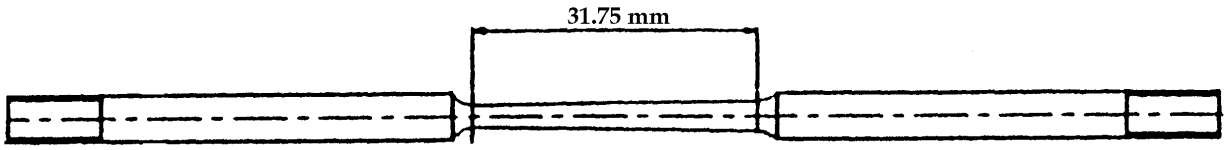

Figure 5-61
Tapered tensile stress corrosion cracking testpiece used in the program

Each specimen contained a 31.8 mm long tapered gauge length from 3.18 mm to 4.07 mm. The gauge length was polished to 4000 grit prior to the commencement of the tests. The specimens were loaded to their nominal yield strength, based on the stress calculated at the minimum gauge diameter, after establishment of the environmental conditions within the test cells. (The latter occurred within 5 minutes of opening the steam admittance valve). Consequently, in any one specimen the stress varies from 60% of the nominal yield strength at the maximum gauge diameter to about 100% of the nominal yield strength at the minimum gauge diameter. Testing was carried out to durations of 500, 1 000, 2 000, 5 000 and 10 000 hours. At the completion of these planned test durations the specimens were metallographically examined to determine the extent of pitting and stress corrosion cracking that had occurred during the tests.

Figures 5-62 and 5-63 show the results of the SCC tests. Although pitting was observed in tests of all durations down to and including 500 hours, cracking was only observed at the narrowest section of the gauge length in the low yield strength specimen exposed for 10 000 hours. The crack observed was, however, small being only 0.11 mm deep x 0.2 mm long and was transgranular and unbranched. Also shown in Figures 5-62 and 5-63, for comparison, are pit and stress corrosion crack boundaries for 3½%NiCrMoV rotor material tested in condensing steam [27]. In general the 2CrMoNiWV rotor material tested in this program seems to exhibit similar or slightly better resistance to

SCC than the 3½%NiCrMoV material [27], although the previous work on 3½%NiCrMoV was confined to higher stress levels than those used in the current work.

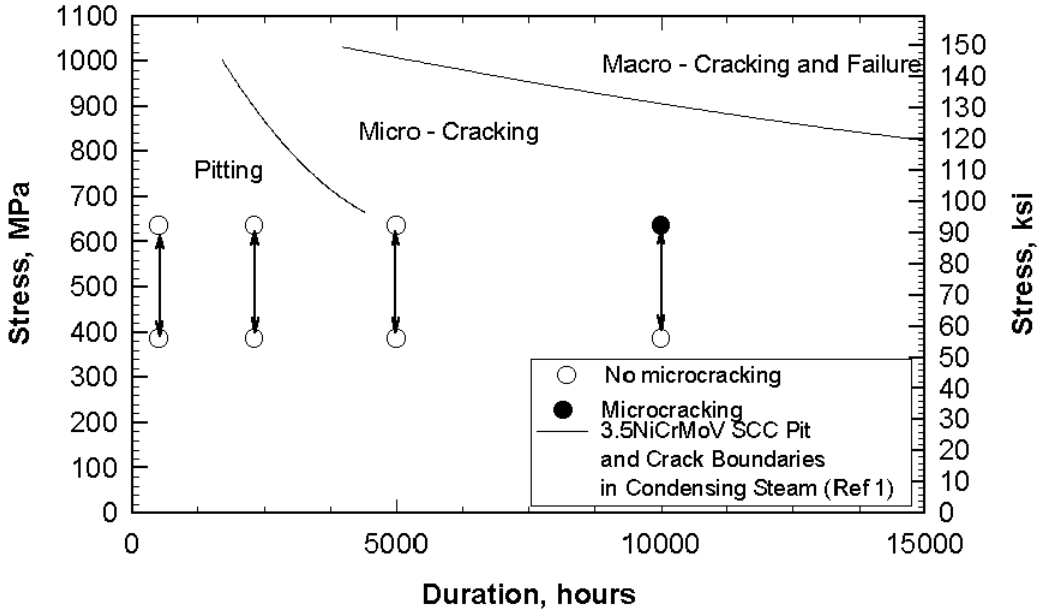

Figure 5-62
Stress corrosion cracking in low oxygen condensing steam at 90-100°C for the low yield strength LP section of the EPRI-Europe rotor

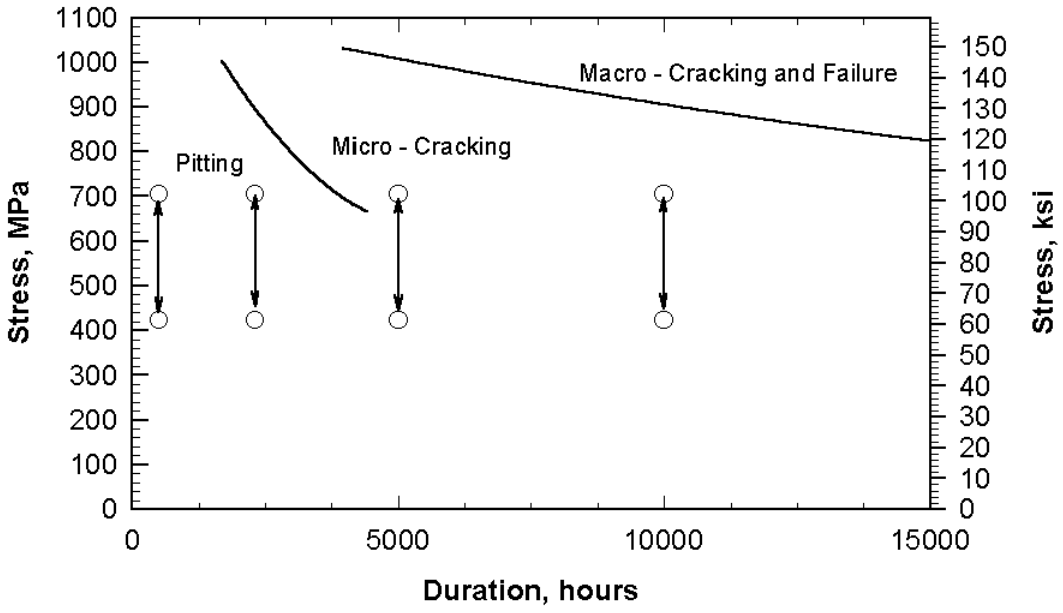

Figure 5-63
Stress corrosion cracking in low oxygen condensing steam at 90-100°C for the high yield strength LP section of the EPRI-Europe rotor

Maximum pit depths measured on the SCC specimens are shown in Fig 5-64. Pit depths did not exceed 0.02 mm and there appeared to be no relationship between pit depth and exposure period. This work appears to confirm previous conclusions [28] that 'Super-clean' steels have a much lower propensity to pitting than conventional steels, presumably due to the lower levels of surface breaking sulfide and other inclusions. This work showed that once a SCC crack had initiated, growth rates were similar to conventional 3½%NiCrMoV steels.

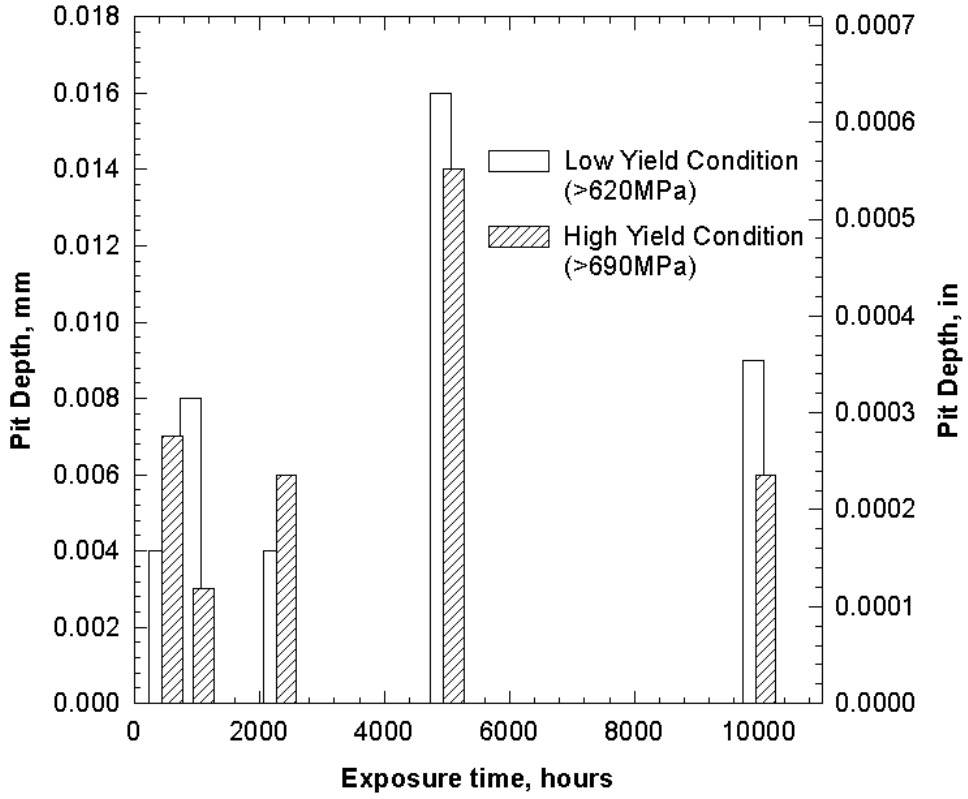

Figure 5-64
Pitting characteristics of the EPRI-Europe rotor LP section with exposure time in low oxygen condensing steam in both low and high yield strength conditions - data from SCC testpieces

Pitting Tests

Pitting tests were conducted on small cubes of the material which were supported from the upper end cap in the same test cell as the constant load tests. The specimens incorporated a polished exposed surface area of approximately 1 cm^2. The exposed surface was polished to an initial surface finish of 4000 grit prior to exposure.

Fig 5-65 shows the maximum measured pit depths as a function of exposure period. Pit depths were found to be of similar magnitude to those observed in the tensile specimens with maximum pit depths not exceeding 0.02 mm.

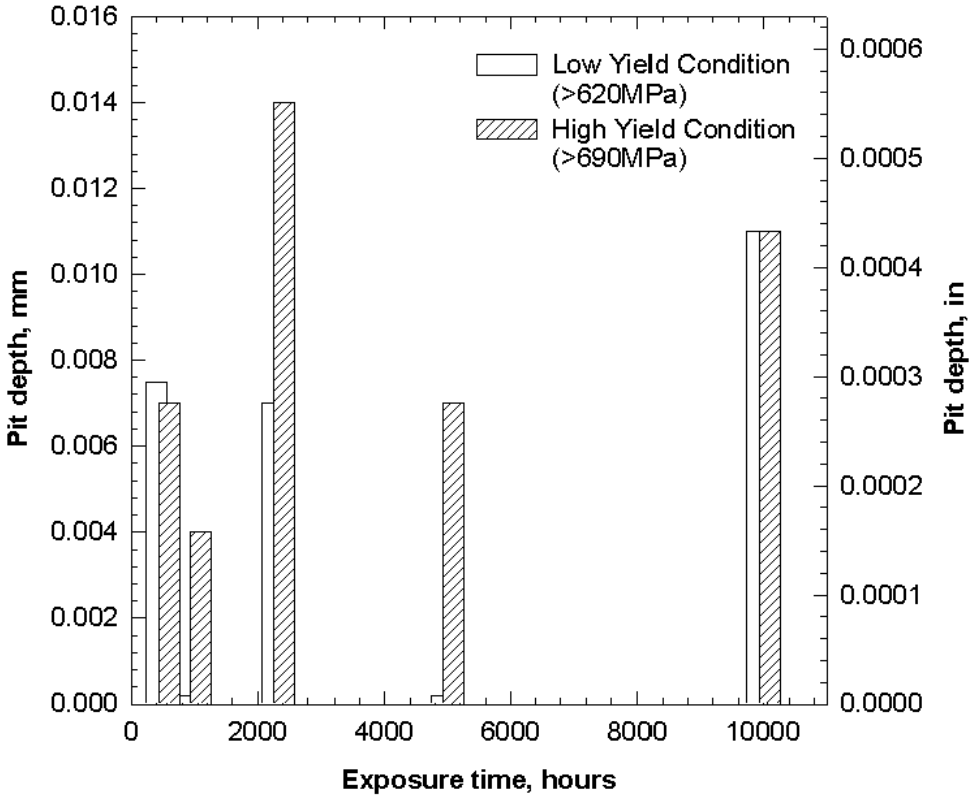

Figure 5-65
Pitting characteristics of the EPRI-Europe rotor with exposure time in low oxygen condensing steam in both low and high yield strength conditions - data from Pitting Cubes

Conclusions

1. The 2CrMoNiWV rotor material tested in this program seems to exhibit similar or slightly better resistance to SCC than the 3½%NiCrMoV material

2. Pit depths did not exceed 0.02 mm and there appeared to be no relationship between pit depth and exposure period

6

CONCLUSIONS

Trial melts of 2%CrMoNiWV steel showed that at least up to 0.2% yield strengths of 700 MPa, decreasing the content of the embrittling elements Si, P, As, Sb and Sn gives better FATT values and can also avoid long-term embrittlement. However increasing the Mo and W contents promises a better FATT only in the rim region of the rotors, and this advantage is offset by poorer creep properties. An addition of 0.04% Nb gives better toughness due to grain refinement, but it too is detrimental to the creep-rupture properties, and results in an unacceptable formation of ferrite + carbide.

A trial LP rotor manufactured to the optimum 2%CrMoNiWV composition with a diameter of 1750 mm exhibited excellent toughness levels compared with the results of previous 2%CrMoNiWV rotors with smaller diameters but with comparable yield strengths. It was possible to attain the toughness level of the previously investigated 2%CrMoNiWV rotors with an increased diameter and a yield strength of >690 MPa.

A study of the embrittlement response in a trial HP/LP forging showed that maximum embrittlement was reached at 425°C, and higher yield strengths lead to greater embrittlement. At temperatures of 540°C, the embrittlement decreased due to matrix softening. At 480°C exposure, the ΔFATT for the EPRI-Europe trial rotor and previously investigated rotors are comparable, however at 425°C the EPRI-Europe rotor ΔFATT is 25°C more than the COST VCD rotor. The high strength and 425°C combination led to a FATT of 100°C. The reason for the above is not clear, and cannot be explained by phosphorus embrittlement alone.

The low cycle fatigue properties of the EPRI-Europe rotor steel at ambient temperature appears to lie just above the upper scatter band limit for 3½%NiCrMoV and this was true up to 350°C, and at 540°C, the results are similar to conventional 1%CrMo¼V. Additionally, the fatigue properties of the material in the high and low yield strength conditions were indistinguishable at all test temperatures. A creep-fatigue interaction was observed at 540°C for the 2% CrMoNiWV steel. This is similar to the findings for the COST 505 rotors, and adds to the confidence in the use of this material for combi rotors.

The creep strength of the HP portion of the trial rotor lies in the upper scatterband of 1%CrMo¼V rotor steel out to 14 000 hours, with a comparable initial creep rupture strength. Material heat treated to the higher yield strength had higher rupture strength,

such that the creep strength lies above the COST 505 data: no notch weakening was observed at either yield strength condition. The 1% creep strain limit of 2%CrMoNiWV rotor steel tended to exceed the scatterband of 1%CrMoV rotor steels with comparable initial strength, and the creep rupture ductility of the 2%CrMoNiWV rotor steel was consistently high and superior to that of 1%CrMo¼V rotors. With increasing Larson-Miller parameter, the 1% creep strain limit of the 2%CrMoNiWV rotor steel exceeds the upper bound of the scatterband for 1%CrMoV rotor steels.

The 2CrMoNiWV rotor material tested in this program seems to exhibit similar or slightly better resistance to SCC than the 3½%NiCrMoV material, and corrosion pit depths did not exceed 0.02 mm and there appeared to be no relationship between pit depth and exposure period.

A

REFERENCES

[1] S.M. Beech and G.A. Honeyman.

A Modified Composition for Improved Creep Resistance in Superclean NiCrMoV Steel. ASM Materials Congress, Robert I. Jaffee Memorial Symposium on Clean Materials Technology 2 - 5, Chicago. 1992

[2] H. Finkler, E. Potthast

Presentation of a new steel for high-pressure shafts. Presented in Palo Alto, CA, USA, 1980; Workshop Proceedings: Rotor Forgings for Turbines and Generators. EPRI WS-79-235, Sept 1981, paper 5.5.1

[3] E. Potthast, H. Finkler

New 2%CrMoNiW steel for high pressure rotors. ASTM Forging Conf. Williamsburg, VA, USA 1986, STP 903

[4] W. Wiemann, C. Berger, K.-H. Mayer, E. Potthast

A new 2% CrMoNiWV creep resistant rotor steel. Intern. Conf. on Advances in Material Technology for Fossil Power-Plants. Chicago, Sept 1987

[5] E. Potthast

Material development in forged turbine shafts. Steel Times 218 (1990), pp 312 - 319

[6] W. Wiemann

2% CrMoNiWV steel - an improved creep resistant rotor material. Proc. Conf. High Temperature Materials for Power Engineering 1990, Liège, Sept 1990

[7] W. Wiemann, W. Engelke, E. Potthast

Advanced 2% CrMoNiV steel for rotors with enhanced requirements. Third Intern. Conf. on Improved Coal Fired Power Plants. San Francisco, April 1991

[8] W. Wiemann, H. Luft, E. Potthast

HP-, IP-rotors and HP-LP combination rotors manufactured from advanced 2% CrMoNiWV steel. Conf. on Materials for Combined Cycle Power Plant, Sheffield UK, June 1991

[9] E. Potthast, J. Poppenhager, W. Wiemann

Advanced 2% CrMoNiWV steel for combination rotors. llth Intern. Forgemasters Meeting, Terni, Italy, June 1991

[10] W. Wiemann

Development of an improved 2%CrMoNiWV HP/LP rotor material. Evaluation report of a joint research programmed for the Commission of European Communities, 1991.

Partners: ABB (CH) M. Staubli, GEC-Alsthom (UK) A. Strang, MAN-Energie K. H. Mayer, MPI-Düsseldorf H.J. Grabke, Parsons-IRD S.M. Beech, Saarschmiede E. Potthast, Siemens-KWU W. Wiemann, EUR 13452 EN

[11] E. Potthast, R. Viswanathan, W. Wiemann

Advanced 2% CrMoNiWV steel for combination rotors. 12th Intern. Forgemasters Conference, Chicago, September 1994

[12] R.L. Bodnar, J.R. Michael, S.S. Hansen, R.J. Jaffee

Progress in the design of an improved high temperature 1%CrMoV steel. Report on EPRI Research Programs RP 2426-4 and RP 2741-4 (1989)

[13] Y. Tanaka, T. Azuma, Y. Ikeda, 0. Watanabe, M. Yamada, A. Kaplan, R.C. Schwant

Production and properties of a superclean 2½%NiCrMoV high pressure/low pressure rotor shaft. ASM/TMS Materials Week, Chicago, 1992, p. 169 - 180

[14] R. Viswanathan

Application of clean steel/ superclean steel technology in the electric power industry - Overview of EPRI Research and Products. EPRI Workshop Clean steel - super clean steel, London, Institute of Materials, 1996, Proceedings, p. 1 - 32

[15] T. Tsuchiyama, M. Miyakawa, M. Okamura, M. Morita, T. Yamamoto, S. Nishida Development and production of a new HP-LP combined turbine rotor of 2%CrMoV steel. ASM/TMS Materials Week, Chicago, 1992, p. 181 - 186

[16] M. Yamada, T. Tsuda, 0. Watanabe, M. lfiyazaki., Y. Tanaka, T. Takenouchi, Y. Ekeda

HLP single cylinder steam turbine rotor forgings for combined cycle power plants. ASM/TMS Materials Week, Chicago, 1992, p. 161 - 168

[17] Y. Fukui, M. Shiga, R. Kaneko, T. Tan, N. Morisada, Y. Ikeda, T. Ishiguro, T. Azuma

Development of super clean 0.2 Mn - 1.8 Ni - Cr - MoV steel rotor for HP-LP steam turbine. llth Int Forgemasters Meeting, Terni, 1991, Proceedings IX.9

[18] JPV RC Report Number2

Temper embrittlement and hydrogen embrittlement in pressure vessel steels. The Iron and Steel Institute of Japan, May 1979

[19] R. Bruscato

Temper embrittlement and creep embrittlement of 2¼Cr-1Mo shielded metal-arc weld deposits. Welding Journal Research Suppl., 49,1970

[20] M. Kohno, M. Miyaawa, S. Kinoshita., A. Suzuki

Effect of chemical composition on properties of high purity 3½%NiCrMoV steel forging. ASM/EPRI Conf. Chicago, Sept 1987

[21] J. Ewald, C. Berger, K.-H. Keienburg, W. Wiemann

Present quality level of large heat resistant rotor forgings made of 1%CrMoV steels - Part 1. Steel research 57, Number 2, 1986, p. 83 - 92

[22] K.H. Mayer and C. Berger

Influence of Steel Cleanness on the Operational Properties of Turbine Components. Conference Proceedings of Fifth EPRI Workshop" Clean Steel, Superclean Steel" 6. - 7. March 1995, London, UK, Page 195 - 211.

[23] Y. Tanaka et al

100 000 Isothermal Aging Test Results of NiCrMoV Steels for Low Pressure Steam Turbines. Conference Proceedings of Fifth EPRI-Workshop “Clean Steel, Superclean Steel” 6 - 7 March 1995 London, UK, Page 181 - 193.

[24] ASTM Standard E1457-92

Standard test method for measurement of creep crack growth rates in metals. Annual Book of ASTM Standards, Section 3, Volume 03.01.

[25] J R Haigh

The mechanisms of macroscopic high temperature crack growth, Part II: Review and re-analysis of previous work. Mat. Sci. Engng., 1975, 20, 225.

[26] S R Holdsworth

Initiation and early growth of creep cracks from preexisting defects. Materials at High Temperatures, 1992,10, 2, May, 127.

[27] M O Speidel, J Denk and B Scarlin

Stress Corrosion Cracking and Corrosion Fatigue of Steam-Turbine Rotor and Blade Materials. CEC Report EUR 13186EN, Edited by J B Marriott

[28] A. Elsender, S.M. Beech

Fatigue and Corrosion Fatigue Crack Initiation and Growth in Various 2-3.5% NCMV Rotor Forging Steels. EPRI Workshop on Superclean Materials Review, Sapporo, Japan. September 1989

B

2% CRMOWVNB ROTORS MANUFACTURED BY SAARSCHMIEDE

From the initial rotors of this steel, which were investigated in an European project known as the COST 505 program (see chapter 1), 108 rotors have been manufactured (See Table B-1). 76 rotors were of the HP-LP combination type with maximum diameters of 1276 mm in the HP section and 1938 mm in the LP section. Manufacturing details and test results for these rotors can be found in References [2 - 10].

Table B-1
Production 2%CrMoNiWV rotor forgings

Customer	Saar-schmiede Ref. #	Type of Forging	Diameter, mm of heat treatment contour HP part	LP part	Delivery Weight, mt	Delivery date	Remarks
Siemens-KWU	6110504	Turbine		1370		Aug 83	COST 505, ESR
MAN-Energie	6110663	HP-Turbine	1000			-	COST 505 VCD
Siemens-KWU	6110921	HP-Turbine	906		11	Sept 88	
Siemens-KWU	6110922	HP-Turbine	846		8	Sept 88	
Siemens-KWU	6110923	HP-Turbine	846		8	Sept 88	
Siemens-KWU	6110976	HP/LP-Turbine	830	1275	24-5	Jul 89	Valadolie, ESR
Siemens-Wesel	6111042	Turbine	1145/990		21.9	Oct 89	
MAN-Energie	6111127	HP/LP-Turbine	1026	1406	17.7	Mar 91	
Siemens-KWU	8111153	HP/LP-Turbine	1080	1486	34.7	Mar 91	
Siemens-KWU	6111164	HP/LP-Turbine	1080	1486	34.7	Oct 91	
Siemens-KWU	6111165	HP/LP-Turbine	1080	1486	34.7	Mar 92	
Siemens-KWU	6111166	HP/LP-Turbine	1080	1486	34.7	Jul 91	
Siemens-KWU	6111167	HP/LP-Turbine	1080	1486	34.7	Jun 91	

2% CRMOWVNB Rotors Manufactured by SAARSCHMIEDE

Customer	Saar-schmiede Ref. #	Type of Forging	Diameter, mm of heat treatment contour HP part	LP part	Delivery Weight, mt	Delivery date	Remarks
Siemens-KWU	6111250	HP/LP-Turbine	1080	1486	36.5	Mar 92	
Parsons	6310326	HP/LP-Turbine	992	1572	45.5	Feb 92	
Siemens-KWU	6111408	HP/LP-Turbine	1086	1539	37.4	Jan93	
Siemens-KWU	6111420	HP/LP-Turbine	938	1148	24.2	Jan93	
GE Schenectady	6411627	HP/LP-Turbine	1025	1647	14.2	May 93	
GE Schenectady	6411758	HP/LP-Turbine	1000	1266	15.1	Jun 93	
Siemens-Wesel	6111491	HP/LP-Turbine	933	1528	31.7	Jun 93	
Siemens-Wesel	6111 527	HP-Turbine	988		15.8	Jun 93	
Siemens-Wesel	6111558	HP-Turbine	953		14.7	Sept 93	
Siemens-Wesel	6111559	HP-Turbine	953		14.7	Sept 93	
ABB Stal	6411873	IP-Turbine	600		1.8	Nov 93	
GE Schenectady	6111908	HP/LP-Turbine	1019	1273	15.1	Jan94	
Siemens-KWU	6111578	HP/LP-Turbine	1088	1538	37.4	Feb 94	
Siemens-KWU	6111579	HP/LP-Turbine	1088	1538	37.4	Feb 94	
Siemens-KWU	6111580	HP/LP-Turbine	1088	1538	37.4	Mar 94	
ABB-Baden	6411938	Shaft end	1076	1374	20.1	Mar 94	
ABB-Baden	6411939	HP-Turbine	674		6	Mar 94	
ABB Stal	6412008	IP-Turbine	600		1.9	Apr 94	
GE Schenectady	6411965	HP/LP-Turbine	966	1388	22.5	May 94	
ABB Stal	6411992	IP-Turbine	911		7.1	May 94	
ABB Stal	6411129	IP-Turbine	565		1.7	Oct 94	
ABB Stal	6412130	IP-Turbine	565		1.7	Oct 94	
ABB Stal	6412096	IP-Turbine	912		7.1	Dec 94	
EPRI-Europe Rotor	6093890	HP/LP-Turbine	1250	1750	53	Aug 94	EPRI-Project RB 1403-21
GE Schenectady	6412101	HP/LP-Turbine	1063	1431	22.5	Nov 95	

Customer	Saar-schmiede Ref. #	Type of Forging	Diameter, mm of heat treatment contour HP part	LP part	Delivery Weight, mt	Delivery date	Remarks
GE Schenectady	6412102	HP/LP-Turbine	1063	1431	22.5	Jan95	
GE Schenectady	6412103	HP/LP-Turbine	1063	1431	22.5	Mar 96	
Siemens-KWU	6111750	HP/LP-Turbine	998	1938	48.5	Jan95	
Siemens-KWU	6111787	HP/LP-Turbine	998	1938	41.9	Jun 95	
ABB Stal	6412177	IP-Turbine	911		7	Jan95	
Siemens-Wesel	6111801	HP/LP-Turbine	938	1033	21.1	Mar 95	
Siemens-Wesel	6111914	HP/LP-Turbine	1005		24.1	May 97	
GE Fitchburg	6412258	HP/LP-Turbine	1144	1644	23.5	Mar 95	
ABB Stal	6412351	IP-Turbine	903		7		
ABB Stal	6412352	IP-Turbine	1374		17.5	Jul 95	
ABB Stal	6412353	IP-Turbine	1374		17.5		
Parsons	6310425	HP/LP-Turbine	1012/922	1582	54	Jun 95	
Siemens-KWU	6111970	HP/LP-Turbine	998	1938	48.5	May 96	
GE Fitchburg	6412375	HP/LP-Turbine	1012	1616	23.2	Sept 95	
GE Fitchburg	6412533	HP/LP-Turbine	1003	1616	23	Mar 96	
GE Fitchburg	6412674	HP/LP-Turbine	1012	1616	23.2	Aug 96	
Ansaldo	6310488	IP-shaft end	1723		29.5	Jul 96	
Ansaldo	6310452	HP/LP-Turbine	1276	1538	37.4	Dec 95	
ABB Stal	6310482	IP-Shaft	541		1.8	Jan96	
ABB Stal	6310505	IP-Shaft	576		1.8		
ABB Stal	6310506	IP-Shaft	576		1.9		
Siemens-Wesel	6112096	HP/LP-Turbine	1092	1502	44.8	Apr 96	
Siemens-Wesel	6112097	HP/LP-Turbine	1092	1502	44.8	Apr 97	
Siemens KWU	6112140	HP/LP-Turbine	998	1938	48.5	Apr 97	
Siemens KWU	6112142	HP/LP-Turbine	998	1938	48.5	Nov 96	

2% CRMOWVNB Rotors Manufactured by SAARSCHMIEDE

Customer	Saar-schmiede Ref. #	Type of Forging	Diameter, mm of heat treatment contour HP part	LP part	Delivery Weight, mt	Delivery date	Remarks
Siemens KWU	6112153	HP/LP-Turbine	998	1938	48.5	Feb 97	
Siemens Wesel	6112165	IP-Shaft	1220		38.15	Jul 96	
ABB-Baden	6412444	HP- Shaft	778		6.4	Sept 95	
ABB-Baden	6412445	IP-Shaft end	1426		1 9.05	Oct 95	
ABB-Baden	6412486	IP-Shaft end	1486		23.57	Dec 95	
ABB-Baden	6412594	HP-Shaft	1130		22.7	Mar 96	
Siemens Wesel	6112217	HP/LP-Turbine	850	1400	38.7	Nov 96	
Siemens Wesel	6111218	HP/LP-Turbine	850	1400	38.7		
GEC-A Nürnberg	6112219	HP/LP-Turbine	1036	1510	23.4	Oct 96	
GEC-A Nürnberg	6112220	HP/LP-Turbine	1036	1510	23.4	Nov 96	
Siemens KWU	6112221	HP/IP-Turbine	1466		36.5		
Siemens KWU	6112138	HP/IP-Turbine	1455		35.4	Dec 96	
Siemens KWU	6112139	HP/IP-Turbine	1455		35.4	Apr 97	
GE Fitchburg	6412716	HP/LP-Turbine	1003	1616	23.2	Oct 96	
GE Fitchburg	6412723	HP/LP-Turbine	1003	1616	23.2	Nov 96	
Siemens KWU	6112286	HP/LP-Turbine	998	1938	48.5	Jun 97	
Siemens KWU	6112222	HP/IP-Turbine	1466		36.5	Apr 97	
Siemens KWU	6112223	HP/IP-Turbine	1466		36.5	Apr 97	
Siemens KWU	6112265	HP/IP-Turbine	1466		36.5		
Siemens KWU	6112265	HP/IP-Turbine	1466		36.5		
Siemens KWU	6112267	HP/IP-Turbine	1466		36.5		
Siemens KWU	6112268	HP/IP-Turbine	1466		36.5		
Siemens KWU	6112271	HP/IP-Turbine	998	1629	38.7		
Siemens KWU	6112272	HP/IP-Turbine	998	1629	38.7		
Siemens KWU	6112273	HP/IP-Turbine	998	1629	38.7		

Customer	Saar-schmiede Ref. #	Type of Forging	Diameter, mm of heat treatment contour HP part	LP part	Delivery Weight, mt	Delivery date	Remarks
Siemens KWU	6112274	HP/IP-Turbine	998	1629	38.7		
Siemens KWU	6112275	HP/LP-Turbine	998	1938	48.5		
GE Fitchburg	6412786	HP/LP-Turbine	994	1384	15.5	Feb 97	
GE Fitchburg	6412846	HP/LP-Turbine	986	1612	22.5		
Siemens KWU	6112347	HP/LP-Turbine	998	1629	38.7		
Siemens KWU	6112348	HP/LP-Turbine	998	1629	38.7		
Ansaldo	6310541	HP/LP-Turbine	880	1364	20.8		
Ansaldo	6310564	HP/LP-Turbine		1270	15.9		
Ansaldo	6310565	HP/LP-Turbine		1270	15.9		
Ansaldo	6310522	IP-Shaft end	1723		29.5	Mar 97	
Ansaldo	6310523	IP-Shaft end	1723		29.5		
Siemens KWU	6112363	HP/LP-Turbine	998	1936	48.5		
Siemens KWU	6112404	HP/LP-Turbine		1466	36.5		
Siemens Wesel	6112402	HP/LP-Turbine		1520	48.5		
Siemens Wesel	6112403	HP/LP-Turbine		1520	48.5		
GE Fitchburg	6412932	HP/LP-Turbine		1612	15.6		
GE Fitchburg	6412919	HP/LP-Turbine		1612	22.9		
GE Fitchburg	6412918	HP/LP-Turbine		1612	22.9		
GE Fitchburg	6412783	HP/LP-Turbine		1612	15.6	Feb 97	
GE Fitchburg	6412780	HP/LP-Turbine		1616	22.5		

C

2% CRMONIWV HP/LP ROTOR SECTIONING DETAILS

Figs. 3-2 - 3-4 show the manner in which the trepanned radial cores were sectioned and the location of the test positions, and Figure 3-1 shows the typical orientations of test specimens with respect to the original trepanned core cross sections.

Table C-1
Investigation program

Position	Diameter 1750, Center						Diameter 1250, Center				Diameter 1250, Rim			
0.2 Yield - Level MPa	690 -720		620 - 650		690 - 720		620 - 650		690 - 720		620 - 650		690 - 720	
Condition	AR	Exp	AR	Exp	AR	Exp	AR	Exp	AR	Exp	AR	Exp	AR	Exp
Basic data: chem comp	KWU		KWU		KWU		KWU		KWU		KWU		KWU	
Tensile, hardness, micro structure														
FATT and upper shelf energy	MAN	MAN	MAN	MAN					MAN	MAN	RR	RR		
Impact energy along radius (RT)	KWU		KWU						KWU		KWU			
Fracture toughness	KWU	KWU	KWU	KWU	GEC				KWU	KWU	KWU	KWU	GEC	
Exposure time/temp	MAN		MAN						MAN		RR			
Fracture toughness	KWU	KWU	KWU	KWU	GEC				KWU	KWU	KWU	KWU	GEC	
Exposure time/temp	MAN		MAN						MAN		RR			
Creep rupture									ABB		GEC			
									ABB		GEC			
									ABB		GEC			
Creep crack growth											GEC			
LCF without dwell					ABB		ABB						ABB	

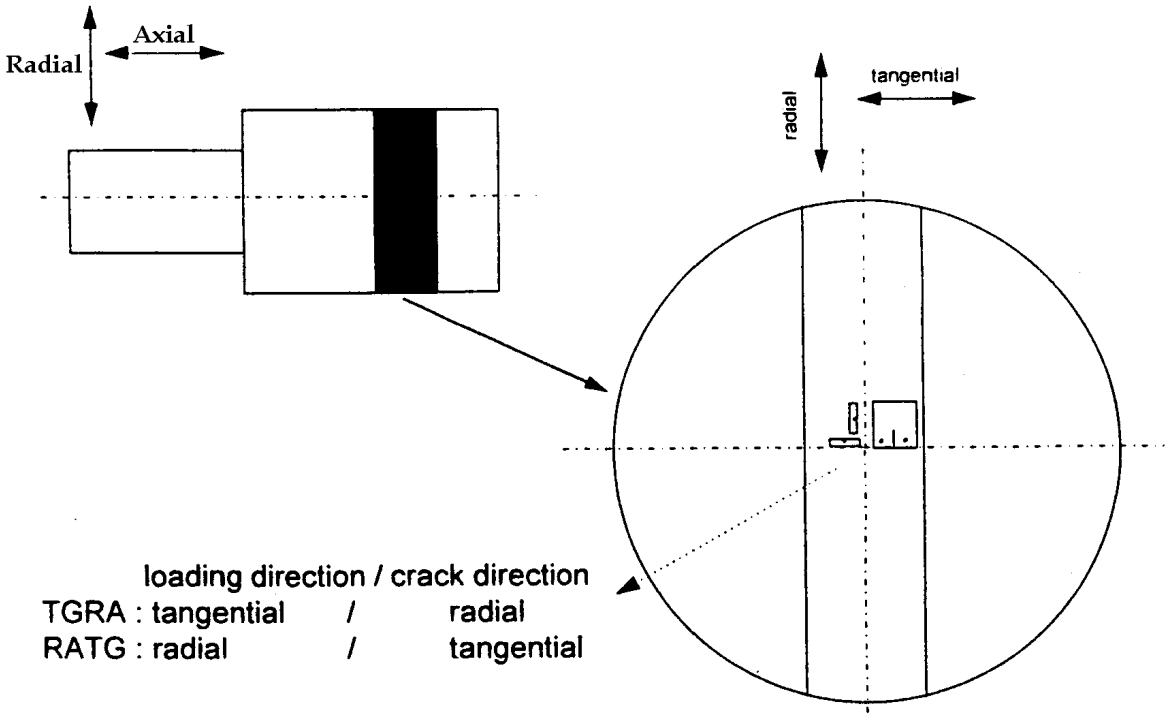

Figure C-1
Definition of specimen orientations

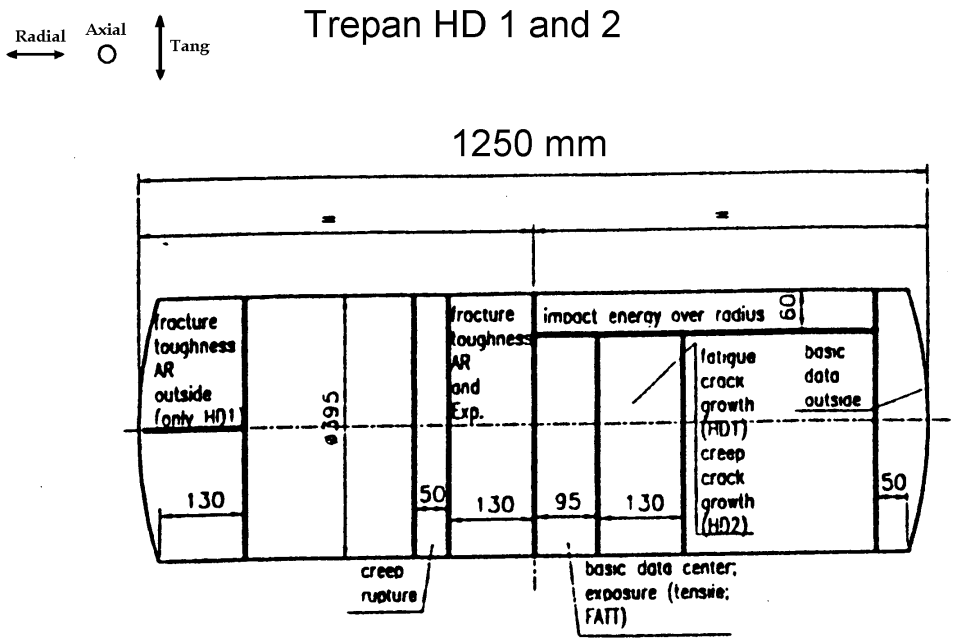

Figure C-2
Radial trepan sectioning in the HP part of the trial rotor

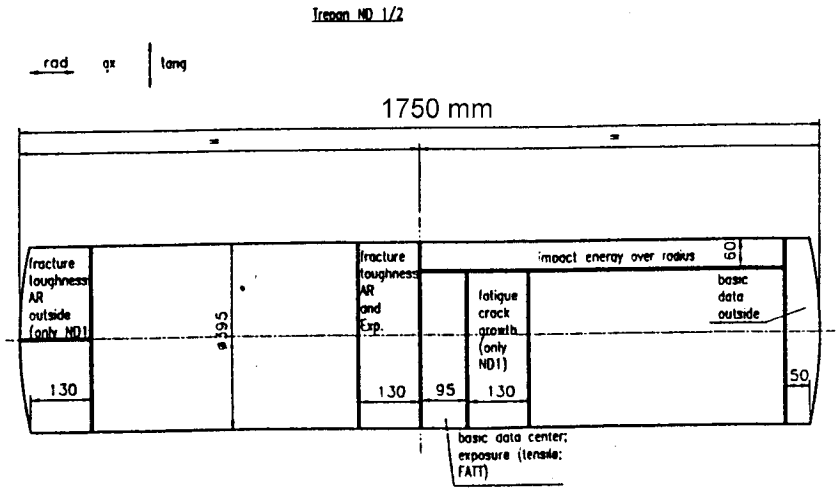

Figure C-3
Radial trepan in LP part of the trial rotor

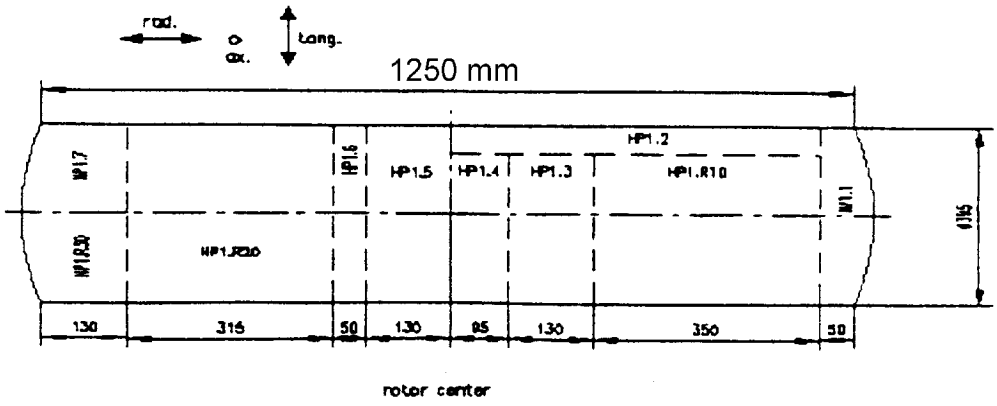

Figure C-4
Sectioning of the LP trepan

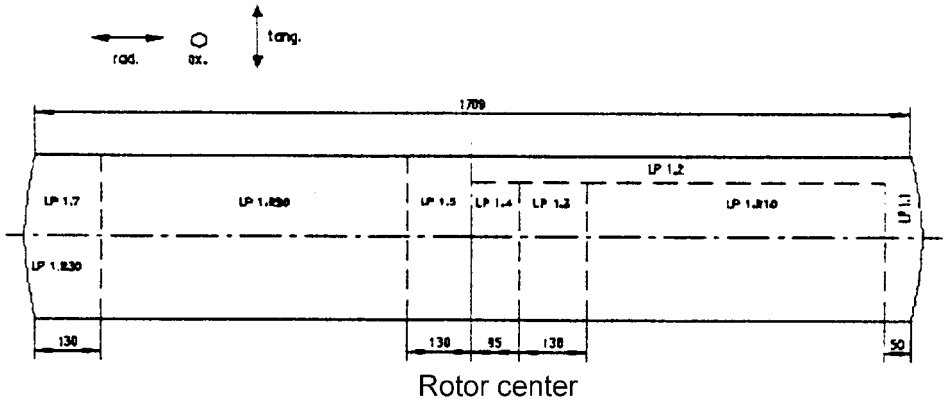

Figure C-5
Sectioning of the HP trepan

Table C-2
Test Matrix Contribution

Segment	Examination	Specimen Orientation
HP 1.R30	Mechanical properties	tangential
	Impact energy	tangential/radial
	Low-cycle fatigue	tangential
HP 1.2	Mechanical properties	tangential
	Impact energy at 20oC	tangential/radial radial/tangential
HP 1.3	Fatigue crack growth	tangential/radial
HP 1.4	Mechanical properties	tangential
	Impact energy	tangential/radial
	Condition: As-received and after exposure	
HP 1.5	Fracture toughness	tangential/radial
	Condition: As-received and after exposure	
HP 1.6	Creep properties	tangential
HP 1.7	Fracture toughness	tangential/radial
	Condition: As-received	
LP 1.1	Mechanical properties	tangential
	Impact energy	tangential/radial
	Low-cycle fatigue	tangential
	SCC testing	tangential
LP 1.2	Mechanical properties	tangential
	Impact energy at 20oC	tangential/radial radial/tangential
LP 1.3	Fatigue crack growth	tangential/radial
LP 1.4	Mechanical properties	tangential
	Impact energy	tangential/radial
	Condition: As-received and after exposure	
LP 1.5	Fracture toughness	tangential/radial

Segment	Examination	Specimen Orientation
	Condition: As-received and after exposure	
LP 1.7	Fracture toughness	tangential/radial
	Condition: As-received	
HP 2.1	Mechanical properties	tangential
	Impact energy	tangential/rad
	Low-cycle fatigue	tangential
HP 2.2	Mechanical properties	tangential
	Impact energy at 20oC	tangential/radial radial/tangential
HP 2.3	Creep crack growth	tangential
HP 2.4	Mechanical properties	tangential
	Impact energy	tangential/radial
	Condition: As-received and after exposure	
HP 2.5	Fracture toughness	tangential/radial
	Condition: As-received and after exposure	
HP 2.6	Creep properties	tangential
LP 2.1	Mechanical properties	tangential
	Impact energy	tangential/radial
	Low-cycle fatigue	tangential
	SCC testing	tangential
LP 2.2	Mechanical properties	tangential
	Impact energy at 20oC	tangential/radial radial/tangential
HP 2.4	Mechanical properties	tangential
	Impact energy	tangential/radial
	Condition: As-received and after exposure	
HP 2.5	Fracture toughness	tangential/radial
	Condition: As-received and after exposure	

Specimens for the exposure tests were cut-up as shown in the figures below

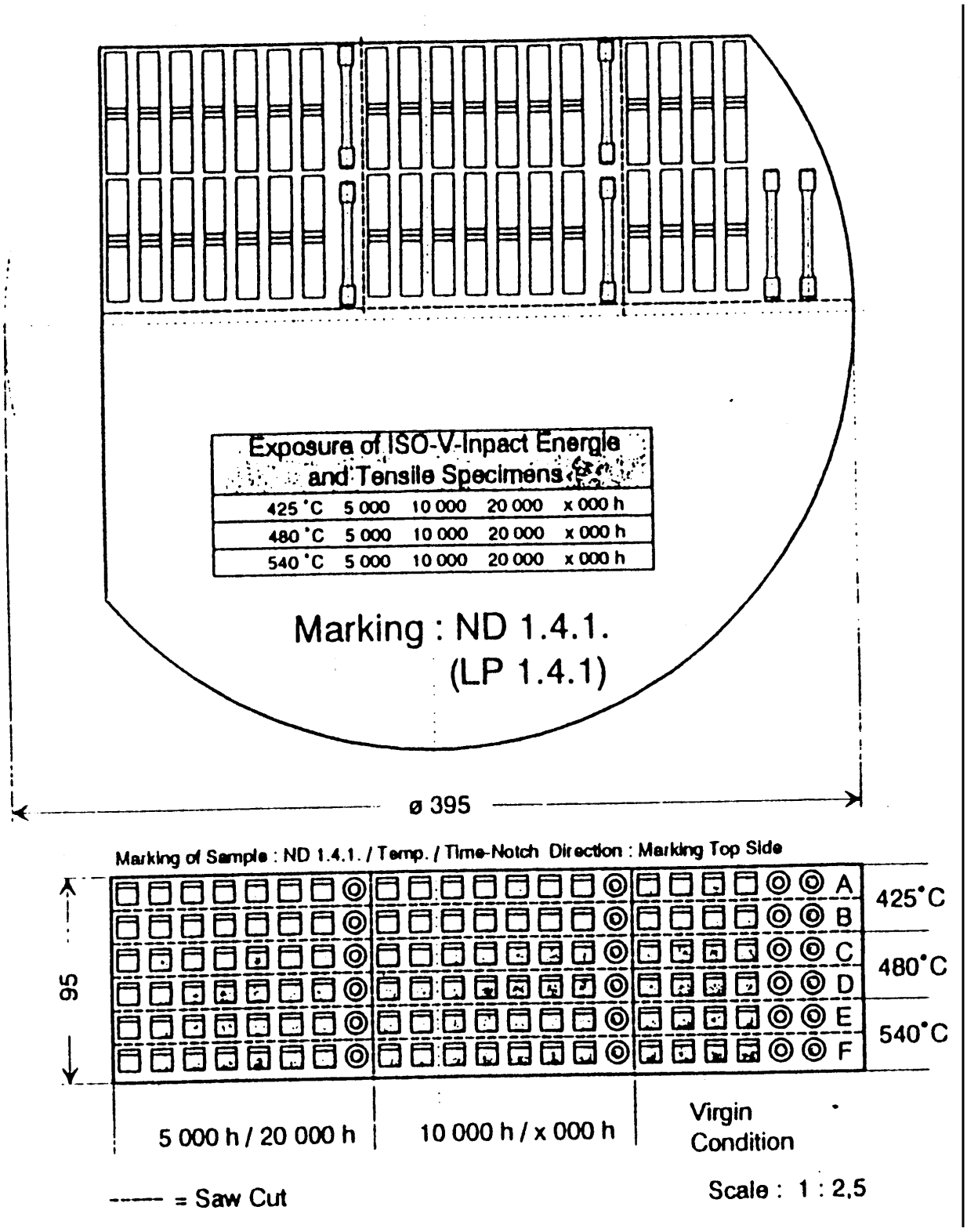

Figure C-6
Specimen Location for Exposure Tests in the low yield strength LP section of the trial rotor

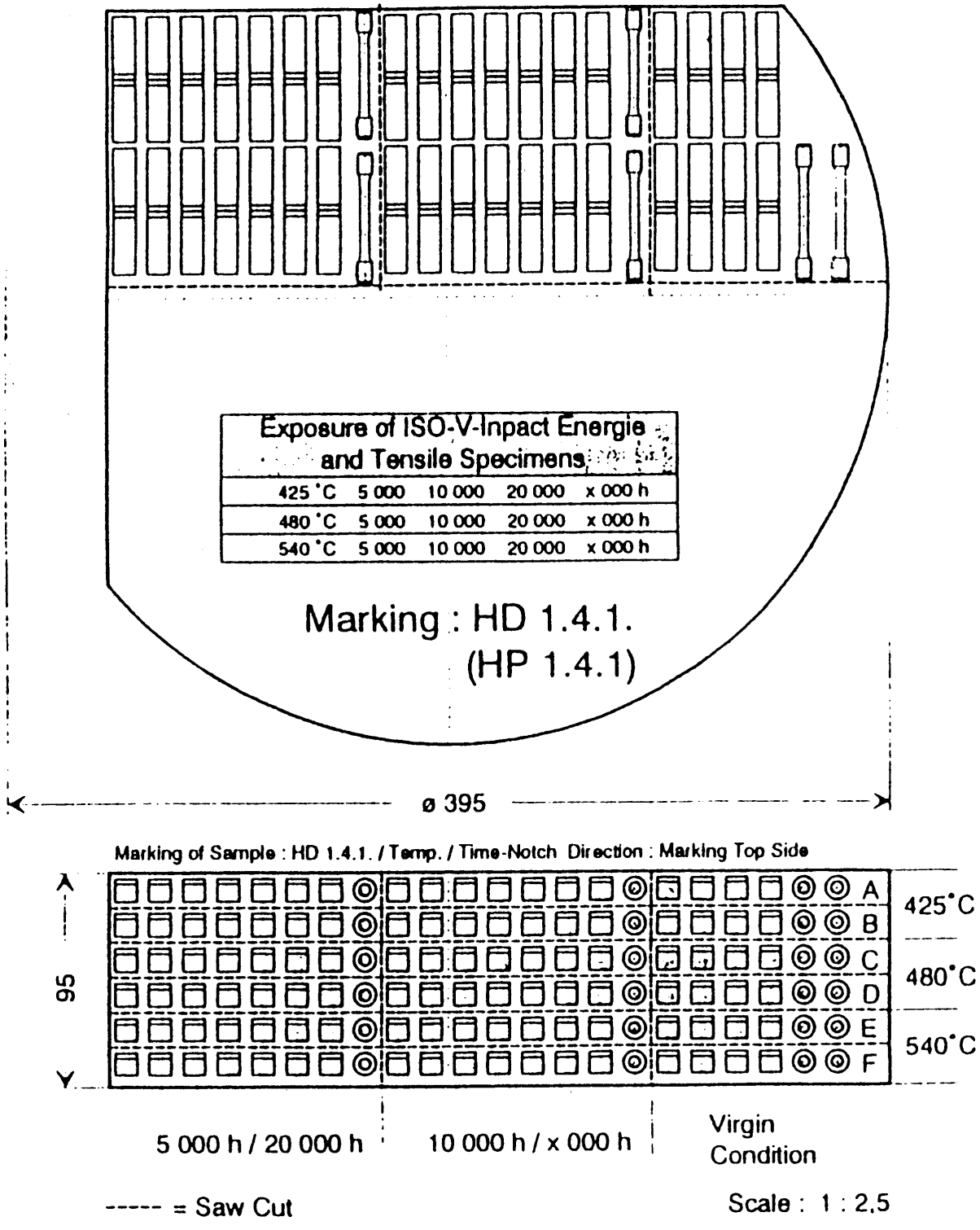

Figure C-7
Specimen Location for Exposure Tests in the low yield strength HP section of the trial rotor

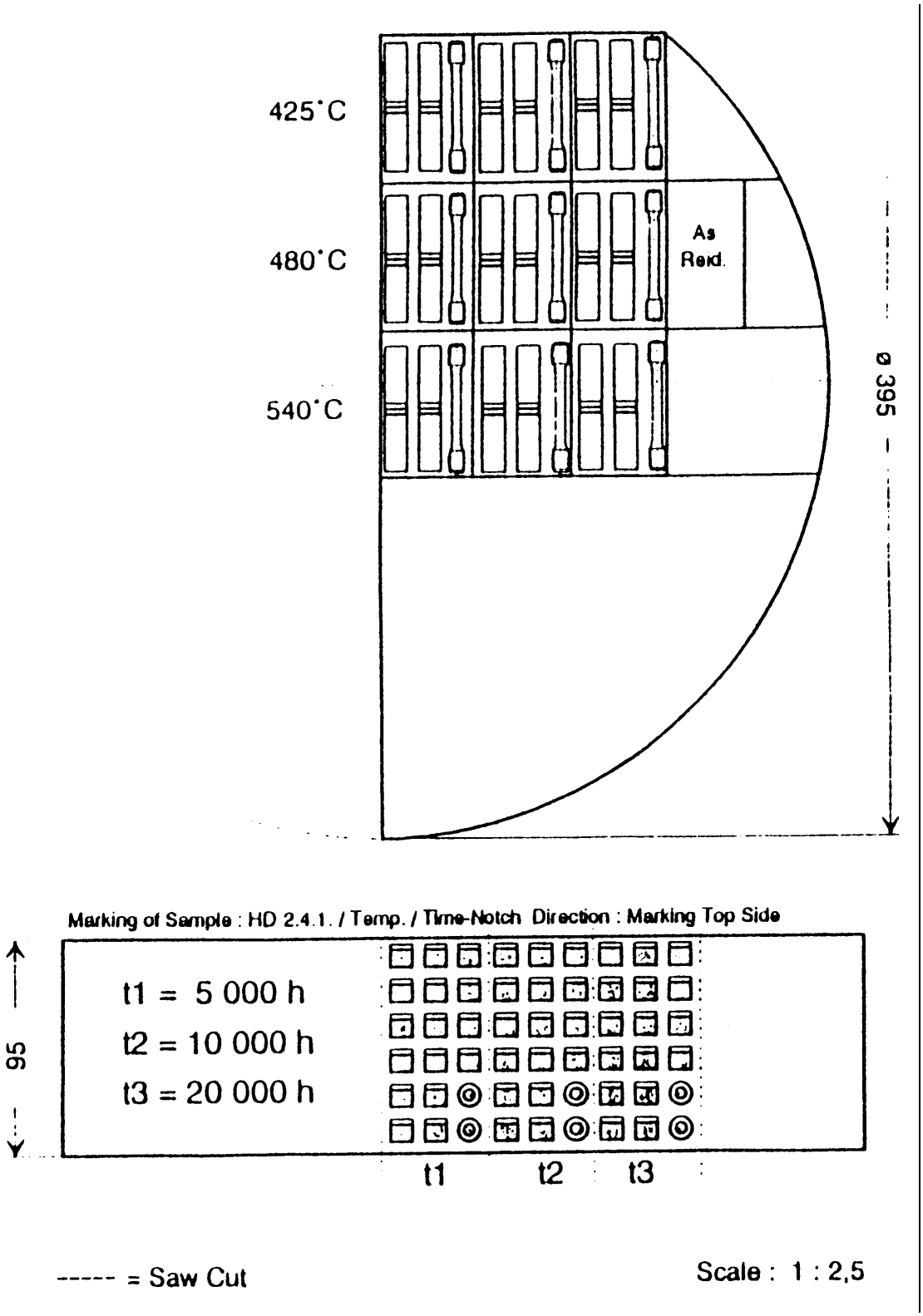

Figure C-8
Specimen Location for Exposure Tests in the high yield strength HP section of the trial rotor

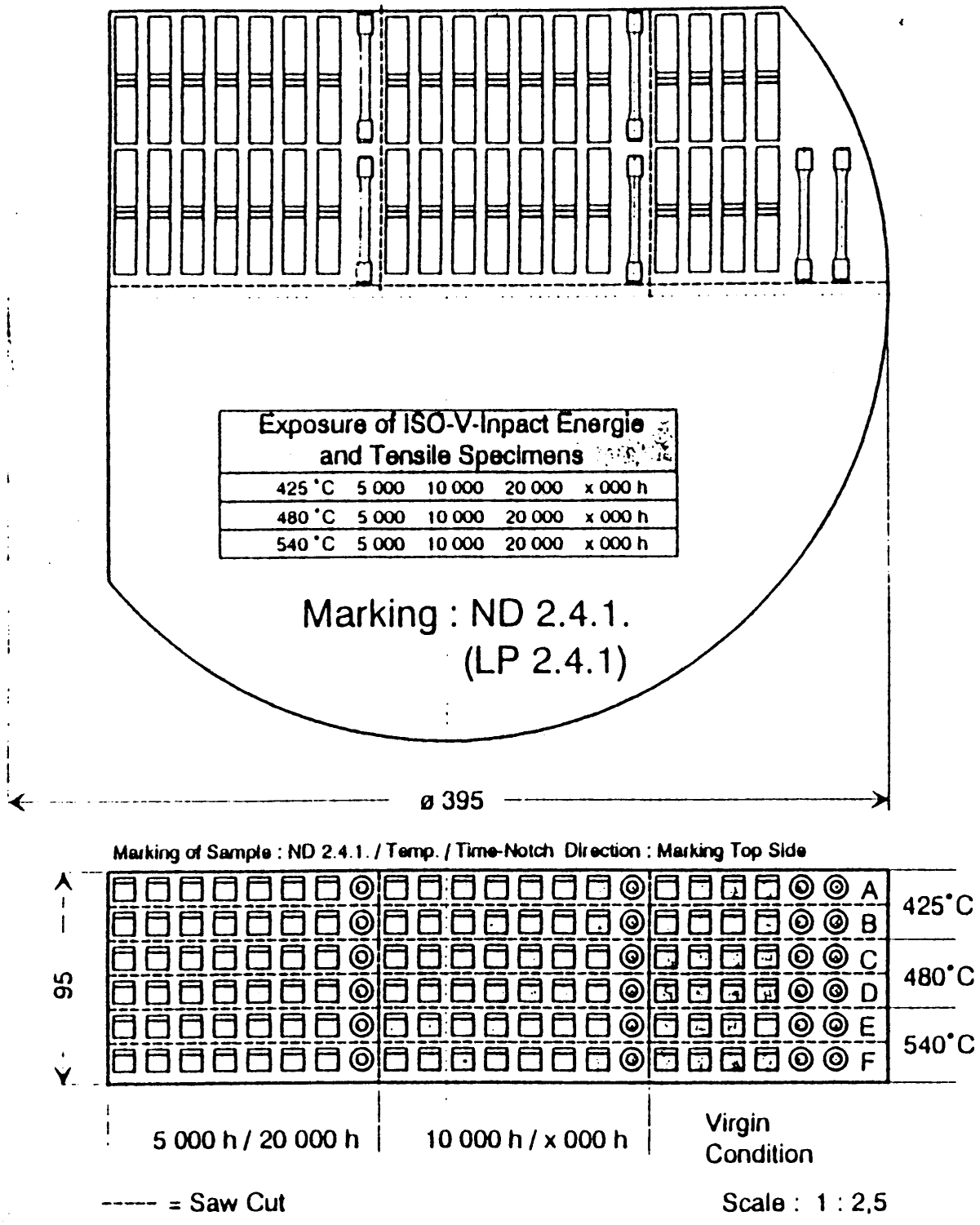

Figure C-9
Specimen Location for Exposure Tests in the LP high yield strength section of the trial rotor

D

LOW STRAIN HIGH CYCLE FATIGUE RESULTS

Table D-1
Low Cycle Fatigue Results for the EPRI-Europe rotor

Segm (Spec) #	Specimen		Temp °C	Dwell Time		Strain Rate %/min	Cycle to Crack Init†	Stress MPa		Youngs Modulus		Strain Range		
	Pos (x/R)	Orient		Ten min	Comp min			Max	Min	EγC MPa	N/nni	Elastic, %	Plastic, %	Total,%
94F60	1	Axis Tan	540	0	0	1.554	720	346	-346	16.8 x 104	0.33	0.413	0.364	0.777
94F61	1	Axis Tan	540	0	0	1.172	1437	346	-346	17.1 x 104	0.29	0.404	0.182	0.586
94F62	1	Axis Tan	540	0	0	1.02	1701	330	-330	16.04 x 104	0.61	0.412	0.098	0.510
94F63	1	Axis Tan	540	0	0	0.826	2380	316	-316	16.9 x 104	0.67	0.374	0.039	0.413
94F65	1	Axis Tan	540	30	0	1.186	650	302	-321	17.1 x 104	0.93	0.363	0.23	0.593
94F66	1	Axis Tan	540	30	0	0.80	1400	236	-343	16.7 x 104	0.23	0.346	0.052	0.398
94F64	1	Axis Tan	540	30	0	1.00	860	309.9	-354.2	18.0 x 104	0.294	0.368	0.132	0.500

Segment 2.1.3

Segm (Spec) #	Specimen		Temp °C	Dwell Time		Strain Rate %/min	Cycle to Crack Init†	Stress MPa		Youngs Modulus		Strain Range		
	Pos (x/R)	Orient		Ten min	Comp min			Max	Min	EγC MPa	N/nni	Elastic, %	Plastic,%	Total,%
94F145	1	Axis Tang	540	0	0	1.56	768	410	-410	17.46 x 104	0.16	0.47	0.31	0.78
94F146	1	Axis Tang	540	0	0	1.16	1990	362	-362	16.72 x 104	0.52	0.433	0.147	0.58
94F147	1	Axis Tang	540	0	0	0.788	3666	331	-331	17.7 x 104	0.30	0.374	0.02	0.394
94F148	1	Axis Tang	540	0	0	0.944	1471	356	-356	16.98 x 104	0.75	0.419	0.053	0.472
94F149	1	Axis Tang	540	30	0	0.98	1250	307	-394	18.2 x 104	0.523	0.386	0.104	0.49
94F150	1	Axis Tang	540	30	0	1.20	800	347	-394.7	18.2 x 104	0.46	0.40	0.18	0.58
94F151	1	Axis Tang	540	30	0	0.78	1305 Disc	248	-386	18.3 x 104	<0.74	0.346	0.043	0.389
94F152	1	Axis Tang	540	30	0	1.56	420	359	-386.8	17.73 x 104	0.75	0.42	0.36	0.78

Segment 1.R.30

Segm (Spec) #	Specimen		Temp °C	Dwell Time		Strain Rate %/min	Cycle to Crack Init†	Stress MPa		Youngs Modulus		Strain Range		
	Pos (x/R)	Orient		Ten min	Comp min			Max	Min	EγC MPa	N/nni	Elastic, %	Plastic,%	Total,%
ND31	1	Tang	RT	-	-	6	203	621	-652	201 300		0.654	2.231	2.885
ND32	1	Tang	RT	-	-	6	276	619	-648	202 800		0.649	1.887	2.536

ND33	1	Tang	RT	-	-	6	725	576	-591	212 700		0.579	0.724	1.303
ND34	1	Tang	RT	-	-	6	5750	505	-509	202 700		0.492	0.228	0.720
ND35	1	Tang	RT	-	-	6	1881	537	-558	203 000		0.545	0.454	0.999
ND41	1	Tang	RT	-	-	6	10 600	497	-501	211 800		0.472	0.094	0.566

† Number of cycles until stress range drop of 5% Segment ND 2.1.2

Segm (Spec) #	Specimen		Temp °C	Dwell Time		Strain Rate %/min	Cycle to Crack Init†	Stress MPa		Youngs Modulus		Strain Range		
	Pos (x/R)	Orient		Ten min	Comp min			Max	Min	EγC MPa	N/nni	Elastic, %	Plastic,%	Total,%
ND11	1	Tang	RT	-	-	6	1031	626	-640	211 400		0.645	0.638	1.283
ND12	1	Tang	RT	-	-	6	248	676	-709	214 200		0.711	1.838	2.549
ND14	1	Tang	RT	-	-	6	6084	568	-579	213 300		0.565	0.114	0.679
ND17	1	Tang	RT	-	-	6	20 512	517	-547	213 700		0.509	0.031	0.540

† Number of cycle us until stress range drop of 5% Segment ND 1.1.2

Segm (Spec) #	Specimen		Temp °C	Dwell Time		Strain Rate %/min	Cycle to Crack Init†	Stress MPa		Youngs Modulus		Strain Range		
	Pos (x/R)	Orient		Ten min	Comp min			Max	Min	EγC MPa	N/nni	Elastic, %	Plastic,%	Total,%
ND36	1	Tang	350	-	-	6	903	454	-465	188 100		0.503	0.832	1.340
ND37	1	Tang	350	-	-	6	15 345	394	-394	187 100		0.412	0.108	0.520
ND38	1	Tang	350	-	-	6	8291	415	-430	191 900		0.458	0.131	0.589
ND39	1	Tang	350	-	-	6	3480	414	-419	195 200		0.449	0.286	0.735
ND40	1	Tang	350	-	-	6	1422	450	-437	184 700		0.503	0.525	1.028
ND42	1	Tang	350	-	-	6	231	521	-543	180 500		0.602	1.957	2.559

† Number of cycles until stress range drop of 5% Segment ND 2.1.2

Segm (Spec) #	Specimen		Temp °C	Dwell Time		Strain Rate %/min	Cycle to Crack Init†	Stress MPa		Youngs Modulus		Strain Range		
	Pos (x/R)	Orient		Ten min	Comp min			Max	Min	EγC MPa	N/nni	Elastic, %	Plastic,%	Total,%
ND15	1	Tang	350	-	-	6	>30 458R	426	-455	193 300		0.464	0.026	0.490
ND16	1	Tang	350	-	-	6	236	582	-601	192 400		0.644	1.913	2.557
ND18	1	Tang	350	-	-	6	13 250	431	-448	199 000		0.468	0.102	0.570
ND19	1	Tang	350	-	-	6	6 413	456	-461	185 700		0.512	0.197	0.709
ND20	1	Tang	350	-	-	6	918	502	-523	204 200		0.565	0.751	1.316
ND21	1	Tang	350	-	-	6	2004	510	-527	199 900		0.555	0.442	0.997
ND22	1	Tang	350	-	-	6	40 200	434	-449	190 000		0.466	0.037	0.503

† Number of cycles until stress range drop of 5% R: Removed before failure

Segment ND 1.1.2

Segm (Spec) #	Specimen		Temp °C	Dwell Time		Strain Rate %/min	Cycle to Crack Init†	Stress MPa		Youngs Modulus		Strain Range		
	Pos (x/R)	Orient		Ten min	Comp min			Max	Min	EγC MPa	N/nni	Elastic, %	Plastic,%	Total,%
HD21	1	Tang	530	-	-	6	2382	345	-351	177 400		0.407	0.202	0.609
HD22	1	Tang	530	-	-	6	703	360	-368	174200		0.427	0.667	1.094
HD23	1	Tang	530	-	-	6	203	393	-407	168 900		0.482	2.238	2.720
HD24	1	Tang	530	-	-	6	8286	329	-334	178 100		0.384	0.069	0.453
HD25	1	Tang	530	-	-	6	1391	345	-356	173 400		0.412	0.363	0.775
HD26	1	Tang	530	-	-	6	193	395	-418	172 900		0.481	2.231	2.722
HD27	1	Tang	530	-	-	6	471	358	-377	172 000		0.440	0.974	1.414
HD28	1	Tang	530	-	-	6	532	363	-382	175 900		0.452	0.966	1.418

† Number of cycles until stress range drop of 5% Segment HD 2.1.2

Segm (Spec) #	Specimen		Temp °C	Dwell Time		Strain Rate %/min	Cycle to Crack Init†	Stress MPa		Youngs Modulus		Strain Range		
	Pos (x/R)	Orient		Ten min	Comp min			Max	Min	EγC MPa	N/nni	Elastic, %	Plastic,%	Total,%
HD1	1	Tang	530	-	-	6	3 685	385	-401	179 500		0.454	0.124	0.578
HD2	1	Tang	530	-	-	6	701	407	-421	179 300		0.484	0.561	1.095
HD3	1	Tang	530	-	-	6	194	452	-475	183 400		0.563	2.077	2.640
HD4	1	Tang	530	-	-	6	10 511	337	-364	180 200		0.410	0.033	0.443
HD5	1	Tang	530	-	-	6	272	436	-455	174 400		0.532	1.147	1.679
HD6	1	Tang	530	-	-	6	485	426	-445	175 600		0.522	0.828	1.350

† Number of cycles until stress range drop of 5% Segment HD 1.1.2

E

CREEP RUPTURE RESULTS FOR THE EPRI-EUROPE ROTOR

Table E-1
Creep Rupture Test Results for the EPRI-Europe Rotor

Position Orient	Heat Treat-ment[†]	Test Temp °C	Stress MPa	Time to Rupture Smooth h	Time to Rupture Notched h	Time to 0.2% Strain h	Time to 0.5% Strain h	Time to 1% Strain h	Elong at Rupt %	Red of Area%	Status of Test[‡]
CORE/TAN	HYS	500	450	141	>141R				19.8	75	B
CORE/TAN	HYS	500	400	769	>769R			120	22.7	78	B
CORE/TAN	HYS	500	350	>3000		500	1100	1800			C
CORE/TAN	HYS	550	350	181	>181R				23.9	79	B
CORE/TAN	HYS	550	320	572	>572R		6	100	26.9	79	B
CORE/TAN	HYS	550	300	872			50	230	23.1	82	B
CORE/TAN	HYS	550	280	1793	>1793R		250	700	25.2	78	B
CORE/TAN	HYS	550	245	5875	>5875R		2500	3000	27.1	81	B
CORE/TAN	HYS	550	220	>10000	>10000	180	1900	5200			C
CORE/TAN	HYS	550	203	>10000	>10000C	1000	3800	7000			C
CORE/TAN	HYS	550	183	>10000	>10000C	1500	4300	8500			C
CORE/TAN	HYS	600	280	81	>81R				30.1	89	B
CORE/TAN	HYS	600	240	277	>277R				26.8	78	B
CORE/TAN	HYS	600	190	830	>830R			250	31.8	88	B
CORE/TAN	HYS	600	170	1665	>1665R		270	800	32.5	89	B

Creep Rupture Results for the EPRI-EUROPE Rotor

CORE/TAN	HYS	600	150	2845	>2845R		500	1200	36.5	89	B
CORE/TAN	HYS	600	110	6777	>6777R	560	1200	2500	42.6	92	B
CORE/TAN	HYS	600	85	>9700	>9700C	450	1900	4400			C
CORE/TAN	HYS	600	65		>10000C	900	3900				
CORE/TAN	LYS	550	250	1563	12140	7	55	250	29	85	B
CORE/TAN	LYS	550	220	4462	>14100C	15	160	800	24	86	B
CORE/TAN	LYS	550	180	>13500	>14100C	15	400	3000			C
CORE/TAN	LYS	550	160	>13500	>14100C	40	900	5700			C
CORE/TAN	LYS	600	160	1363	4565				36	92	B
CORE/TAN	LYS	600	125	4178	8056			2300	35	88	B
CORE/TAN	LYS	600	90	12452	>13500C		1700	3100			B
CORE/TAN	LYS	600	70	>13200		850	2850	5300			C

[†]HYS 950°C / 31.5h / water - air + 655°C / 35.5h / furnace
LYS 950°C / 31.5h / water - air + 655°C / 35.5h / furnace + 655°C / 35h / furnace
[‡]Status of test B - Broken C - Continuing R - Removed